The Dissertation Committee for Saamiya Seraj Certifies that this is the approved version of the following dissertation:

Evaluating Natural Pozzolans for Use as Alternative Supplementary Cementitious Materials in Concrete

Committee:

Maria C.G. Juenger, Supervisor

Raissa P. Ferron, Co-Supervisor

David W. Fowler

Howard M. Liljestrand

Jinying Zhu

Kitty L. Milliken

Evaluating Natural Pozzolans for Use as Alternative Supplementary Cementitious Materials in Concrete

by

Saamiya Seraj, BSCE; MSE

Dissertation

Presented to the Faculty of the Graduate School of

The University of Texas at Austin

in Partial Fulfillment

of the Requirements

for the Degree of

Doctor of Philosophy

The University of Texas at Austin

December 2014

Dedication

Dedicated to my mom, for instilling the love of learning in me,

To my dad, for inspiring me to dream big,

To my sister, for being my being my daily dose of laughter,

And to my husband for loving and supporting me every step of the way.

Acknowledgements

First, I would like to acknowledge my parents, my sister and my husband for their unconditional love and support throughout the years. You are the light of my life and I would not have been able to finish this Ph.D. without your constant encouragement, guidance and inspiration. I wanted to give special thanks to my maternal grandparents, who were instrumental in my decision to come study in UT Austin, and to my paternal grandparents who have always played a crucial role in my education. I also wanted to thank everyone in my extended family for being so supportive throughout graduate school, and for providing me with Ph.D. related humor!

Next, I would like to thank my supervisors, Dr. Maria Juenger and Dr. Raissa Ferron. Dr. Juenger, thank you for all your support and guidance, not only through graduate school, but during my undergraduate years as well. You always know how to encourage and inspire me, whether it's through sending a Ph.D. comic strip, offering me chocolates that look like martensite steel, or sending me articles about pozzolans that you know will inspire me. Dr. Ferron, thank you as well for your support throughout my Ph.D., and for challenging me to look at things from a different and innovative perspective. I would also like to thank my committee members, Dr. Fowler, Dr. Liljestrand, Dr. Milliken and Dr. Zhu for their support, encouragement and advice throughout my Ph.D.

Next, I would also like to thank the Texas Department of Transportation for providing funding for my Ph.D., and to Cliff Coward at TxDOT for helping with some of the data collection. I wish to give special thanks to Rachel Cano, Shukui Liu, Victoria Valdez and Juan Pablo Gevaudan for their help and involvement in the project for my dissertation. Rachel, you were an awesome project partner and I wanted to thank you for teaching me the ropes at the lab when I initially joined. Shukui, thank you for your help with all the big concrete mixtures. Victoria and JP, you were the best undergraduate research assistants I had and I wanted to thank you for the countless hours of work (especially all the crushing and sieving) that you put into this project.

I would like to thank all my friends at Building 18B for their love and support! Mike, thank you for all your help around the lab with various equipment and experiments – I could not have finished my research without you. Sherian, thank you for always helping me to order research supplies and answering all my administrative questions. Sarah, I wanted to thank you for being an amazing mentor and for teaching me calorimetry and XRD. Ramya, I wanted to acknowledge all your help with my rheology work and thank you for being a constant source of inspiration and encouragement. Sarwar, thanks for being the best office mate and for all the wonderful conversation and Ph.D. advice. Beth Anne, thank you for always providing a sympathetic ear to my research troubles and for being a willing participant in my whimsical food/dessert adventures! Mitchell, Jose, Chris, Fred, Trevor, Rachel, Simon and Nick, thank you for helping me with the heavy ASR buckets, and for all your interesting conversations and pranks around the lab. To my old friends scattered all across the globe, especially

Gaurav, Kim, Piyal, Azrin, Kishore and Najeli – thank you for always being there for me and loving me.

My acknowledgements would not be complete without thanking all the anonymous UT librarians who provide help to students through chat and email. You guys are amazing, and I wanted to thank you for chasing down articles for me from the 1950's and in many different languages.

Finally, I would like to acknowledge and thank God for all the blessings that He has provided in my life, and for giving me the strength, peace and intellect needed to finish this dissertation.

Evaluating Natural Pozzolans for Use as Alternative Supplementary Cementitious Materials in Concrete

Saamiya Seraj, Ph.D.

The University of Texas at Austin, 2014

Supervisors: Maria C.G. Juenger and Raissa P. Ferron

Abstract: Concerns over the future availability of traditional SCM sources, such as fly ash, have left the concrete industry in need of alternative sources of SCMs. The research presented here has evaluated natural pozzolans such as pumice, perlite, vitric ash, zeolites, shale and calcined clay as alternative sources of SCMs. Unlike previous research that has only concentrated on empirically evaluating the performance of natural pozzolans in concrete, the research presented in this dissertation has measured both the performance of the pozzolans in cementitious mixtures as well as their physical and chemical characteristics, to draw meaningful relationships between pozzolan properties and performance. The physical and chemical characteristics of these natural SCMs were measured using techniques like particle size analysis, Brunauer–Emmett–Teller (BET) surface area, scanning electron microscope (SEM) imaging, x-ray fluorescence (XRF), x-ray diffraction (XRD), and thermal gravimetric analysis (TGA). The performance of the pozzolans as alternative SCMs was examined by looking at their effect on mortar strength and mixture workability, as well as by their ability to mitigate expansions from durability problems like alkali silica reaction (ASR) and sulfate attack. The performance of the pozzolans was related back to their physical and chemical characteristics to gain an understanding of the underlying mechanisms of cement and pozzolan interaction, and to draw insights as to why some pozzolans perform better than others in cementitious

mixtures. Using this knowledge, some of the under-performing pozzolans were modified to see if changes in their properties could improve performance. Results of the research showed that other than the two coarse zeolites, the rest of the pozzolans tested could be used as Class F fly ash replacements in concrete, with the pumice, perlite, metakaolin and fine zeolite being the best performers in terms of mortar strength and durability. Although the pumice mortar had lower strengths than the control at early ages, results from the performance improvement studies showed that the reactivity of pumice could be enhanced by grinding the pozzolans to a finer particle size distribution. Zeolites were found to negatively affect mixture workability, but calcination of the zeolites helped to improve the workability of zeolite mixtures.

Table of Contents

List of Tables

List of Figures

Chapter 1: Introduction

The push towards more sustainable concrete mixtures has made supplementary cementitious materials (SCMs) very important to the concrete industry. According to ASTM International (formerly known as American Society of Testing and Materials), SCMs are inorganic materials that can contribute to the properties of cementitious mixtures through hydraulic and/or pozzolanic activity (ASTM C 125, 2012). As such, SCMs can be used to partially replace the cement content of hydraulic-cement concrete (referred to as "concrete" elsewhere in this dissertation). Typically, SCMs are naturally occurring materials or industrial byproducts, which make their use in concrete mixtures more sustainable than that of ordinary portland cement, whose worldwide production is responsible for 5% of the global anthropogenic CO_2 emissions (Humphreys and Mahasenan, 2002). SCMs provide other benefits as well, such as improving long-term strength and durability in concrete. Despite such advantages, only a few SCMs are widely used in practice, with fly ash being one of the most popular. The use of fly ash improves the fresh and early age properties of concrete as it can increase workability of the concrete mixture (Ravina and Mehta, 1986) and lower heat production during hydration (Nocun-Wczelik, 2001), which helps to reduce thermal cracking after final set. Additionally, fly ash with low calcium content, known as Class F ash (ASTM C 618, 2012), can improve long term concrete strength and durability by mitigating expansions due to alkali silica reaction (ASR) and sulfate attack (Dhole et al., 2013; Thomas, 2011; Shehata and Thomas, 2000; Papadakis, 1999).

The popularity of fly ash as an SCM is stimulated not only by its benefits in concrete, but also by its price and availability. Being a by-product of coal burning power plants, fly ash is usually cheaper than cement, costing approximately $40/ton in the US

(ARTBA, 2011) compared to $115/ton for cement (Engineering News Record, 2014), and is widely available in regions using coal generated electricity. In 2010, the estimated worldwide production of coal combustion products was 780 million metric tons (Heidrich et al., 2013), out of which approximately 70-85% was fly ash (Heidrich et al., 2013; Mukherjee et al., 2008). However, even with such an enormous global production, the future availability of fly ash has become a source of concern in places like the US, Canada, Europe and Japan, where fly ash is classified as a waste material and is subjected to existing and evolving regulations about its use, handling and storage (US EPA, 2014-a; Heidrich et al., 2013; Sear, 2009; Barnes and Sear, 2006). Furthermore, environmental regulations that aim to reduce air pollution (US EPA, 2014-b; US EPA, 2014-c) have forced power plants to adopt emission reduction techniques that have consequently led to a lower quality of fly ash. For example, in order to reduce nitrogen oxide (NOx) emissions, power plants have switched to low NOx burners that do not fully combust the coal. This results in coarser ashes with higher carbon contents, making the fly ashes unsuitable for use in concrete mixtures with air entraining agents (Hill et al., 1997). Additionally, in order to decrease sulfur dioxide (SO_2) emissions, plants have started to combust low-sulfur coals, which produce Class C fly ash, instead of the more beneficial Class F fly ash (Jones et al., 2006; Tishmack et al., 1999). An additional problem with the use of low-sulfur coals is that ammonium has to be added to the fly ashes they produce, since these ashes do not retain sufficient electrostatic charge to be attracted towards the electrostatic precipitators that are used for dust control. This results in ammoniated fly ash, which can cause odor problems when used with alkaline cement (Jones et al., 2006). Finally, changes in the fuel source in power plants are also lowering the quality and supply of fly ash. For example, co-combustion of secondary fuels to reduce CO_2 emissions in coal burning power plants results in fly ash with very different

characteristics than the conventional coal fly ash (Barnes and Sear, 2006; Jones et al., 2006), which makes it undesirable for use in concrete. Additionally, in the long run, it has been projected that the low cost and increasing availability of natural gas will motivate power plants to use natural gas for production of electricity instead of coal (US EIA, 2014). Since these worldwide changes in the power generation industry are causing considerable uncertainty for the future availability and quality of fly ash, it becomes imperative to identify and test other SCMs that can provide similar benefits of strength, durability and mixture workability to concrete as Class F fly ash.

Promising alternative SCMs to Class F fly ash could be natural pozzolans. A pozzolanic SCM, as defined in ASTM C 125, is "a siliceous or siliceous and aluminous material that in itself possesses little or no cementitious value but will, in finely divided form and in the presence of water, chemically react with calcium hydroxide at ordinary temperatures to form compounds possessing cementitious properties" (ASTM C 125, 2012). Pozzolanic SCMs differs from hydraulic SCMs in that hydraulic SCMs can form cementitious products in water, without the presence of calcium hydroxide (ASTM C 125, 2012). Since the definition of "pozzolan" does not have any requirements for material origin, pozzolanic materials can be natural or man-made. Natural pozzolans, which is what this dissertation focuses on, can have a volcanic or a sedimentary origin and are typically materials that can be used as pozzolanic SCMs in their naturally occurring form after some minor conditioning processes like grinding, sieving or calcination (Snellings et al., 2012; ASTM C 125, 2012). Examples of natural pozzolans include volcanic materials like pumice, perlite, vitric ash and zeolites, as well as sedimentary materials like diatomaceous earth, clay and shale.

Before the advent of modern cement, the ancient Greeks and Romans extensively used natural pozzolans like pumice, powdered clay bricks and zeolitic tuff to enable

mixtures of lime and water to have hydraulic properties, or, in other words, be able to set and form cementitious products underwater (ACI 232-1R, 2012; Colella et al., 2001). Even after modern cement was developed in the 19th century, natural pozzolans were used for making mass concrete in the construction of canals, bridges and dams. Some notable examples from the 19th century, where natural pozzolans were used in construction, are the Suez Canal in Egypt and the Corinthian Canal in Greece (ACI 232-1R, 2012). Natural pozzolans were also extensively used in the US, before the availability and low price of fly ash in the late 20th century propelled fly ash to be the SCM of choice instead of natural pozzolans. Examples of US projects using natural pozzolans in the early to mid-20th century include the Golden Gate Bridge, the San-Francisco Oakland Bay Bridge, the Davis Dam and the Flaming Gorge Dam, all of which used shale as a pozzolan (Meissner, 1950; Elfert, 1974). Pumice was also a popular pozzolan to use in mass concrete during this time and was utilized in the construction of the Los Angeles aqueducts, the Friant Dam, the Altus Dam and the Glen Canyon Dam (ACI 232-1R, 2012, Elfert, 1974; Meissner, 1950).

With the threat of fly ash scarcity, natural pozzolans are experiencing a renaissance in concrete research and construction. Recent studies have shown that volcanic pozzolans like finely ground pumice, perlite and vitric ash meets most of the requirements listed in ASTM C 618, the "Standard Specification for Natural Pozzolans" (Erdem et al., 2007; Hossain, 2003; Campbell et al., 1982). Researchers have also observed lower calcium hydroxide contents, an indication of pozzolanic reaction, in cementitious mixtures where pumice, volcanic ash and zeolites were used as SCMs compared to control mixtures made with only cement (Lilkov et al., 2011; Perraki et al., 2010; Hossain and Lachemi, 2006). Research has also been conducted on sedimentary pozzolans like clay and shale, and has shown that these pozzolans require calcination to

activate their pozzolanic properties (Snellings et al., 2012; ACI 232.1R, 2012; He et al., 2000; Mielenz et al., 1950).

Although previous literature has shown natural pozzolans to be beneficial in improving durability properties of concrete like resistance to alkali silica reaction (Gokce et al., 2013; Karakurt and Topcu, 2011; Ahmadi and Shekarchi, 2010; Bektas et al., 2005; Ramlochan et al., 2000; Campbell et al., 1982) and chloride ion penetration (Uzal et al., 2007; Hossain and Lachemi, 2006; Zhang and Malhotra, 1995), studies have also found some drawbacks of using natural pozzolans as SCMs, mainly in terms of strength, mixture workability and cost. Previous research on volcanic pozzolans like pumice, perlite, vitric ash and zeolite have found that using these natural pozzolans as a cement replacement generally led to decreased compressive strength of mortar and concrete at 28 and 90 days (Lilkov et al., 2011; Erdem et al., 2007; Hossain, 2003; Campbell et al., 1982). However, there have not been any subsequent investigations to understand the reasons behind this decreased compressive strength and whether there are ways to mitigate it. Unlike volcanic pozzolans, previous literature has shown sedimentary pozzolans, such as high reactivity metakaolin, to have an early reactivity, surpassing the strength of the control concrete mixture by the first week (Guneyisi et al., 2008; Zhang and Malhotra, 1995). However, the cost of high reactivity metakaolin, which is made by purifying thermally activated kaolinite clay from lesser reactive calcined clay pozzolans (Ramlochan et al., 2000), often makes its use in concrete prohibitive. Although not as reactive as high reactivity metakaolin, research on non-commercial calcined kaolinite and calcined shale have shown that concrete mixtures with these pozzolans are also able to achieve strengths similar to or higher than the control within 28 days (Badogiannis et al., 2004; Ramsburg and Neal, 2002; Khanna and Puri, 1957; Mielenz et al., 1950). Compared to volcanic pozzolans, significantly more research, correlating pozzolan

properties to performance in cementitious mixtures, has been conducted for sedimentary pozzolans. For example, researchers have examined the effect of clay mineralogy and opaline silica on the reactivity of the clay and shale pozzolans (Fernandez et al., 2011a; He et al., 2000; Ambroise et al., 1985; Meilenz, 1950). However, there have not been any studies that have compared the physical and chemical characteristics of sedimentary pozzolans to those of volcanic origin to better understand the reasons behind the differences (or similarities) in their performance and draw meaningful relationships between pozzolan characteristics and performance.

Previous research on the effects of natural pozzolans on mixture workability is also limited. Although there are several studies that have shown natural pozzolans, like zeolites and clays, to decrease the workability of cementitious mixtures (Bilim, 2011; Ahmadi and Shekarchi, 2010; Perraki et al., 2010; Zhang and Maholtra, 1995), most of these studies use the slump test, which only gives a simplistic indication of mixture workability, instead of a scientific understanding of how the viscosity and yield stress of the mixture change with the addition of pozzolans. Additionally, other than some limited research on the workability of clay mixtures (Fernandez et al., 2011a; He et al., 2000; Foster, 1954) there has not been any significant work in trying to understand how the physical and chemical characteristics of different pozzolans correlate with their effects on mixture workability and whether there are ways to mitigate these effects.

The main objective of this dissertation is to address these aforementioned gaps in previous pozzolan literature, to determine whether natural pozzolans could be used as alternative SCMs when the use of fly ash in concrete is no longer feasible. To accomplish this objective, a variety of natural pozzolans were critically examined along with Class F fly ash, and their performance in cementitious mixtures was evaluated in terms of compressive strength, durability and mixture workability. A critical difference between

previous pozzolan research and the research presented in this dissertation is that here, the performance of the natural pozzolans was correlated back to their physical and chemical characteristics to understand why some pozzolans performed better as SCMs than others. Finding such relationships between pozzolan properties and performance is critical, not only for understanding the underlying mechanisms of cement and pozzolan interaction, but also for discovering ways to mitigate the problems of low strength and poor mixture workability that are typically associated with the use of pozzolans as SCMs in previous literature.

The rest of the dissertation is organized as follows. Chapter 2 gives descriptions of the test methods and materials used in this research. It also provides information from previous literature on the geological formation process of the natural pozzolans to help understand how the properties of the pozzolans came about. Chapter 3 presents the physical and chemical characteristics of the pozzolans, found using test methods such as laser particle size analysis, surface area measurements, scanning electron microscope (SEM) imaging, x-ray florescence (XRF) and x-ray diffraction (XRD). Chapter 4 compares the performance of the natural pozzolans in cementitious mixtures along with that of a Class F fly ash, in terms of compressive strength, durability and mixture workability. Unlike previous literature, which has typically measured compressive strength up to 28 or at most 90 days, the current study observed the strength of pozzolan mortars for a year, to assess whether strength gains from the later age pozzolanic reactions could offset the early age strength decrease that is generally associated with pozzolans. Isothermal calorimetry and thermal gravimetric analysis (TGA) was also conducted along with the compressive strength testing to gain insight on the mechanisms through which pozzolans influence the mixture compressive strength. Additionally, the research presented in this dissertation used a more advanced and scientific method than

what has been used in previous literature to assess the effect of pozzolans on mixture workability. Instead of using simplistic methods like the slump test, the research here used a rheometer to measure the actual viscosities and yield stresses of the pozzolan-containing mixtures. At the end of chapter 4, a brief synopsis is given on the problems of using natural pozzolans as SCMs that were identified during the performance testing.

Chapters 5 and 6 are devoted to techniques that can mitigate the aforementioned problems of low compressive strength and poor mixture workability, as they can serve as deterrents to the use of natural pozzolans as replacements for Class F fly ash in concrete. Using inert quartz filler and a variety of pumices, Chapter 5 illustrates the reasons behind the low early age strength of volcanic pozzolans and the ways through which this problem can be mitigated. Chapter 6 highlights how different modification techniques can change the water absorption of zeolites and ultimately improve the workability of zeolite mixtures. The dissertation concludes with Chapter 7, which provides a summary of the main findings of the current research and lists ways in which the research can be expanded in the future.

Chapter 2: Materials and Methods

Chapter 2 describes the materials and test methods used for the research presented in this dissertation. Section 2.1 provides information about all the materials used in this study and explains the geological formation process of the natural pozzolans tested, to help understand how the properties of the pozzolans came about. Section 2.2 describes the characterization test methods that were used to find the physical and chemical properties of the pozzolans. Section 2.3 presents details about the performance tests that were conducted to evaluate the suitability of the natural pozzolans as Class F fly ash replacements in concrete. Section 2.4 presents the test method for calcination that was used in Chapter 6, to improve the performance of the zeolite pozzolans.

2.1 MATERIALS

2.1.1 Natural Pozzolans

Natural pozzolans can be divided into two large categories depending upon whether the pozzolans are of a volcanic or sedimentary origin. Volcanic pozzolans, which are created from the lava and ash of volcanic eruptions, can be further divided into two more categories depending on whether they underwent any physical, chemical or biological change in nature, often referred to as diagenetic alteration, after being formed (Snellings et al., 2012). Pumice, perlite and vitric ash are examples of unaltered volcanic pozzolans, whereas zeolites are examples of altered volcanic pozzolans. On the other hand, sedimentary pozzolans are formed from the deposition of chemical and detrital sediments over time. Chemical sediments include micro-organism skeletons and chemical precipitates from hydrothermal waters, whereas detrital sediments are formed through erosion and weathering of pre-existing rocks (Snellings et al., 2012). Examples of

sedimentary pozzolans include materials like diatomaceous earth, clay and shale. Figure 2.1 shows an illustration of this breakdown.

Candidate natural pozzolans for the research presented in this dissertation were identified through published literature searches and discussions with university researchers and industrial users of SCMs. While searching for materials, the focus was kept on pozzolans that were either sourced locally or could be shipped from nearby areas at a low cost. Preference was also given to materials that were already being marketed and used as SCMs commercially. However, some of the pozzolans that were used in this research were created in the research lab by grinding down fine aggregate from aggregate producers.

Originally, 15 materials were identified, out of which only eight were tested as Class F fly ash replacements. The rest of the materials were deemed to be unsuitable as Class F fly ash replacements due to their high cost, problems in availability or poor performance in initial ASTM C 618 (2012) screening tests (the procedures of which are described in Section 2.2.1). As such, these unsuitable materials were discarded from the testing matrix, except for two unaltered volcanic pozzolans, Pumice-N and Pumice-S, which were kept for the research presented in Chapter 5, to help illustrate how the early age strength of pozzolan-containing mixtures can be improved. These two pumice pozzolans were only evaluated in selected characterization and strength tests, and were not assessed as Class F fly ash replacements. Table 2.1 provides details on the cost, sourcing and availability of these two pozzolans.

The eight materials, out of the original fifteen, which were tested as Class F fly ash replacements are also presented in Table 2.1. There are two sedimentary pozzolans, Metakaolin-D and Shale-T, and six volcanic ones. Out of the volcanic pozzolans, Pumice-D, Perlite-I and Vitric Ash-S fall under the category of unaltered volcanic

pozzolans, while the three zeolites, Zeolite-Z, Zeolite-T and Zeolite A, are altered volcanic pozzolans. The next subsections describe each of the natural pozzolans in more detail.

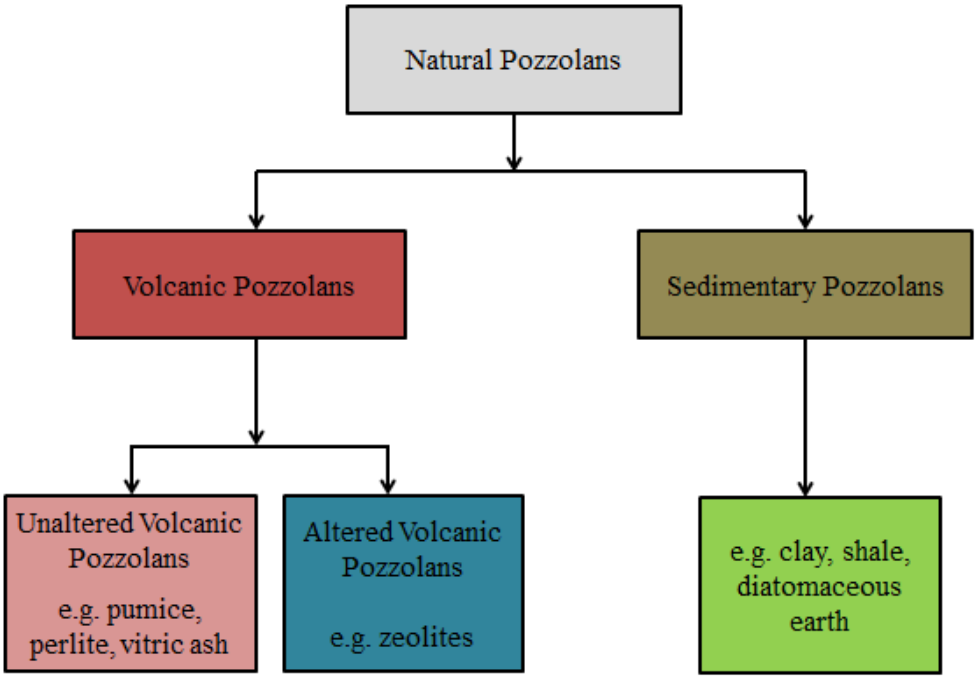

Figure 2.1: Categorization of natural pozzolans

Table 2.1: The Classification, Cost, Source and Availability of the Natural Pozzolans

Classification	Material Name	Cost ($/ton)^	Source	Availability (tons/year)
Unaltered Volcanic	Pumice-N*	$526	Idaho	200,000
	Pumice-S*	N/A	N/A	N/A
	Pumice-D	$116	Idaho	200,000
	Perlite-I	$124	Idaho	N/A
	Vitric Ash-S	$100-160	Nevada	300,000 - 1,000,000
Sedimentary	Metakaolin-D	$325~	Missouri/Indiana	30,000
	Shale-T	$49-51	Streetman, TX	4500
Altered Volcanic	Zeolite-Z	$100	Idaho	50,000
	Zeolite-T	$200~	Tilden, TX	10,000
	Zeolite-A	$150	Marfa, TX	500,000

* Not tested as Class F fly ash replacements
^ US ton = 2000 lbs = 907 kg
~ Does not include shipping

2.1.1.1 Unaltered Volcanic Pozzolans

Pumice is a porous volcanic rock formed by extruded lava containing dissolved gases. As the lava rapidly cools down and hardens, the dissolved gases separate out from the lava as bubbles, which form pores (known as vesicles) that result in a low density amorphous rock. Generally, pumice is formed from felsic or highly siliceous lava, which tends to hold dissolved gases due to its high viscosity. Lava with a lower silica content than felsic lava tends to de-gas quickly without being able to create the stable vesicular structure of a pumice rock. As such, pumice usually has a very siliceous composition (Presley, 2006).

Pumice-D, the pumice tested as a Class F fly ash replacement in this research, is a commercial SCM that is sourced in Idaho, USA. This pozzolan was processed by the manufacturer to have a certain fineness by sieving the pumice through a No. 325 sieve

(45 μm sieve opening) Since the price of Pumice-D is higher than that of fly ash, but similar to that of cement, the main benefits anticipated from the use of Pumice-D are enhancement of concrete properties (through pozzolanic reaction) and lowering the carbon foot print of concrete (through partial replacement of cement), instead of an economic one. The two additional pumice pozzolans that are used in this research, to illustrate ways to improve early age strength of cementitious mixtures, are Pumice-N and Pumice-S. Like Pumice-D, Pumice-N is also a commercial SCM from Idaho. However, Pumice-N is much finer than Pumice-D since Pumice-N was ground by its manufacturers to have a median particle size (d_{50}) close to 3 μm. The extra processing required to achieve the fineness of Pumice-N makes it very costly, and was one of the reasons why it was not selected to be tested as a fly ash replacement. The other pumice pozzolan, Pumice-S, was supplied by the manufacturer as a fine aggregate. It was later ground down in the university laboratory, where the research for this dissertation was conducted, using a Bico Inc. UA V-Belt Drive Pulverizer and sieved through a No. 200 sieve (75 μm opening). Since the supplier for Pumice-S could not be located after initial contact, the pozzolan was not tested as a fly ash replacement.

Like pumice, perlite is also an amorphous, volcanic rock, often characterized as displaying a "pearly, vitreous luster." Although the formation of perlite is similar to that of pumice, its high water content of 2-5% is what differentiates it from other volcanic rocks (Bektas et al., 2005). It is generally hypothesized that perlite has a high internal water content because its hydration (ingress of water into the rock) occurs in two steps. The primary hydration takes place during the formation of the volcanic glass and the secondary hydration occurs late in the cooling history of the glass. Water for the primary hydration mostly comes from the siliceous lava, whereas water for the secondary hydration is generally attributed to external sources, such as ground water or surface

water (Denton et al., 2009; Rotella and Simandl, 2002). When heated rapidly, natural perlite expands to form a white, porous, lightweight aggregate known as expanded perlite (Bektas et al., 2005; Rotella and Simandl, 2002). The high water content of natural perlite is crucial in the formation of expanded perlite. As perlite is heated to temperatures ranging between 870-1100°C, the glassy structure becomes soft enough for the internal water to boil (Rotella and Simandl, 2002). The resultant steam forms bubbles within the perlite structure, which allows the perlite to expand up to 20 times its original volume and form expanded perlite (Bektas et al., 2005; Rotella and Simandl, 2002). The perlite used in this research, Perlite-I, is a commercially available expanded perlite from Idaho, USA, which was ground and sieved by the manufacturers to pass the No. 325 sieve (45 μm sieve opening). The price of Perlite-I is similar to that of cement, so no economic benefit is expected to be derived from replacing cement with Perlite-I.

Volcanic or vitric ash is formed when gas bubbles in molten lava rock expand rapidly from exposure to atmospheric temperature and pressure. As a result of this expansion, a violent explosion occurs that breaks the molten rock apart. These fragments then cool down quickly and form amorphous volcanic glass. Fragments that are less than 2 mm in diameter are considered volcanic ash and can be composed of rock, minerals, and/or volcanic glass (ACI 232.1R, 2012). Explosive eruptions, which form large plumes of volcanic ash and hot gases, are predominantly indicative of highly siliceous lava, making volcanic ash similar in chemical composition to pumice or perlite (Presley, 2006). However, due to its formation process, volcanic ash is more likely to contain significant amounts of mineral impurities that may increase the crystallinity of the ash. The Vitric Ash-S used in this project is from Nevada, USA. The price of the pozzolan without shipping costs is $50-80/ton, which makes it cheaper than cement. However, the

suppliers estimate shipping costs to also be between $50-80, which makes the final cost between $100-160/ton, negating the economic benefit of the SCM.

2.1.1.2 Altered Volcanic Pozzolans (Zeolites)

Zeolites are hydrated crystalline aluminosilicate minerals. The crystalline framework consists of silicate and aluminate tetrahedra that are arranged in rings (Snellings et al., 2012), which connect together to form pores of a consistent diameter throughout the crystal structure (Snellings et al., 2012; ACI 232.1R, 2012). The pores, which can comprise as much 50% of the total volume (Pabalan and Bertetti, 2001), contain exchangeable cations, which help to balance the net negative charge of the zeolite framework that is caused by the substitution of Al^{3+} for Si^{4+} in the tetrahedra (Snellings et al., 2012). Water molecules are also held in these pores due to charge-dipole interactions (Snellings et al., 2012). Zeolites fall under the category of altered volcanic pozzolan since they are typically formed from the diagenetic alteration of volcanic glasses by alkaline fluids. Although the structure of zeolites is significantly more crystalline, their chemical composition is similar to that of their unaltered counterparts. There are many different types of natural zeolites with clinoptilolite, a silica-rich polymorph of heulandite, being the most commonly identified zeolite mineral (Snellings et al., 2012).

Three zeolites were used in this research. Zeolite-Z, is a commercially available, finely ground zeolite from Idaho, USA, whereas Zeolite-T and Zeolite-A, which are more coarsely ground, are from Texas, USA. Surprisingly, the cost of the finer zeolite, Zeolite-Z, is cheaper than the cost of the two coarser zeolites, Zeolite-T and Zeolite A. At $100/ton, the price of the fine grained Zeolite-Z is closer to that of cement, whereas the cost of Zeolite-T and Zeolite-A are much higher at $200 and $150 per ton, respectively.

2.1.1.3 Sedimentary Pozzolans

Metakaolin is made from calcining kaolinite clays. Clays are fine-grained soils and rocks, which are typically dominated by phyllosilicate particles, known as clay minerals (Snellings et al., 2012). Although they are considered to be sedimentary materials, clay minerals originally developed from diagenetic alteration of volcanic rocks in low temperatures or by mild alkaline fluids (Snellings et al., 2012). These minerals are composed of tetrahedrally (T) coordinated sheets of SiO_4 and AlO_4, connected to octahedrally (O) coordinated sheets composed of cations, such as Al^{3+}, Mg^{2+}. These sheets then come together in a T-O or a T-O-T formation to create a layered structure (Snellings et al., 2012), with interchangeable cations that can adsorb water in between the layers (Snellings et al., 2012; Fernandez et al., 2011a; Foster, 1954). This arrangement of the clay minerals has important implications in the use of clays as pozzolans, as the highly stable layered crystal structure makes clays less reactive than other pozzolans, despite being highly siliceous. As such, before they can be used as pozzolans, clays have to be calcined beyond their dehydroxylation point to make their structure more amorphous and reactive (Snellings et al., 2012; He et al., 2000). Kaolinite clays have an advantage over other types of clays, in that the layers of the kaolinite mineral have only two sheets, forming a T-O structure, with no interlayer cations. This structure allows kaolinite clay to have a low water demand (Fernandez et al., 2011a) and undergo the highest amount of decomposition during calcination, which makes it the most reactive of all clays once it has been thermally activated (Fernandez et al., 2011a; Ambroise et al., 1985). The metakaolin pozzolan used in this research, Metakaolin-D, is a commercially available SCM, sourced from Missouri and Indiana in the US. Please note that Metakaolin-D is not a high reactivity metakaolin, which is derived from a highly refined kaolinite clay that had its impurities removed prior to calcination (ACI 232.1R, 2012;

Ramlochan et al., 2000). Although not a high reactivity metakaolin, the cost of Metakaolin-D at $325/ton is much higher than that of cement, making its use as a cement replacement detrimental to mixture cost.

Shale is a fine grained sedimentary rock formed from compaction of clay minerals and other particulate debris that initially creates a mudrock. Eventually the mudrock transforms into shale when cleavage or laminations are developed (Snellings et al., 2012; Cook, 1986). Although in geology, current nomenclature suggests that the term "mudstone" be used for fine grained sedimentary rock instead of "shale" (Macquaker and Adams, 2003), for the purposes of this dissertation the term shale will be used, since the manufacturers of the material used in this research refer to their product as shale. Shale generally exhibits similar chemical composition but lower water content compared to the clay from which it was derived. Since shale is mostly composed of clay minerals, it also needs to be heated in order to activate its pozzolanic potential (ACI 232.1R, 2012; Mielenz et al., 1950). The calcined shale used in this research, Shale-T, was originally a fine aggregate from Texas, USA that was crushed in the laboratory using Bico Inc. UA V-Belt Drive Pulverizer and passed through a No. 200 sieve (75 μm opening). Although Shale-T is not a commercially available material, the suppliers of the shale aggregate stated that a lot of fines are produced as a by-product during processing of the aggregate, which could be used as SCMs. Since the Shale-T SCM would be a by-product of the shale aggregate processing, the estimated cost is similar to that of fly ash, making its use in concrete as a cement replacement very economical.

2.1.2 Cement, Sand, Fly Ash and Quartz

The cement used for all the mixtures was an ASTM C 150 (2011) Type I portland cement from Texas Lehigh, in Buda, Texas. The sand used for all mortar mixtures, except for those testing resistance to ASR, was standard graded sand from Ottawa, Illinois, which met all the requirements of ASTM C 778 (2012). A fine aggregate mixture of quartz and chert sand from Texas, which has been shown to be reactive in previous literature (Ideker et al., 2012), was used in the ASR mortar mixtures. This reactive fine aggregate was re-graded in the laboratory to meet the requirements of ASTM C 1567 (2013). The Class F fly ash used to compare the natural pozzolans was from Rockdale, Texas. Inert quartz filler was also used for the strength improvement research presented in Chapter 5. The inert quartz was produced by Old Hickory Clay Company and distributed by Clay World, Inc.

2.1.3 Admixtures

A polycarboxylate-based ASTM C 494 (2013) Type F Water Reducing Admixture (WRA) distributed by the Sika Corporation under the trade name Sika ViscoCrete 2100 was used in the ASR mortar mixtures. However, some of the pozzolan mixtures required more than the recommended dosage of the polycarboxylate admixture to achieve the required flow. As such, the admixture was changed for the subsequent sulfate attack tests. Instead of a polycarboxylate, the mortar mixtures used to test sulfate-resistance used a napthalene-based ASTM C 494 (2013) Type F WRA. This admixture was also distributed by the Sika Corporation, under the trade name of Sikament N. The admixture dosages can be found in Appendix A.

2.2 CHARACTERIZATION METHODS

This section describes the test methods that were used to characterize the physical and chemical properties of the eight natural pozzolans tested as Class F fly ash replacements in this research. Although Pumice-N and Pumice-S were not tested as fly ash replacements, their physical and chemical characteristics were also evaluated along with the eight other pozzolans, to understand the similarities and differences between the three pumice powders used in this study. This will be critical for the research presented in Chapter 5. Some of the characterization tests that were conducted for the natural pozzolans were also done for the cement, fly ash and quartz filler. Details are provided if the test method had to be changed when testing these other materials.

Section 2.2.1 describes the ASTM C 618 (2012) test procedures for characterizing natural pozzolans. Since ASTM C 618 (2012) is the governing specification for coal fly ash (Class C and F) and natural pozzolans (Class N), it is important to qualify SCMs for concrete using this specification. Sections 2.2.2 – 2.2.6 describe more advanced characterization test methods, like laser particle size analysis, Brunauer–Emmett–Teller (BET) surface area measurements, scanning electron microscope (SEM) imaging, x-ray diffraction (XRD), thermal gravimetric analysis (TGA), which were used to supplement the information found using the basic ASTM C 618 (2012) characterization tests. Table 2.2 presents a list of all the characterization test methods used in this research.

Table 2.2: Characterization Test Methods Used

Category	Test Method	Found Using
ASTM C 618 Tests	Oxide Composition	X-ray Florescence (XRF)
	Moisture Content	Oven Drying
	Loss on Ignition	Oven Drying
	Fineness	No. 325 sieve (45 um opening)
	Density	Pycnometer
	Soundness	Autoclave
	Strength Activity Index	Compression Testing
	Water Requirement	Flow Table
Advanced Characterization Tests	Particle Size	Laser Particle Size Diffraction
	Surface Area	BET Surface Area with Nitrogen
	Particle Shape/Texture	SEM Imaging
	Crystalline Phase Composition	X-ray Diffraction (XRD)
	Phase Composition	Thermal Gravimetric Analysis/Differential Scanning Calorimeter (TGA/DSC)

2.2.1 ASTM C 618

ASTM C 618 (2012) is the governing specification for coal fly ash (Class C and F) and natural pozzolans (Class N) used in concrete. The criteria set forth in the ASTM specification are divided into three categories: chemical requirements, physical requirements and supplementary optional requirements. The chemical requirements look at variables like the oxide composition, moisture content and loss on ignition of SCMs, while the physical requirements examine properties like fineness, density, soundness, strength and water requirement. A uniformity criteria is also listed under the physical requirements but was not considered for this study because the materials were collected and used from a single batch. The supplementary optional requirements, which mainly

look at the effect of the SCMs on the durability characteristics of concrete, were also not considered during the characterization phase of this study. Instead, the effect on durability was conducted during the performance tests for the eight natural pozzolans that were tested as Class F fly ash replacements.

2.2.1.1 Oxide Composition

ASTM C 618 (2012) requires materials to have a minimum combined silica (SiO_2), alumina (Al_2O_3), and iron oxide (Fe_2O_3) composition of 70.0% by mass to be classified as Class N pozzolans. It also limits the maximum sulfur trioxide (SO_3) composition to 4.0% by mass for Class N pozzolans. The oxide compositions of the natural pozzolans were found using X-ray florescence (XRF). Fused pellets for XRF analysis were prepared in a Claisse M4 Fluxer according to TxDOT test procedure Tex-317-D (2012), using 0.5 g of SCM and 6.5 g of lithium borate-lithium bromide. The fused pellets were then analyzed in a Bruker S4 Explorer according to ASTM D 4326 (2011), as specified in ASTM C 311 (2011).

XRF analysis was also conducted for the cement and fly ash. The XRD procedure for both the fly ash and cement was identical to that used for the natural pozzolans. The only difference was that the fused pellets used in the cement XRF analysis contained 1 g of cement and 6 g of lithium borate-lithium bromide powder, instead of 0.5 g of SCM and 6.5 g of lithium borate-lithium bromide powder that were used in fused pellets for the natural pozzolans and fly ash.

2.2.1.2 Moisture Content and Loss on Ignition

Moisture content measures the weight lost upon drying at 110°C, whereas loss on ignition (LOI) measures the total weight lost when the moisture free sample is heated from 110°C to 750°C. High values in these tests provide possible warnings about the effect of the SCM on concrete workability and admixture demand. ASTM C 618 (2012) specifies that Class N pozzolans must have moisture contents less than 3.0% and LOI less than 10.0% (by mass). The moisture content and LOI of the natural pozzolans was determined according to the procedures of ASTM C 311 (2011). For the LOI determination, ASTM C 311 (2011) uses a modified ASTM C 114 (2011) procedure, which calls for the material to be heated in uncovered porcelain, instead of platinum, at 750°C.

2.2.1.3 Fineness

The fineness test determines the amount of material that is retained on a No. 325 sieve (with a 45 μm opening) after wet sieving the SCM under a water pressure of 10 psi. The fineness test, as the name implies, is useful to get a general idea of how fine the pozzolan particles are, which is related to their reactivity in cementitious systems. ASTM C 618 (2012) specifies that Class N pozzolans must have less than 34% by mass retained on the No. 325 sieve after wet-sieving. As specified in ASTM C 311 (2011), the fineness test was conducted according to the procedures of wet sieving described in ASTM C 430 (2008).

2.2.1.4 Density

Although the uniformity criteria, which uses variations in density to reject materials, was not considered for this research (since all the pozzolans came from a single batch), density measurements of the materials were still conducted. As specified in ASTM C 311 (2011), the density of the natural pozzolans was measured using a modified ASTM C 604 (2007) procedure. The modification listed in ASTM C 311 (2011) calls for the materials to be tested as received, instead of following the sample preparation steps of ASTM C 604 (2007). Along with the natural pozzolans, the density of the fly ash and the quartz filler was also measured. A Quantachrome Corporation Ultra Pycnometer 1000 was used for the density measurements.

2.2.1.5 Soundness

The soundness of a cement/SCM combination is tested to identify materials that have the potential to produce delayed expansion due to magnesium and calcium oxides. Soundness of a material is determined by measuring the autoclave expansion using the procedures specified ASTM C 151 (2009). In this method, specimens made of cement paste are exposed to high temperature and pressure for 3 hours, after which they are brought back down to atmospheric pressure and room temperature. The expansion (or contraction) that occurs due to this process is expressed as a percentage of the effective gage length. ASTM C 618 (2012) specifies that paste samples with Class N pozzolans must not have an autoclave expansion (or contraction) of more than 0.8%. Soundness testing was conducted on paste samples containing 20% SCM – 80% cement by weight. The pastes were mixed to normal consistency according to ASTM C 187 (2011) and tested according to ASTM C 151 (2009), as specified in ASTM C 311 (2011).

2.2.1.6 Strength Activity Index

The strength activity index (SAI) gives an indication of the reactivity of an SCM, by comparing the compressive strength of mortar cubes made with 80 wt.% cement and 20 wt.% SCM to the compressive strength of the control mortar cubes made with only cement. The SAI is performed in conjunction with the water requirement test (described in section 2.2.1.7), which requires the mortar mixtures to have a constant flow. ASTM C 618 (2012) requires the compressive strength of the SCM mortar to be at least 75% of the control mortar's compressive strength at either 7 or 28 days. The SAI tests on the natural pozzolans were conducted according to the instructions in ASTM C 311 (2011), which further refer to ASTM C 109 (2011) for the molding, curing and testing procedures for the mortar cubes.

2.2.1.7 Water Requirement

The mortars with SCM that are made for the SAI test are required to have a flow which is ± 5% of the control mortar, made with 100% cement. ASTM C 618 (2012) dictates that the amount of water necessary to meet this flow requirement should not exceed 115% of the control mortar. The water requirement test is a simplistic method of evaluating the effect of an SCM on mixture workability, which refers to "the ease and homogeneity with which concrete can be mixed, placed, consolidated and finished" (ACI 116.R, 1990). Therefore, failing the water requirement test gives an indication of the relative increase in difficulty of mixing, placing and finishing the SCM concrete mixture compared to the control mixture. The water requirement tests on the natural pozzolans were performed using the instructions in ASTM C 311 (2011), which further refer to ASTM C 1437 (2007) for the flow measurement procedures.

2.2.2 Particle Size

Laser particle size analysis was conducted to supplement the ASTM C 618 fineness test, which only gives a basic indication of material fineness. Using laser particle size analysis, the entire particle size distribution of a material can be found, which is essential in predicting early age properties, such as the stimulation of cement hydration through the filler effect, or increased reactivity or decreased workability due to the presence of finer particles. The particle size distributions of the natural pozzolans, along with those of the cement, fly ash and quartz, were analyzed using a Horiba Partica LA 950-V2 Laser Scattering Particle Size Distribution Analyzer. All samples were tested as received without any sample preparation.

2.2.3 Brunauer–Emmett–Teller (BET) Surface Area

Although surface area can be calculated from particle size after some assumptions, these calculations do not work well for porous materials like pumice and zeolites which have a high internal surface area. As such the BET surface area of all the natural pozzolans were measured using an ASAP 2020 Micromeritics Surface Analyzer with nitrogen gas. The surface area of the fly ash and quartz filler was also tested along with the natural pozzolans. Before testing, all samples were dried in a vacuum desiccator and then heated to 300°C in the degas chamber of the BET machine, to drive off any volatile materials that were adsorbed onto the sample surface.

2.2.4 Scanning Electron Microscope (SEM) Imaging

To get an understanding of the particle shape and surface texture, SEM imaging was conducted on selected pozzolans. Imaging was conducted in high vacuum using the

FEI Quanta 650 SEM. Before the test, the samples were mounted on a holder using carbon tape. The test specimens were gold-coated to prevent charging of the pozzolan samples.

2.2.5 X-ray Diffraction (XRD)

XRD is a compositional characterization test that complements the XRF oxide composition results, as the XRD results can differentiate whether the oxides are present in amorphous or crystalline phases. The XRD tests on the natural pozzolans were carried out using a Siemens D-500 X-ray Diffractometer with Cu-Kα radiation. The range of 2θ measured was 5-70°, and a dwell time of 4 seconds was used. To ensure adequate packing, all the pozzolan samples were ground to pass through the No. 325 sieve (with a 45 μm opening).

2.2.6 Thermal Gravimetric Analysis/ Differential Scanning Calorimeter (TGA/DSC)

Results from TGA and DSC can also be used to get an insight on the phases present in a material. TGA and DSC were conducted on the pozzolans using a Mettler Thermogravimetric Analyzer, Model TGA/DSC 1. The pozzolan samples were crushed and sieved through a number No. 325 sieve (45 μm opening) prior to being tested. The weight loss of each sample was recorded as it was heated from 40°C to 1000°C, at a rate of 20°C/min. The measured weight loss was used to plot the TGA curve. The heat flow during this interval was recorded as well and was used to plot the DSC curve. The weight loss and the heat flow can both give an indication of phase decomposition which can be used to describe the original phase composition of the natural pozzolan, especially when other characterization data like XRD is available for comparison purposes. During the

test, the chamber gas used was nitrogen and each pozzolan sample was contained in an alumina crucible.

2.3 Performance Evaluation Methods

The performance of the eight natural pozzolans, being tested as Class F fly ash replacements in this research, was evaluated in terms of their effect on compressive strength, durability and mixture workability. The tests methods used to evaluate these performance aspects of the natural pozzolans are detailed in this section. In some cases, additional testing was performed to gain further insight into the performance results. Table 2.3 provides a list of all the performance tests that were conducted. Mixtures containing Class F fly ash was evaluated in all these tests for comparison purposes. Since Pumice-N, Pumice-S and the quartz filler was presented in this research to illustrate ways of improving mixture strength, these materials were also evaluated in tests related to compressive strength.

Table 2.3: Performance Tests Conducted

Category	Performance	Found Using
Strength	Compressive Strength	ASTM C 109
	Heat of Hydration	Isothermal Calorimeter
	$Ca(OH)_2$ Content	TGA/DSC
Mixture Workability	Viscosity and Yield Stress	Rheometer
Durability	Resistance to ASR	ASTM C 1567
	Resistance to Sulfate Attack	ASTM C 1012

2.3.1 Compressive Strength

Compressive strength of a cementitious mixture is one of the most important measures of performance. Since previous literature has found pozzolans to decrease compressive strength (Lilkov et al., 2011; Erdem et al., 2007; Hossain, 2003; Campbell et al., 1982), additional tests like isothermal calorimetry and TGA were performed to better understand the underlying mechanisms of how pozzolans affect the compressive strength of cementitious mixtures.

2.3.1.1 Compressive Strength

Although the SAI test from ASTM C 618 (2012) measures compressive strength, it does so, on the basis of constant flow instead of constant water to cementitious material ratio (w/cm). As such, the results are often unfavorable for mixtures incorporating SCMs with high water demands, like zeolites. To remedy this, compressive strength tests were carried out on pozzolan-containing mortar cubes with a constant w/cm. Other than the fixed w/cm, the cubes were made according to the instructions in ASTM C 109 (2011). The w/cm for the zeolite mixtures was fixed at 0.55, due to their high water demand. The w/cm of the other mixtures, containing unaltered volcanic and sedimentary pozzolans, was fixed at 0.5. For each w/cm, a control mixture (with no SCMs) and a mixture containing fly ash was also made. The SCM replacement dosage used for all the natural pozzolan and fly ash mortars was 20% by weight of cement, as specified in ASTM C 109 (2011).

Additionally, the SAI tests only measure compressive strength at 7 and 28 days. To get a better indication of early age as well as long term strength, the compressive strength of the fixed w/cm mortar mixtures was tested at 1, 3, 7, 28, 90 and 365 days. The average compressive strength was calculated using three mortar cube specimens from

two separate batches that were made consecutively, on the same day. In certain cases, if the range of the compressive strength data from the three mortar cubes was greater than 8.7% of the average, the result that deviates most from the average was discarded, as instructed by ASTM C 109 (2011). The average was then calculated from two mortar specimens instead of three and the final range of the two samples was checked to see it was less than or equal to 7.6% of the average, as required by ASTM C 109 (2011). The results section reports if the 7.6% range was exceeded when the average compressive strength was calculated from two mortar cubes.

2.3.1.2 Isothermal Calorimetry

Isothermal calorimetry was performed with the compressive strength tests to see if the decreased strength of pozzolan mixtures seen in previous literature (Lilkov et al., 2011; Erdem et al., 2007; Hossain, 2003; Campbell et al., 1982) was a result of retardation in cement hydration caused by the addition of pozzolans. The data from the isothermal calorimetry tests, which measure the heat from ongoing hydration reactions of cementitious pastes, can be used to plot heat of hydration curves. Comparing the hydration curves of the pozzolan mixtures to that of the control mixture or the inert quartz mixture can give valuable information on whether the addition of the SCMs accelerates or retards the hydration process of cement.

The control paste mixture was made with 50 g of cement and 22.5 g of water, giving the paste a w/cm of 0.45. For the SCM paste mixtures, 20% of the cement by mass was replaced with the SCM being tested. The water content was kept the same as the control mixture, giving the pozzolan-containing paste a w/cm of 0.45 as well. Prior to each test, the pastes were mixed by hand for 2 minutes. Approximately 10 g of paste was

added to the calorimetry vials after mixing and the heat evolution from hydration was measured at 23°C for 72 hours using a Thermometric TAM Air Isothermal Calorimeter.

2.3.1.3 Thermal Gravimetric Analysis/Differential Scanning Calorimeter (TGA/DSC)

While isothermal calorimetry is a good characterization test to understand the early age effect of pozzolans on cement hydration, it does not provide any information on pozzolanic reactions that typically occur at a later stage. Since a pozzolanic reaction involves the conversion of calcium hydroxide into calcium silicate hydrate (C-S-H), an easy way to track the progress of a pozzolanic reaction is to monitor the decrease of calcium hydroxide in a cementitious mixture over time, using thermal gravimetric analysis (TGA) and differential scanning calorimeter (DSC).

For the thermal gravimetry tests, the paste designs were identical to those used for isothermal calorimetry. After mixing the pastes by hand for 2 minutes, they were cured at room temperature and 100% relative humidity, until they reached the desired test age, which was 7, 28 and 90 days for the current study. After curing, the samples were weighed and then broken into small chunks (approximately less than 10 mm in length) that were stored in a vacuum desiccator for 14 ± 1 days. The samples were reweighed after being removed from the desiccator at 14 days, and the change in weight was recorded as the amount of water lost on drying. The samples were then crushed and sieved through a No. 325 sieve (45 μm opening) to ensure uniformity during testing. The sieved samples were stored under vacuum in a desiccator until they were tested on a Mettler Thermogravimetric Analyzer, Model TGA/DSC 1. During the test, the chamber gas used was nitrogen and the samples were contained in alumina crucibles with lids. The weight losses of the samples were recorded as they were heated from 40°C to 1000°C, at

a rate of 20°C/min. The measured weight loss was used to plot the TGA curve. The heat flow during this interval was recorded as well and was used to plot the DSC curves. Figure 2.2 shows a representative TGA/DSC plot. The DSC curve was used to pinpoint the exact temperatures between which the calcium hydroxide in the paste decomposed (labeled points A and B in Figure 2.2). Using those temperatures, the weight loss due to calcium hydroxide decomposition was calculated from the TGA curve. Finally using molecular weights and the recorded weight change from water loss in the desiccator, the weight loss from calcium hydroxide decomposition was converted to the calcium hydroxide content per gram of cement in the initial paste.

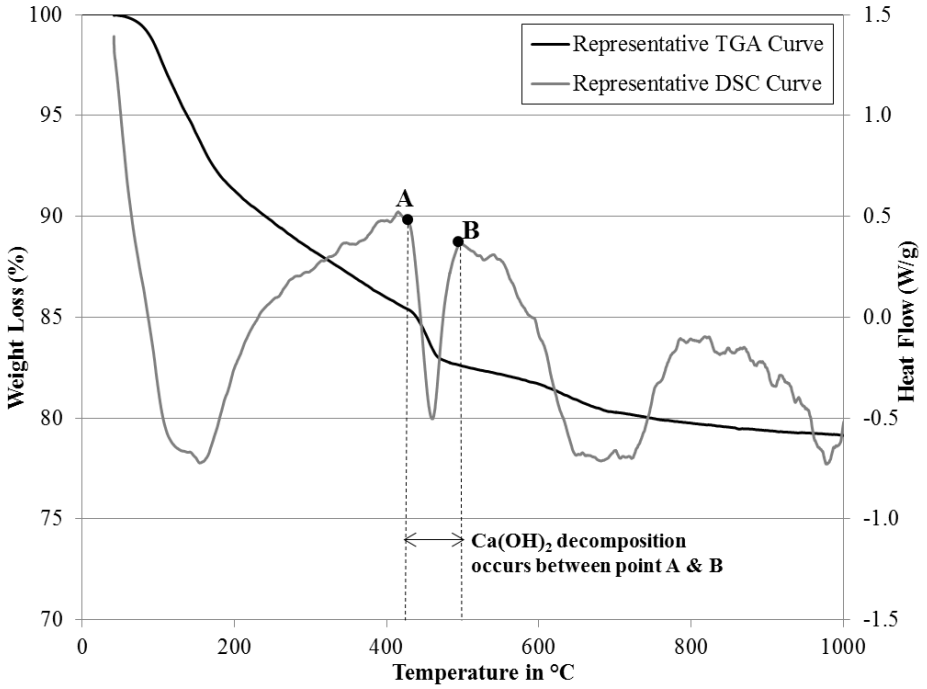

Figure 2.2: Representative TGA and DSC curve to illustrate $Ca(OH)_2$ content calculation

2.3.2 Mixture Workability

Workability, a property which is often overlooked in literature, is defined to be "the ease and homogeneity with which concrete can be mixed, placed, consolidated and finished" (ACI 116.R, 1990) in its fresh state. Workability is a very important measure of performance, since the fresh state properties of concrete ultimately affects its hardened state properties as well (Mindess et al., 2002). For example, mixtures with poor workability may leave voids in the formwork (known as honeycomb), be improperly compacted, exhibit segregation or excessive bleeding, all of which can affect the long term strength and durability of concrete (Mindess et al., 2002). Typically, the level of workability required for a concrete mixture depends on the application. Since the research presented here does not focus on one particular application, the level of workability desired for the pozzolan pastes in this research were the same as that of the control mixture without any pozzolans.

The water requirement test of ASTM C 618 (2012) provides a simplistic assessment of a pozzolan's effect on mixture workability. However, it cannot measure the actual rheological properties of the mixture, like yield stress and viscosity. The viscosity of a material can be defined as a measurement of the material's internal resistance to flow. More specifically, viscosity refers to the amount of shear stress that is needed to increase the shear rate or the velocity gradient of the fluid flow cross-section by one unit (Mindess et al., 2002). On the other hand, the yield stress of the material is the shear stress that must be exceeded before the material can start to flow (Mechtcherine et al., 2014). Having a thorough scientific understanding of these properties is crucial when trying to optimize fresh state properties of concrete mixtures or finding ways to mitigate the high water demand of materials like zeolites. As such, in this research, mixture workability was evaluated using an MCR 301 Anton Paar rotational rheometer than can

measure the rheological properties of cementitious pastes. A cup and bob measuring system geometry was used, with a 1.0 mm gap between the bottom of the cup and the bob. Similar to the mixture design for isothermal calorimetry and TGA, the control paste (with no SCMs) was made with 50 g of cement and 22.5 g of water, giving the paste a w/cm of 0.45. For the pozzolan pastes, 20% of the cement by mass was replaced with the pozzolan being tested. The water content was kept the same as the control mixture, giving the pozzolan pastes a w/cm of 0.45 as well. The pastes were mixed mechanically for 2 minutes using a Caframo Compact Digital BDC 2002 overhead stirrer at 1000 rpm. Approximately 19 mL of the mixed sample was added to the cup for rheological testing. Prior to each test, the pastes were pre-sheared for 4 minutes at a shear rate of 50 s^{-1}. This was done to reduce the effects of shear history on the samples and to ensure a similar starting point across all tests. After pre-shearing, the samples were allowed to rest for 30 seconds. Then, the shear rate was gradually increased from 10 s^{-1} to 50 s^{-1} and then brought back down to 10 s^{-1}. Both the increase and decrease in shear rate were done in increments of 10 s^{-1}. Furthermore, the shear rate was held constant for 3 minutes after each increment to ensure that an equilibrium state had been reached. Ten data points were used in each equilibrium range to determine the average shear stress of the paste at each shear rate. The shear stress and the shear rate obtained from the test are then used to graph a rheological flow curve, from which the viscosity and yield stress of the mixture can be determined by fitting different models. The total time for the rheology test (including the time to pre-shear) was 31.5 minutes. For each type of paste, the entire test was repeated at least two times.

In the current study, cementitious mixtures that showed a linear trend in their flow curves were analyzed using the Bingham model, a popular method to describe the rheological behavior of cementitious mixtures (Mechtcherine et al., 2014; Roussel et al.,

2007). Using a linear trend line to fit the flow curve data, the Bingham model defines the slope of the linear trend line to be the viscosity, and the y-axis intercept to be the yield stress (Mindess et al., 2002). For mixtures that showed a non-linear trend in their flow curves, instead of using the Bingham model, the average apparent viscosity of the mixture was calculated from ten data points measured in equilibrium range of each shear rate. Apparent viscosity is defined to be "the quotient of shear stress divided by rate of shear when this quotient is dependent on the rate of shear" (Tattersall and Banfill, 1983). In other words, unlike the Bingham viscosity, which is independent of the shear rate applied to the mixture, apparent viscosity refers to the viscosity (or the ratio of shear stress to shear rate) of a mixture at a particular shear rate. Finally, it must be noted that all the rheological analysis was based on the region of the flow curve where the shear rate was being gradually decreased from 50 s^{-1} to 10 s^{-1}, as the data is considered to be more stable when the shear rate is being decreased, rather than when it is increased.

2.3.3 Durability

Degradation of concrete from ASR is a common durability problem that occurs from the use of reactive aggregates that form expansive silica gel in the highly alkaline environment of concrete. Cracking of concrete from sulfate attack is a concern in marine environments and in areas where the concrete is in contact with soils that have a high concentration of sulfate ions. Class F fly ash has been shown in previous literature to mitigate expansions from both ASR and sulfate attack (Dhole et al., 2013; Thomas, 2011; Shehata and Thomas, 2000). As such, the natural pozzolans in this study were tested for resistance against ASR and sulfate attack, to assess their suitability as Class F fly ash replacements in concrete.

2.3.3.1 Alkali Silica Reaction (ASR)

The accelerated mortar bar test method, from ASTM C 1567 (2013), was used to evaluate the ability of the natural pozzolans to control expansion from ASR. As described in the standard, the mortar mixtures contained 2.25 parts of the reactive fine aggregate to 1 part of cementitious material (cement + SCM) by weight. The dimensions of the mortar bars were 25.4 mm x 25.4 mm x 285.75 mm (1 in. x 1 in. x 11 ¼ in.). The steel gage studs at each end of the mortar bar made the gage length to be 254 mm (10 in.). The standard requires the mortar mixes to have a constant w/cm of 0.47 and a measured flow that is ±7.5% of the control mortar, with no SCMs. To meet the required flow, a polycarboxylate-based ASTM C 494 (2013) Type F WRA distributed by Sika Corporation under the trade name Sika ViscoCrete 2100 was used in the mortar mixtures. The admixture dosages for these mortar mixtures are shown in Appendix A. It must be noted that some of the ASR mortar mixtures required more than the recommended dose of this polycarboxylate WRA.

After mixing and verifying that the consistency was acceptable, the mortar was placed and compacted into molds. After 24 hour curing at 23 °C and 100% relative humidity, the mortar bars were removed from the molds and their lengths were measured using a comparator (initial reading). After this, the bars were submerged in room temperature water, and placed in a sealed container in an oven set to 80°C. After 24 hours in the oven, the mortar bars were taken out of the water and measured again using the comparator (zero reading). They were then submerged in a 1 N sodium hydroxide (NaOH) solution (that had already been heated to 80°C) and placed back in the oven. Additional length readings were taken at 3, 7, 11, and 14 days after submersion in the NaOH solution. Expansion was calculated by determining the length change of the mortar bars expressed as a percentage of the gage length.

ASTM C 1567 (2013) states that if expansion of the mortar bars after 14 days of submersion in NaOH solution is less than 0.10% then the mixture has "a low risk of deleterious expansion when used in concrete under field conditions." The initial SCM replacement dosage for the ASTM C 1567 (2013) mortar bars was 20% by mass of cement. Depending upon the results of the test, the SCM percentage was increased or decreased, to find the minimum SCM replacement dosage at which expansions were kept below the 0.1% limit of ASTM C 1567 (2013).

2.3.3.2 Sulfate Attack

The ability of the natural pozzolans to resist sulfate attack was tested using ASTM C 1012 (2013), which measures the length change of mortar bars submerged in a 5% sodium sulfate (Na_2SO_4) solution. Two different sets of sulfate mixtures were prepared. For the first set, the w/cm of the control mortar (with no SCMs) was 0.485. As specified by the standard, the water content for the SCM mortar mixtures was such that the mortar flow measured by ASTM C 1437 (2007) was within ± 5% of the control mortar. However, it was seen that the zeolite mortar mixtures were requiring very high w/cm to meet the flow requirements. Therefore, a second set of mortar mixtures was prepared for the zeolites, where the w/cm was kept constant at 0.51 for all mixtures. A napthalene-based ASTM C 494 (2013) Type F WRA distributed by Sika Corporation under the trade name Sikament N was used for the constant w/cm mortar mixtures to achieve the required flow. A naphthalene based admixture was chosen since the polycarboxylate admixture was shown to not be as effective for the zeolites in the ASR tests (described in Section 2.3.3.1).

As specified by this method, the mortar mixture contained 2.75 parts standard graded sand to 1 part cementitious material (cement + SCM). Six mortar bars with dimensions of 25 mm x 25 mm x 285 mm (1 in. x 1 in. x 11 ¼ in.) and six mortar cubes with sides of 50 mm (2 in.) were made from each mortar mixture. After mixing, the filled mortar bar molds and cube molds were sealed and submerged in a water bath set to 38 °C to accelerate curing. After 24 hours, the molds were taken out of the water bath, and the specimens were removed from the molds. After removal from the molds, the compressive strength of two mortar cubes was tested. If the compressive strength was less than 20 MPa (2850 psi), the mortar bars were placed in saturated lime water with the remaining mortar cubes until the average compressive strength of two mortar cubes reached 20 MPa (2850 psi). When the average compressive strength of the cubes reached this value, the length of the mortar bars were measured using a comparator. They were then submerged in a 5% Na_2SO_4 solution at room temperature. Subsequent length measurements of the mortar bars were taken at 1, 2, 3, 4, 8, 13, 15, 16, 24, 36, 48, 60 and 72 weeks.

ASTM C 1012 (2013) lists a maximum permissible range that the length change data must not exceed depending upon the number of samples. Due to the variable nature of the test, the range of data for a few samples with high sulfate expansions was found to be higher than the tolerance listed under the “Report” section of ASTM C 1012 (2013). Although not explicitly stated (as is the case for ASTM C 109, 2011), the language of the standard implies that bars that have expansions outside the tolerance limit of the data should be treated as outliers. Therefore in this study, the bar that deviated the most from the average out of the 6 bars was discarded and the value of the range was checked to see if it met the listed tolerance of ASTM C 1012 (2013). If the range was still higher, then the bar with the second highest deviation from the average was also discarded and the range was checked again to ensure it was within the ASTM C 1012 tolerance. It must be

noted that no more than 2 bars were removed for any mixtures testing sulfate resistance in this study. Therefore, each of the average expansions was always calculated from 4 or more bars. ASTM C 1012 (2013) requires a minimum of 3 bars for calculating the average expansion.

Finally, instead of using the standard replacement dosage of 20%, the sulfate mortar mixtures used the minimum SCM replacement dosages that were found to keep ASR expansions in the ASTM C 1567 (2013) test below the 0.1% limit after 14 days of submersion in NaOH solution. The rationale in doing so was to try and find the minimum SCM dosage that would mitigate expansion from both ASR and sulfate. However, the natural pozzolans that needed replacement dosages of less than 20% to mitigate ASR expansion were tested at two different dosages in the ASTM C 1012 (2013) sulfate test. Since sulfate attack is considered more damaging than ASR, and because the ASTM C 1012 (2013) test runs for a much longer time than the ASTM C 1567 (2013) ASR test, it was considered prudent to test two dosages for the natural pozzolans that needed a low replacement dosage to mitigate ASR. Additionally, it must be noted here, that the reason why SCM replacement dosages were tried to be minimized instead of maximized is because the price of all the natural pozzolans (except Shale-T) were similar to or above that of cement.

2.4 Performance Improvement Methods - Calcination

For the research presented in Chapter 6, three zeolites were calcined to see whether calcination mitigated their high water demand. The zeolites were calcined at a temperature of 800°C. 50g of the zeolite was placed in the oven and the temperature was steadily increased from room temperature to 800°C for 160 minutes (approximate rate of

5°C/min). Once the oven temperature reached 800°C, the temperature was kept constant for 5 hours. After five hours, the temperature was steadily reduced back down to room temperature over 160 minutes.

Chapter 3: Material Characterization Results

This chapter presents the results of the characterization tests conducted on the eight natural pozzolans that were evaluated as Class F fly ash replacements. The characterization results of Pumice-N and Pumice-S, which are relevant to the research presented in Chapter 5, are also described in this chapter. Finally, this chapter also provides the results of the characterization tests done on the cement, fly ash and quartz. Section 3.1 describes the results from the ASTM C 618 (2012) characterization tests. Sections 3.2 - 3.6 describes the results of the more advanced characterization tests, like laser particle size analysis, BET surface area measurements, SEM imaging, XRD and TGA/DSC, which were used to supplement the information found from the ASTM C 618 (2012) characterization tests.

3.1 ASTM C 618 Characterization Results

Five out of the eight materials that were tested as Class F fly ash replacements fulfilled all the requirements of ASTM C 618 (2012) for Class N pozzolans. The materials that qualified as Class N pozzolans were Pumice-D, Perlite-I, Vitric Ash-S, Metakaolin-D and Shale-T. The three materials that failed the Class N pozzolan criteria were Zeolite-Z, Zeolite-T and Zeolite-A. The ASTM C 618 (2012) results of Pumice-N and Pumice-S show them to pass all the requirements for a Class N pozzolans. Table 3.1 shows a summary of the ASTM C 618 results. The next sub-sections discuss the ASTM C 618 (2012) results in detail.

3.1.1 Oxide Composition

All the natural pozzolans met the ASTM C 618 (2012) requirement to have a minimum combined SiO_2, Al_2O_3 and Fe_2O_3 composition of 70.0% by mass. All the pozzolans were also below the SO_3 limit of 4% by mass. Table 3.2 shows detailed oxide results from the XRF analysis of the natural pozzolans. Most of the volcanic pozzolans had similar oxide compositions. However, Zeolite-A had a lower SiO_2 content than the rest of the volcanic pozzolans and a higher CaO content. Metakaolin-D, which has a sedimentary origin, had the lowest SiO_2 content but the highest Al_2O_3 content out of all the pozzolans tested. Although Shale-T is a sedimentary pozzolan like Metakaolin-D, its oxide composition was similar to that of the volcanic pozzolans, except for its Fe_2O_3 content, which was higher than all the other sedimentary and volcanic pozzolans tested in this research.

Table 3.3 shows the XRF results of the fly ash and cement. The sum of the combined SiO_2, Al_2O_3 and Fe_2O_3 has to be a minimum of 70% for Class F fly ash (ASTM C 618, 2012). The XRF results show the sum of SiO_2, Al_2O_3 and Fe_2O_3 to be almost 80% for the fly ash used in this research.

3.1.2 Moisture Content and Loss on Ignition (LOI)

Other than the three zeolites, all the natural pozzolans passed the moisture content requirements. Although Zeolite-Z and Zeolite-A failed the moisture content requirement, their values were only about 2% higher than the maximum limit set by ASTM C 618 (2012). However, the moisture content of Zeolite-T was about 8% higher than the limit. The high moisture content value of Zeolite-T indicated that the material had a high absorption capacity, which further suggested that the use of Zeolite-T in concrete could result in very stiff mixtures due to the mixture water being absorbed into the zeolite. In

terms of LOI, all the natural pozzolans had values less than the maximum limit prescribed by ASTM C 618 (2012).

3.1.3 Fineness

Other than Zeolite-T and Zeolite-A, all materials passed the fineness requirements for Class N pozzolan. This was not surprising as these two zeolites appeared to be coarse from a visual inspection. The coarseness of these two zeolites could reduce the available surface area where pozzolanic reactions can occur, which in turn could lead to a lower reactivity of the SCM in concrete. Although Shale-T passed the fineness test, it had a higher retention percentage compared to the other pozzolans that passed the fineness test. This is most likely due to the fact that Shale-T was crushed in the research laboratory where the experiments for this dissertation was undertaken, instead of being ground down in a commercial facility like the other materials.

3.1.4 Density

The average densities of the natural pozzolans, fly ash and quartz are presented in Table 3.4. All the natural pozzolans were seen to have densities between 2.30 and 2.75 g/cm^3. This indicates that the natural pozzolans were less dense than cement, which is typically assumed to have a density of 3.15 g/cm^3 (Lamond and Pielert, 2006). This is not surprising considering that a lot of the volcanic pozzolans like pumice and zeolites are porous. The density test for Zeolite-Z was not able to be performed correctly due to the airy nature of the powder. As such, the density of Zeolite-Z was assumed to be similar to that of the other two zeolites. The densities of the fly ash and quartz were found to be

2.34 g/ cm^3 and 2.76 g/cm^3, respectively, making these materials less dense than cement, as well.

3.1.5 Soundness

All the mixtures with natural pozzolans had autoclave expansions that were well below the ASTM C 618 (2012) limit.

3.1.6 Strength Activity Index (SAI)

Other than Zeolite-T and Zeolite-A, all materials passed the SAI requirements of having at least 75% of the control compressive strength at 7 or 28 days. It should be noted that Vitric Ash-S, Shale-T and Zeolite-Z had SAI values lower than 75% at 7 days. However, overall they passed the SAI requirements, since by 28 days their SAI values were above 75%. As predicted from the fineness test results, the two coarser zeolites, Zeolite-T and Zeolite-A, had lower reactivities than the finer materials. Similarly, it was not surprising that Vitric Ash-S and Shale-T, which had a higher material retention than the other pozzolans in the fineness test, could not meet the minimum SAI requirement at 7 days. However, the 7 day SAI value of Zeolite-Z was unexpected, considering that all of the SCM passed the No. 325 sieve during the fineness test. The low strength was most likely due to the fact that the zeolite mortar cube was made with a much higher w/cm than the control to keep a constant flow for the water requirement test.

3.1.7 Water Requirement

All three zeolites failed the water requirement test, indicating that mixtures incorporating these pozzolans will have a lower workability than that of the control

mixture without any pozzolans. The high water demand of zeolites and their ability to decrease mixture workability, compared to control mixtures with only cement, has also been seen in previous literature (Bilim, 2011; Ahmadi and Shekarchi, 2010; Perraki et al., 2010). Among the zeolites, Zeolite-T had the highest water requirement.

Table 3.1: Summary of ASTM C 618 Results of Natural Pozzolans

Material Name	**Si+ Al+ Fe (%)**	**SO_3 (%)**	**MC (%)**	**LOI (%)**	**F (%)**	**SAI, 7 d (%)**	**SAI, 28 d (%)**	**WR (%)**	**S (%)**	**Class N?**
Pumice-D	83	0.04	1.5	4.4	2	82	93	104	-0.02	Yes
Perlite-I	84	0.05	0.6	3.4	2	86	94	100	-0.02	Yes
Vitric Ash-S	77	0.33	2.3	5.9	15	72	83	102	-0.01	Yes
Metakaolin-D	89	0.06	0.9	1.0	7	94	108	102	-0.05	Yes
Shale-T	86	0.39	0.3	0.4	30	72	81	103	-0.16	Yes
Zeolite-Z	79	0.07	5.1	2.7	0	71	100	116	-0.01	No
Zeolite-T	75	0.14	11.6	4.7	59	47	61	132	0.00	No
Zeolite-A	75	0.29	4.8	4.1	61	60	64	118	0.00	No
Pumice-N	83	0.05	2.2	4.0	0	99	119	107	-0.01	Yes
Pumice-S	82	0.05	0.7	4.4	19	79	83	103	0.02	Yes
Criteria in ASTM C 618	***70% min***	***4% max***	***3% max***	***10% max***	***34% max***	***75% min***	***75% min***	***115 % max***	**± *0.8% max***	

Si+Al+Fe = SiO_2+Al_2O_3+Fe_2O_3; MC = Moisture Content; LOI = Loss on Ignition; F = Fineness (Amount retained on No. 325 sieve); SAI = Strength Activity Index, WR = Water Requirement, S = Soundness

Table 3.2: XRF Oxide Composition Results of Natural Pozzolans

Material Name	SiO_2 (%)	Al_2O_3 (%)	Fe_2O_3 (%)	CaO (%)	MgO (%)	SO_3 (%)	Na_2O (%)	K_2O (%)
Pumice-D	69.42	12.42	1.08	0.94	0.44	0.04	3.81	5.16
Perlite-I	70.26	12.84	1.16	0.86	0.14	0.05	4.70	4.74
Vitric Ash-S	64.72	11.27	0.87	3.31	1.38	0.33	3.65	5.64
Metakaolin-D	51.66	35.23	1.98	0.57	0.45	0.06	0.10	1.42
Shale-T	65.43	14.55	5.72	2.44	2.30	0.39	1.14	2.88
Zeolite-Z	65.29	10.90	2.36	2.52	0.59	0.07	0.52	4.82
Zeolite-T	62.23	11.88	1.12	2.21	0.64	0.14	1.00	1.68
Zeolite-A	59.50	12.93	2.17	5.07	0.82	0.29	3.07	2.58
Pumice-N	68.86	12.69	1.03	0.96	0.45	0.05	3.97	4.91
Pumice-S	68.88	12.24	1.19	1.37	0.33	0.05	5.13	4.41

Table 3.3: XRF Oxide Composition Results of Fly Ash and Cement

Oxide Composition	Fly Ash	Cement
SiO_2 (%)	52.1	19.1
Al_2O_3 (%)	23.1	5.2
Fe_2O_3 (%)	4.0	2.5
CaO (%)	11.6	62.9
MgO (%)	2.1	1.1
SO_3 (%)	0.48	3.2
Na_2O (%)	0.4	0.12
K_2O (%)	0.74	0.91

Table 3.4: Density of Natural Pozzolans, Fly Ash and Quartz

Material Name	Average Density (g/cm^3)
Pumice-D	2.44
Perlite-I	2.44
Vitric Ash-S	2.46
Metakaolin-D	2.75
Shale-T	2.58
Zeolite-Z	---
Zeolite-T	2.29
Zeolite-A	2.46
Pumice-N	2.46
Pumice-S	2.38
Fly Ash	2.34
Quartz	2.76

3.2 PARTICLE SIZE DISTRIBUTION

Figure 3.1 shows the particle size distributions for the eight natural pozzolans, tested as Class F fly ash replacements. The laser particle size analysis showed that, among the eight pozzolans, Zeolite-Z had the smallest median particle size (d_{50}) at approximately 6 μm. Pumice-D, Perlite-I, Metakaolin-D, Vitric Ash-S and Shale-T were in the middle with their d_{50} values ranging from 13 μm to 23 μm. Zeolite-A and Zeolite-T were the coarsest SCMs, with d_{50} values around 180 μm and 280 μm, respectively.

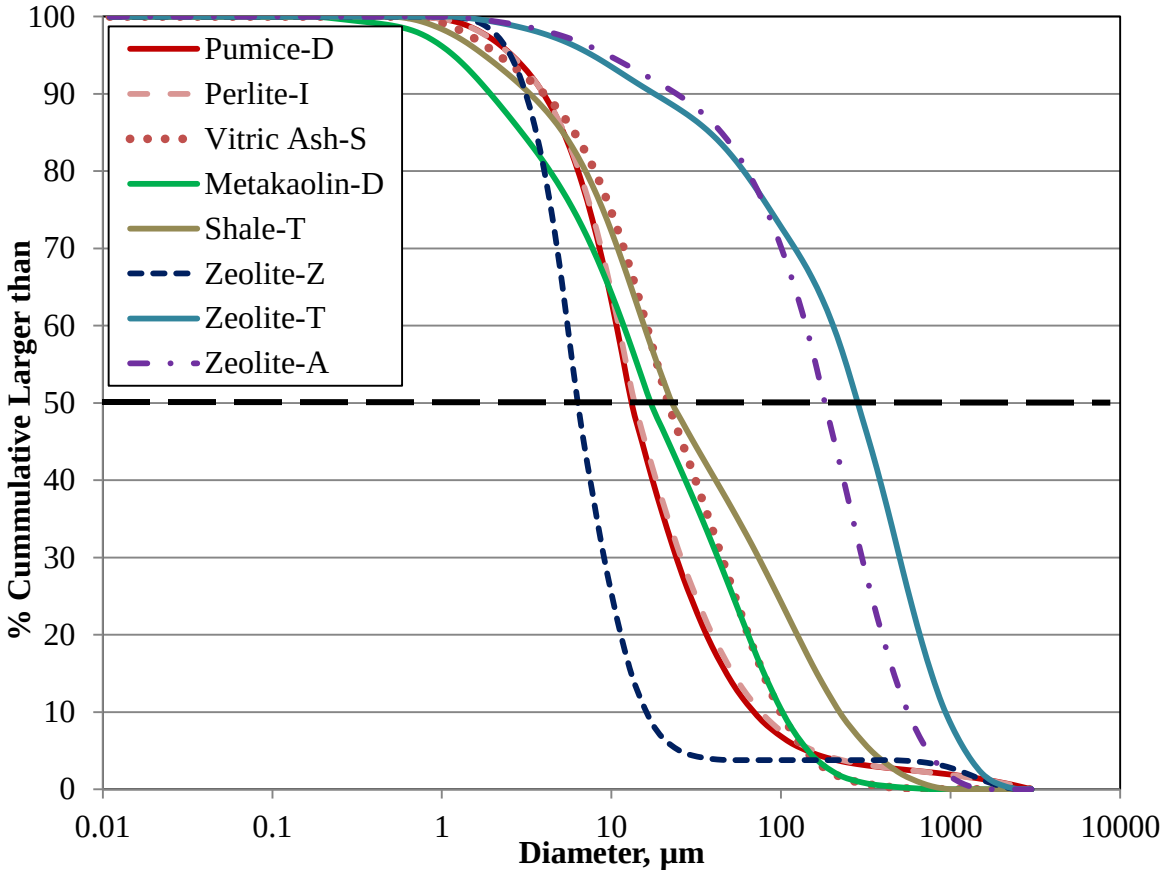

Figure 3.1: Particle size distribution of pozzolans, tested as Class F fly ash replacements

Particle size distributions of the cement, quartz, fly ash and the two additional pumice pozzolans were also evaluated. For purposes of clarity, these particle size distributions are presented in a different plot in Figure 3.2. The particle size distribution of Pumice-D has been added to this plot as well for comparison purposes. The d_{50} value of Pumice-N was approximately 3 µm, making it the finest material out all the materials tested. This is not surprising as Pumice-N is a commercial SCM that was ground by its manufacturers to have a d_{50} value close to 3 µm. The particle size distributions of the cement, quartz, and Pumice-D are similar, with their d_{50} values ranging between 11 µm to 13 µm. Although its d_{50} value is around 12 µm, the particle size distribution of the fly ash

is slightly coarser than that of the cement and quartz. Finally, Pumice-S was observed to have a coarser distribution than Pumice-D, with its d_{50} value being close to 20 µm. This was expected, as Pumice-S was originally a fine aggregate that was ground down in the laboratory.

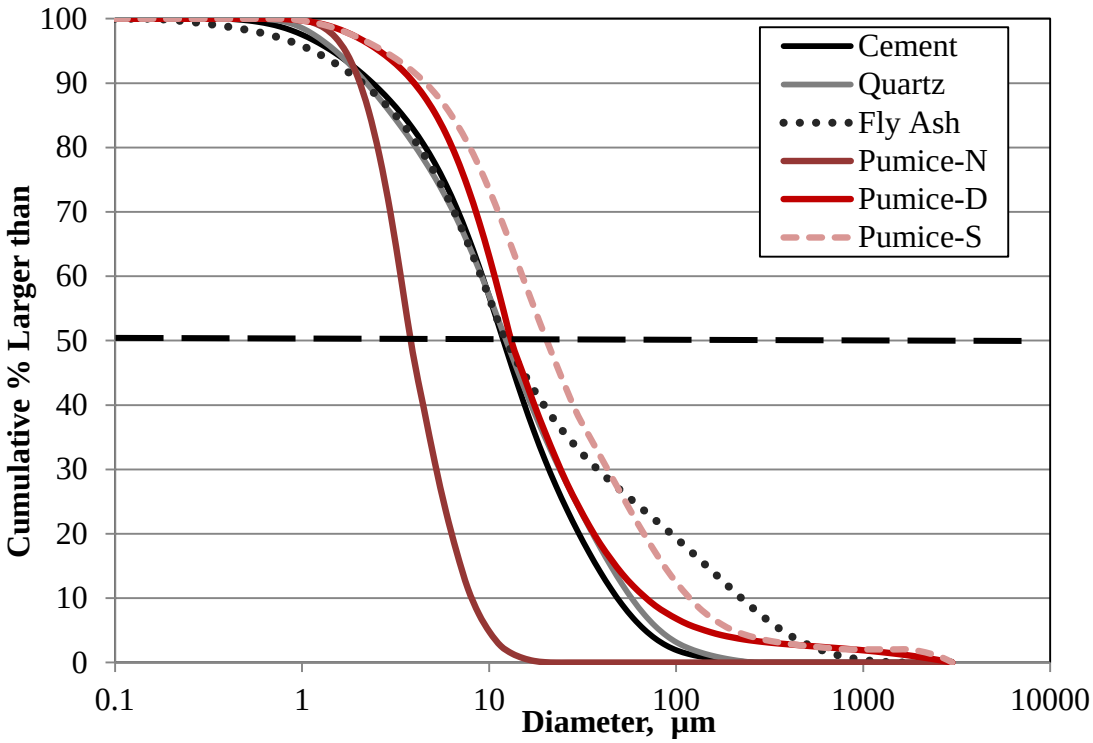

Figure 3.2: Particle size distribution of cement, quartz, fly ash and pumice pozzolans

3.3 BET Surface Area

The BET surface areas of the natural pozzolans, fly ash and quartz are shown in Table 3.5. The zeolites were seen to have larger specific surface areas than all the other materials. With a value approaching 60 m^2/g, Zeolite-T had the highest specific surface area out of all the tested materials, despite having the coarsest particle size distribution, as

shown in Section 3.2. This highlights the importance of measuring surface area for porous materials like zeolites. Among the unaltered volcanic pozzolans, the BET results showed Vitric Ash-S to have the highest surface area with a value of 20 m^2/g. This was unexpected, as the fine pumice pozzolan, Pumice-N, was expected to have the highest surface area among the unaltered volcanic pozzolans, due to its fine particle size distribution. Among the sedimentary pozzolans, Metakaolin-D had the highest surface area with a value approaching 15 m^2/g. Perlite-I, Pumice-S, Shale-T, fly ash and quartz have the lowest surface areas out of all the materials, with values less than 5 m^2/g. Please note that the BET surface area for the quartz shown in Table 3.5 is the result of a single test only, while the other values represent at least duplicate tests with the error representing the range of values measured.

Table 3.5: BET Surface Area Results

Material Name	BET Surface Area (m^2/g)
Pumice-D	7.58 ± 0.12
Perlite-I	3.16 ± 0.27
Vitric Ash-S	20.33 ± 0.10
Metakaolin-D	14.78 ± 0.32
Shale-T	2.51 ± 0.02
Zeolite-Z	42.00 ± 0.57
Zeolite-T	59.01 ± 0.47
Zeolite-A	25.98 ± 0.01
Pumice-N	10.90 ± 0.08
Pumice-S	1.57 ± 0.09
Fly Ash	2.89 ± 0.18
Quartz	1.26

3.4 SEM IMAGE ANALYSIS

SEM images of the pozzolans revealed their particles to be mostly angular, with many variations of texture between particles of a given material. Figures 3.3 – 3.5 show SEM images of the unaltered volcanic pozzolans. The SEM images of Pumice-D and Vitric Ash-S were similar in that they both had particles with smooth and rough textures, interspersed among each other. Due to the apparent similarity in particle texture, the SEM images of Pumice-D and Vitric ash-S did not offer any additional insight as to why Vitric Ash-S had a much higher surface area, despite its particle size distribution being coarser than Pumice-D. Perlite-I, on the other hand, was seen to have comparatively higher proportion of smooth textured particles than rough particles. This is most likely the reason why Perlite-I has a lower surface area compared to Pumice-D, despite having a similar particle size distribution. Increased magnification on the smooth textured particles in Pumice-D and Vitric Ash-S revealed that they were covered with smaller particles with an irregular and rough texture, as is shown in Figures 3.6 and 3.7. Previous literature with SEM images of unground pumice showed them to have a porous, honeycomb-like structure (ACI 232-1R, 2012). Even under high magnification (Figure 3.8), a honeycomb structure was not observed for the pumices in this study, most likely because the pumice particles had been ground finely.

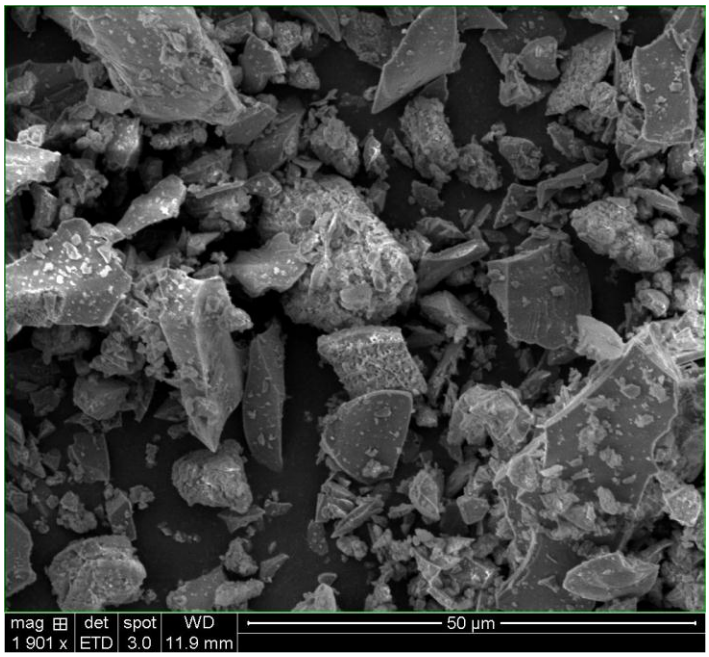

Figure 3.3: Smooth and rough textured particles interspersed in Pumice-D

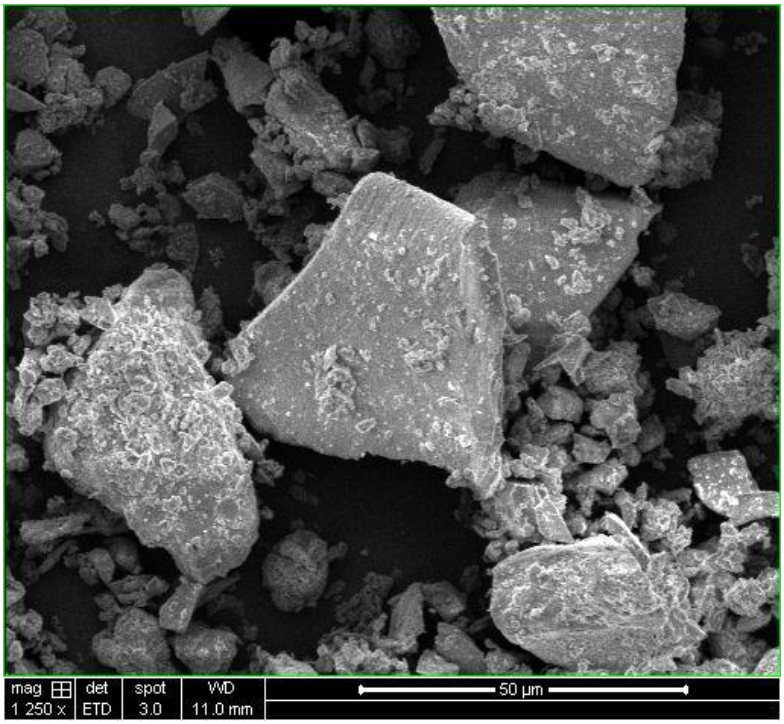

Figure 3.4: Smooth and rough textured particles interspersed in Vitric Ash-S

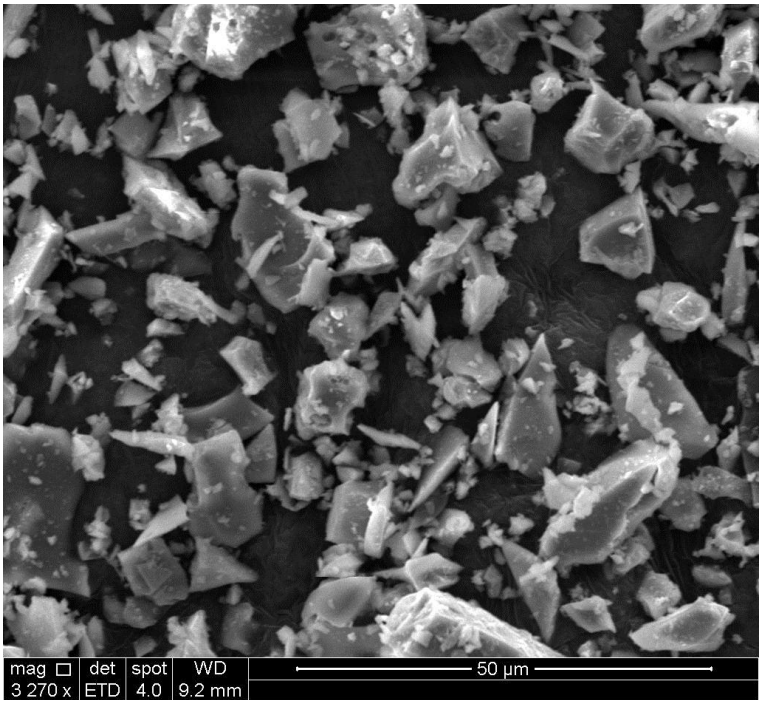

Figure 3.5: Smooth textured particles in Perlite-I

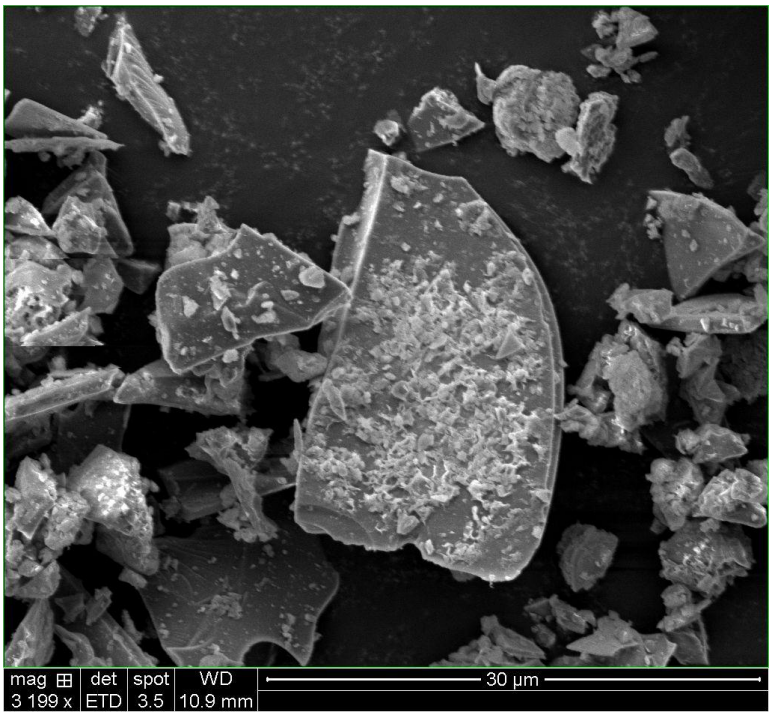

Figure 3.6: Smooth particle covered with smaller, rougher particles in Pumice-D

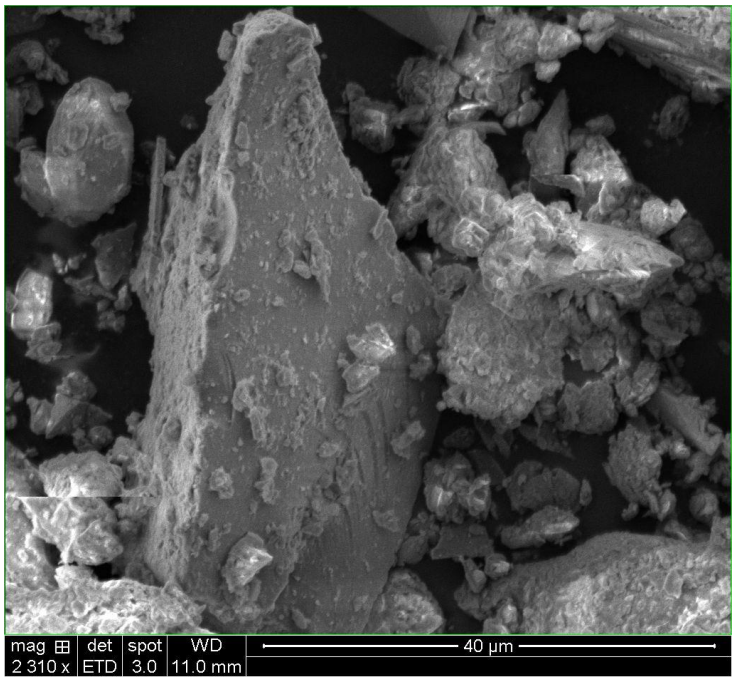

Figure 3.7: Smooth particle covered with smaller, rougher particles in Vitric Ash-S

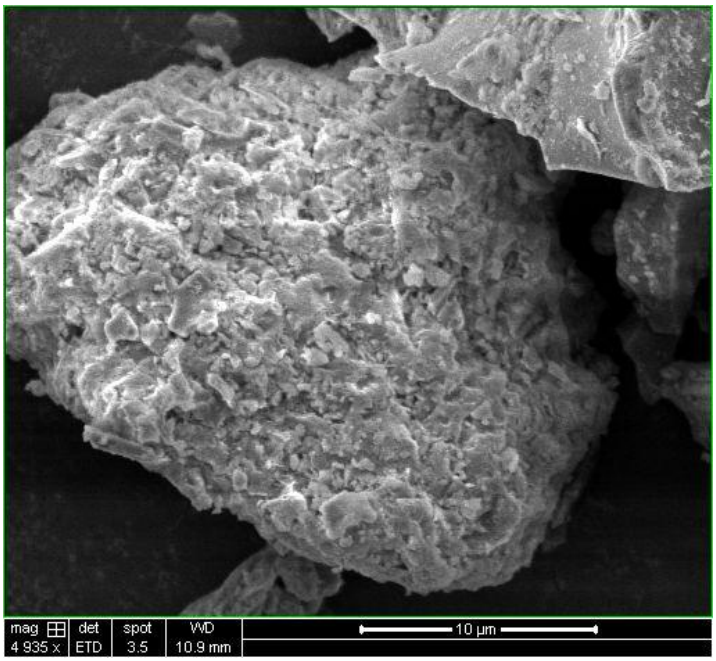

Figure 3.8: Pumice particle under higher magnification

Figures 3.9 – 3.10 show SEM images of Metakaolin-D. There was less variety of surface texture in the SEM images of Metakaolin-D than in the unaltered volcanic pozzolans. Under high magnification, the surfaces of a majority of Metakaolin-D particles seemed uneven and rough. Shale-T, however, had a variety of different particle shapes and textures. Some particles were flat shaped with laminations (Figure 3.11), some had an angular shape with rough pitted surfaces (Fig 3.12), and others had a smooth surface with pores full of smaller particles (Figure 3.13). The smooth walled pores of Shale-T, shown in Figure 3.13, are most likely natural gas vesicles that are remnants of the original material, which the shale was formed from.

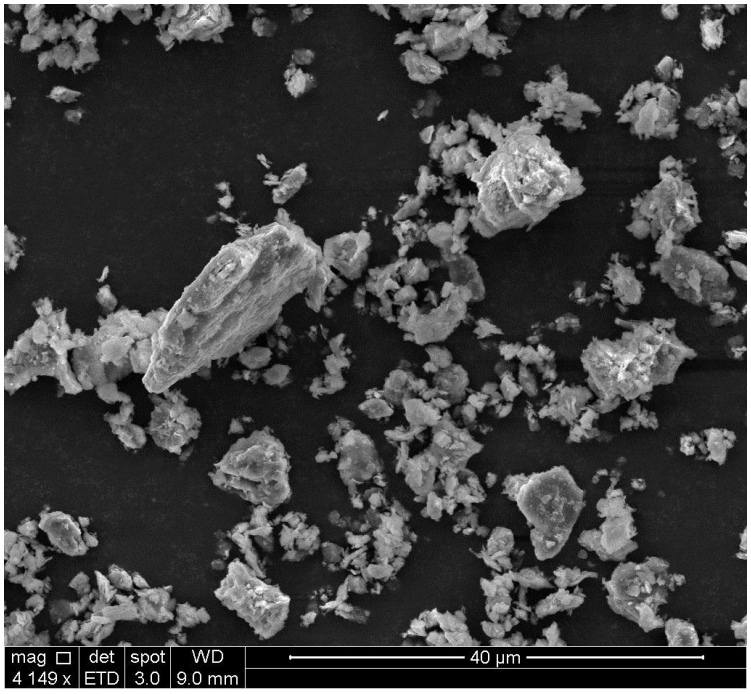

Figure 3.9: SEM image of Metakaolin-D

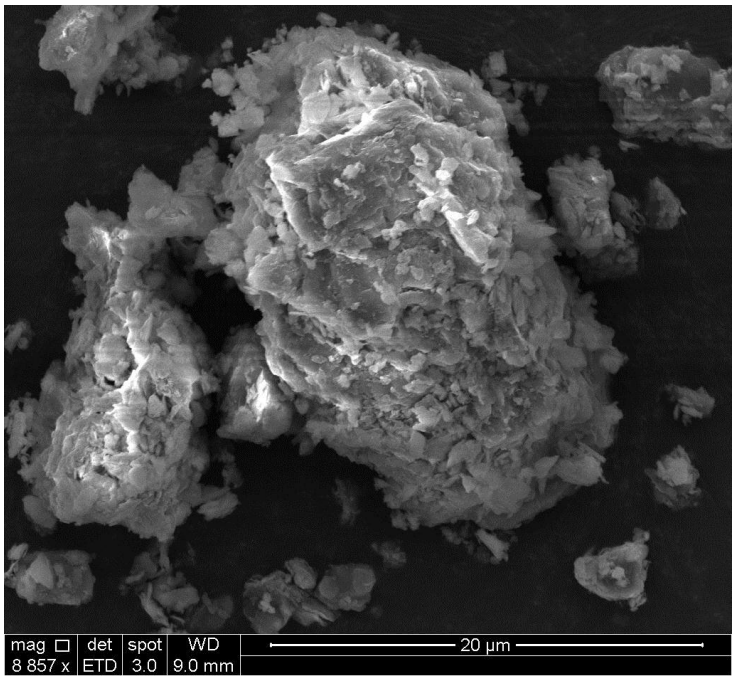

Figure 3.10: Metakaolin-D under high magnification

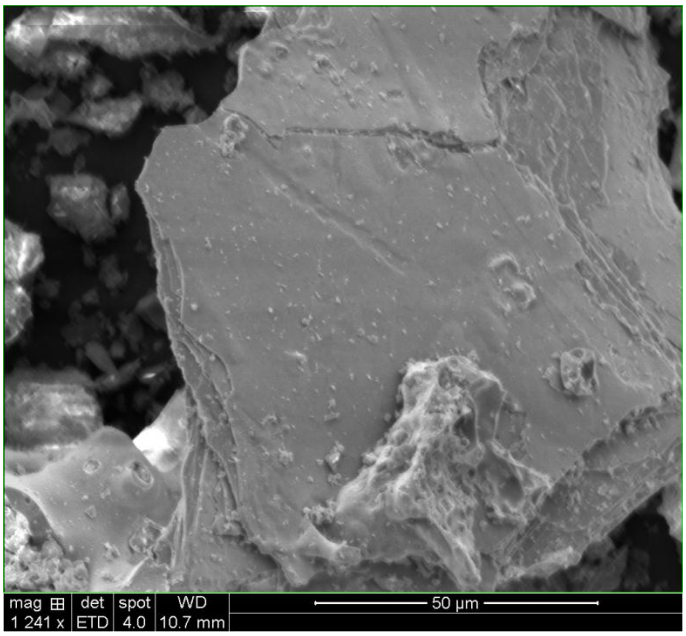

Figure 3.11: Flat particles with laminations observed in Shale-T

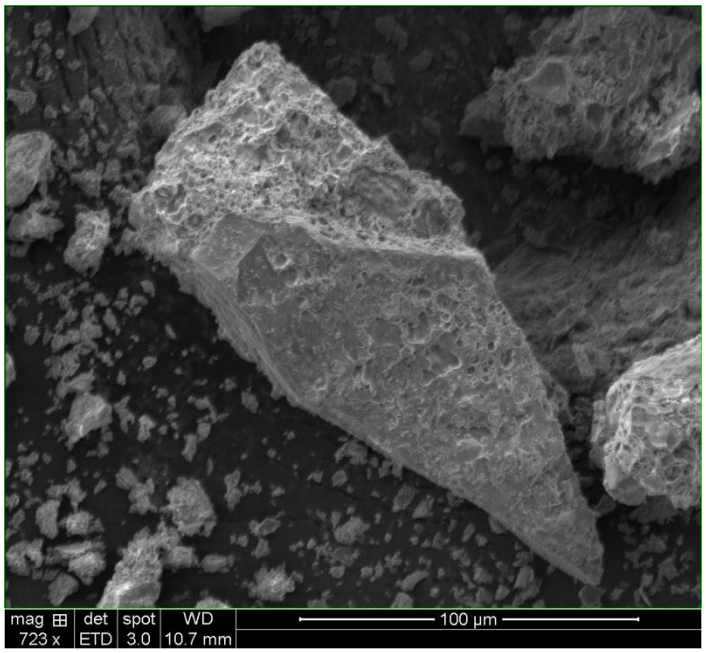

Figure 3.12: Particles with a rough pitted surface observed in Shale-T

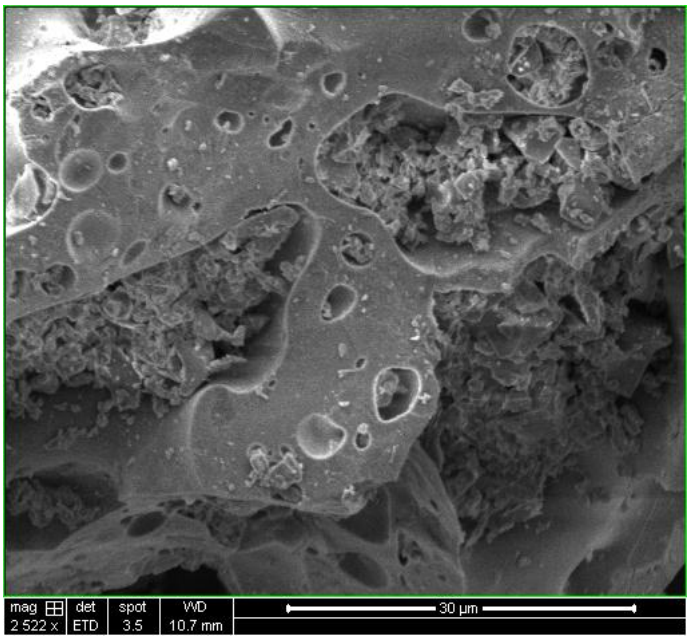

Figure 3.13: Particles with pores observed in Shale-T

Figures 3.14 – 3.16 show SEM images of the three zeolites. Under low magnification, the surface of the Zeolite-T has an intricate mesh-like appearance, which is what gives rise to its high surface area. The surface texture of Zeolite-A was also found to be highly uneven. Since the particle size of Zeolite-Z was smaller compared to the two coarser zeolites, a much higher magnification was needed to study the Zeolite-Z particles. At very high magnification, the Zeolite-Z particles were observed to have a sponge-like structure as shown in Figure 3.16.

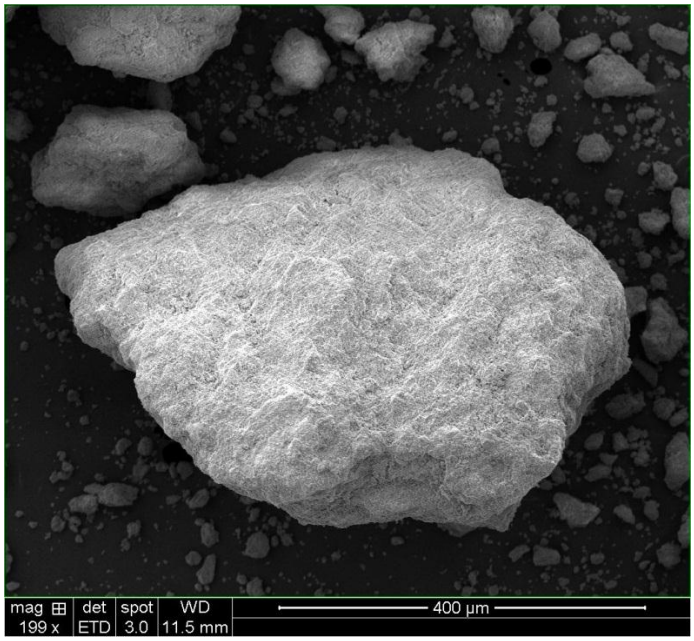

Figure 3.14: Mesh-like texture of Zeolite-T

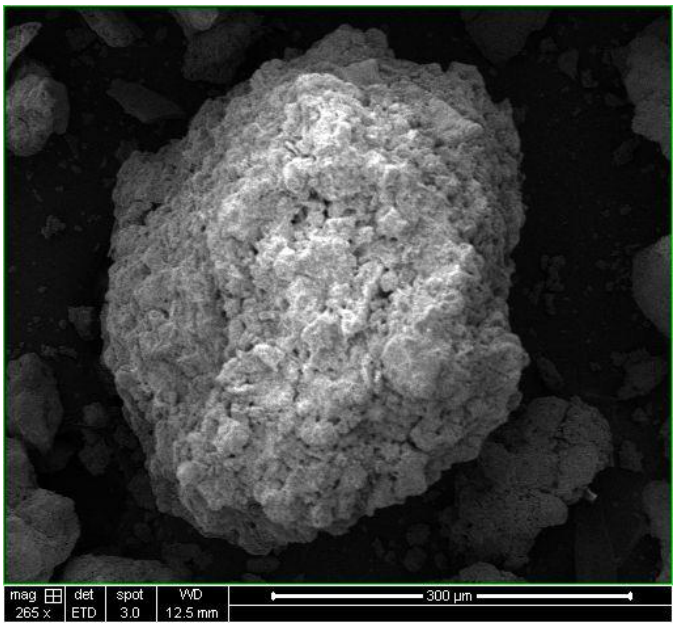

Figure 3.15: SEM image of Zeolite-A

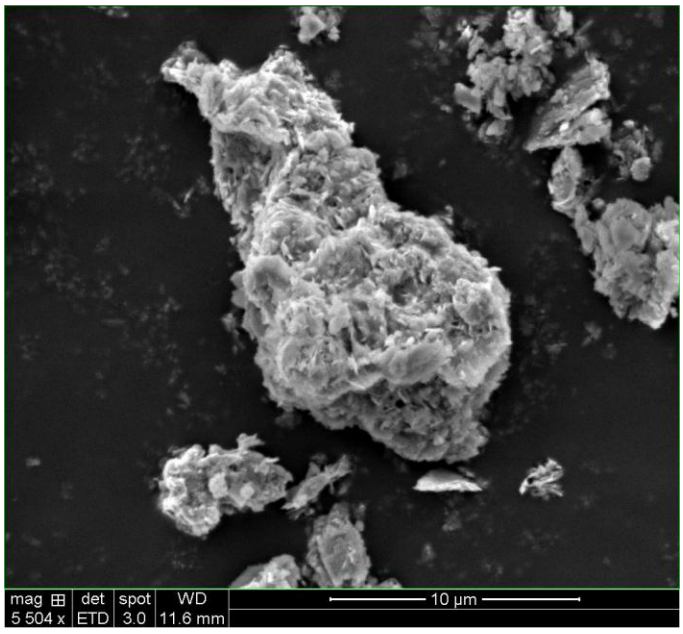

Figure 3.16: SEM image of Zeolite-Z under higher magnification

3.5 XRD ANALYSIS

Table 3.6 contains a summary of the phases found in the natural pozzolans through XRD. The x-ray diffractograms are shown in Appendix B. XRD results show the three pumices and Perlite-I to be mainly amorphous. Vitric Ash-S is also amorphous with a few crystalline impurities such as quartz, calcite and albite. For Metakaolin-D, the x-ray diffractogram did not show any kaolinite peaks, which conforms with previous literature that have observed the XRD peaks of kaolinite to disappear as the clay is calcined to become metakaolin (Fernandez et al., 2011a). However, some muscovite peaks were seen in the XRD images for Metakaolin-D, as well as the peaks for crystalline impurities like quartz, anatase and microcline. Although, shale is formed from the compaction of clay, (Snellings et al., 2012) the XRD plots of Shale-T did not show any peaks from clay minerals. This is not surprising as the clay minerals might have been dehydroxylated when the original shale was calcined. Shale-T also contained crystalline impurities like quartz, albite and microcline. XRD plots of all three zeolites confirmed that they contain clinoptilolite, one of the most common zeolite minerals. Zeolite-Z seemed to be the most purified zeolite out of the three that were tested, as the XRD plots of Zeolite-Z did not show any significant impurities. On the other hand, the XRD plots of Zeolite-T showed some peaks for cristobalite and montmorillonite, along with the clinoptilolite peaks. Presence of the montmorillonite, which can absorb due to the presence of interlayer cations (Fernandez et al., 2011a; Foster, 1954), could be one of the reasons why Zeolite-T showed such a high water demand in the ASTM C 618 (2012) water requirement tests. The XRD plot for Zeolite-A, also showed some impurities, like quartz, calcite and anorthite, along with clinoptilolite.

Table 3.6: Summary of Natural Pozzolan XRD results

SCM	Main Phases in XRD
Pumice-D	Amorphous
Pumice-N	Amorphous
Pumice-S	Amorphous
Perlite-I	Amorphous
Vitric Ash-S	Quartz, Calcite, Albite
Metakaolin-D	Quartz, Anatase, Muscovite, Microcline
Shale-T	Quartz, Albite, Microcline
Zeolite-Z	Clinoptilolite
Zeolite-T	Clinoptilolite, Cristobalite, Montmorillonite
Zeolite-A	Clinoptilolite, Quartz, Calcite, Anorthite

3.6 TGA/DSC ANALYSIS

Table 3.7 gives a summary of the TGA mass loss for the pozzolans. The TGA/DSC plots can be found in Appendix B. The DSC results for Pumice-D, Pumice-N and Perlite-I did not show any major phase changes after the initial dehydration below 200°C. Although the DSC curve for Pumice-S is similar to the other two pumices, it shows a small endothermic peak between 600-700°C. This could be from the decomposition of minor impurities. However, since the XRD plot of Pumice-S was highly amorphous, it was difficult to conclusively pinpoint any minor impurities in the results. Overall, the three pumices and Perlite-I lost about 3-5% of their total mass when heated to 1000°C. The DSC data for Vitric Ash-S also show dehydration below 200°C. Unlike the other unaltered volcanic pozzolans, the DSC plot of Vitric Ash-S has two distinctive endothermic peaks between 650-850°C, which correspond to the decomposition of the impurities detected through XRD analysis. The first endothermic

peak most likely corresponds to a phase change of the quartz impurity, while the second endothermic corresponds to the decomposition of calcite. Vitric Ash-S lost about 7% of its mass, after being heated to 1000°C.

The DSC plots of all three zeolites had two major endothermic peaks. According to previous literature (Villa et al., 2013), the initial endothermic peak at lower temperature corresponds to dehydration, while the later peak at a higher temperature corresponds to the collapse of the zeolitic structure. Overall, the zeolites lost about 10% of their total mass when heated to 1000°C. The DSC data for Metakaolin-D and Shale-T did not show any significant phase changes after the initial dehydration. This is expected, since both materials were already heat treated during production. The DSC plot for Metakaolin-D has an endothermic peak after 900°C, which is most likely due to recrystallization of high temperature phases. The phenomenon of phase recrystallization at high temperatures has been shown for kaolinite in previous literature (Habert et al., 2009). Metakaolin-D and Shale-T lost less than 2% of their mass when heated to 1000°C.

Table 3.7: Summary of Natural Pozzolan TGA results

SCM	**% Total Mass Loss when heated to**			
	100°C	***200°C***	***500°C***	***1000°C***
Pumice-D	0.41	0.99	4.45	5.21
Pumice-N	0.48	1.71	4.89	5.46
Pumice-S	0.04	0.35	3.44	4.62
Perlite-I	0.09	0.32	2.94	3.50
Vitric Ash-S	0.67	1.40	4.17	7.11
Metakaolin-D	0.25	0.56	1.20	1.69
Shale-T	0.08	0.16	0.27	0.69
Zeolite-Z	2.19	5.76	8.70	9.72
Zeolite-T	1.82	5.68	8.47	9.99
Zeolite-A	1.62	4.73	6.84	9.65

Chapter 4: Performance of Natural Pozzolans in Cementitious Mixtures

Performance of the eight natural pozzolans being evaluated as Class F fly ash replacements was assessed in terms of their effects on mortar compressive strength, mixture workability and durability. This chapter presents the results of the performance tests conducted on the natural pozzolans, and compares these results with those from a Class F fly ash to evaluate whether these pozzolans can be suitable Class F ash replacements. Additionally, this chapter also correlates the performance results of the natural pozzolans to their physical and chemical characteristics, presented in Chapter 3, to understand the underlying mechanisms of cement and pozzolan interaction and discover ways to mitigate problems that are typically associated with the use of pozzolans as SCMs.

Section 4.1 presents data from the compressive strength testing of mortars, along with results from isothermal calorimetry and TGA, which were conducted to gain further insight into the effects of natural pozzolans on mortar compressive strength. Section 4.2 presents rheology results to show how natural pozzolans change mixture workability. Section 4.3 describes the results of the durability testing on mortar to show whether the pozzolans were effective in suppressing expansions from ASR and sulfate attack. Finally, Section 4.4 summarizes the performance data and presents a discussion about the problems with natural pozzolan use in cementitious mixtures that were identified during the performance testing.

4.1 COMPRESSIVE STRENGTH

4.1.1 Compressive Strength

Figure 4.1 shows the average compressive strength of natural pozzolan mortars made with a w/cm of 0.5. The control mortar, with no SCMs, and the fly ash mortar shown in Figure 4.1 were also made with the same w/cm of 0.5. The error bars represent the range of the data. All the ranges are within the limits prescribed by ASTM C 109, except for the 1 day compressive strength of the Metakaolin-D mortar and the 3 day compressive strength of the Pumice-D mortar. The ranges for these two readings were approximately 8% of the average, instead of being less than or equal to 7.6%, as suggested by ASTM C 109 (2011). For more information about the compressive strength data analysis, please refer back to Section 2.3.1.1.

From Figure 4.1, it can be seen that all the natural pozzolan mixtures have lower strengths than the control at 1 and 3 days. However by 28 days, there is a considerable improvement in the compressive strengths of the pozzolan mortars, with many of their strengths being similar to that of the control, if not higher. A similar trend of strength gain was observed for the fly ash mortar, which has a lower strength than the control during the first week of hydration, but a higher strength after 28 days. By 90 days, all the natural pozzolan mortars had compressive strengths that were equal to or higher than that of the control. When compared to the fly ash mortar, only the Metakaolin-D, Pumice-D and Perlite-I mortars were seen to have equivalent or higher strengths at 90 days. By 365 days, the Pumice-D and Perlite-I mortars significantly surpassed the strength of the fly ash mortar.

Out of all the pozzolan-containing mortars, the mortar with Metakaolin-D had the fastest rate of strength gain, surpassing the strength of control by approximately 22% at 28 days. Its compressive strength was also higher than that of the fly ash mortar at 28

days. From the XRF oxide composition, presented in Table 3.2, it can be seen that Metakaolin-D has a higher percentage of alumina, and consequently a lower percentage of silica compared to the other natural pozzolans. It is likely that the proportionally high alumina content is one of the main reasons behind the early reactivity of Metakaolin-D. Previous research has linked the reactivity of metakaolin to the transformation of aluminum in the clay structure to be penta-coordinated during calcination of the kaolinite clay (Fernandez et al., 2011a). Other reasons behind the early strength gain of Metakaolin-D mortar could be because of its particle characteristics. In Figure 3.1, Metakaolin-D was seen to have a coarser particle size distribution than pozzolans like Pumice-D and Perlite-I. However, the d_{10} value of Metakaolin-D was the lowest out of all the pozzolans at 1.9 μm, indicating the presence of very fine particles that contribute to an increased surface area of the calcined clay pozzolan. The rough and uneven particle texture of the Metakaolin-D particles, shown in Figure 3.10, could also contribute to an increased surface area. In fact, when the BET surface results from Table 3.5 were compared, the surface area of Metakaolin-D was seen to be higher than those of Pumice-D and Perlite-I. A high surface area can lead to increased compressive strength in the early stages of hydration, when the hydration process is dominated by the availability of sites where hydration products can nucleate and grow (Oey et al., 2013; Lothenbach et al., 2011). This is often referred to as the "filler effect" in previous literature, since the addition of inert filler materials with a high surface area can also promote nucleation and growth of hydration products in a cementitious system (Oey et al., 2013; Lothenbach et al., 2011). In this dissertation this effect will be referred to as the "size filler effect" to differentiate it from the "space filler effect," which will be discussed later.

Although initially the Pumice-D and Perlite-I mortars gained strength at a slower rate than the Metakaolin-D mortar, by 90 days both the Pumice-D and Perlite-I mixtures

displayed higher compressive strengths than the Metakaolin-D mixture. This indicates that although Metakaolin-D is fast to react, highly siliceous pozzolans like Pumice-D and Perlite-I contribute more to the long term strength of cementitious mixtures than pozzolans like Metakaolin-D, which are less siliceous due to its high alumina content. When comparing the strengths of the Pumice-D and Perlite-I mortars against each other, the slightly lower strength of the Perlite-I mortar at 7 and 28 days can be attributed to the lower surface area of Perlite-I compared to Pumice-D, but the difference in strength is very small.

Despite having the highest surface area out of the unaltered volcanic pozzolans, Vitric Ash-S did not seem to improve the long term strength of the mortar mixtures as much as Pumice-D and Perlite-I. Although the strength differences between the Vitric Ash-S mortar and the other unaltered volcanic pozzolan mortars were not apparent at 28 days, by 365 days the difference in strength was significant. The reason for the lower strength of Vitric Ash-S mortar compared to the Pumice-D and Perlite-I mortars could be related to its crystalline impurities. The XRD results, presented in Table 3.6, showed that unlike Pumice-D and Perlite-I, which were mostly amorphous, Vitric Ash-S had crystalline impurities, such as quartz, calcite and albite, which could lower the overall reactivity of the pozzolan.

Despite being a sedimentary pozzolan like the fast reacting Metakaolin-D, Shale-T had the lowest contribution to mortar compressive strength among the eight pozzolans tested as Class F fly ash replacements. This is not surprising as the BET surface area of Shale-T, presented in Table 3.5, was the lowest out of the eight pozzolans. Not only that, the SEM images (Figures 3.11 - 3.13) of Shale-T showed the presence of smooth particles, which might not promote as good dissolution. The smooth texture of

Shale-T particles has also been observed in previous literature (Ramsburg and Neal, 2002).

Figure 4.2 presents the average compressive strength of the natural pozzolan mortars made with a w/cm of 0.55. The control mortar, with no SCMs, and the fly ash mortar shown in Figure 4.2 were also made with the same w/cm of 0.55. The error bars represent the range of the data and are within the limits allowed by ASTM C 109 (2011). From Figure 4.2, it can be seen that Zeolite-Z has a good performance in terms of compressive strength, surpassing the strength of the control by 28 days. On the other hand, even at 365 days, Zeolite-T and Zeolite-A had strengths that were only about 70-75% of the control.

Correlating the compressive strength of the zeolite mortars to the properties of the zeolites themselves showed that, unlike the other pozzolans, early mortar compressive strengths did not correlate with BET surface area of the zeolites. For example, Zeolite-T had a higher surface area than Zeolite-Z, but did not perform as well in compressive strength. This is most likely because the BET surface area measurements include both the external surface area, shown in the SEM images of the zeolites (Figure 3.14 - 3.16), as well as the internal surface area from mesopores of the zeolites that are created from voids left between crystal aggregates (Elaiopoulos et al., 2010). Therefore, despite the BET surface area of the zeolites being high, certain portions of the surface area are from internal porosity and cannot participate as nucleation sites during cement hydration. As such, for porous materials like the zeolites the particle size distribution might give a better indication of the surface area available for the nucleation and growth of cement hydration products than the BET surface area that measure both external and internal surfaces. From Figure 3.1, it can be observed that Zeolite-Z had the finest particle size distribution out of the eight natural pozzolans tested as Class F fly ash replacements,

while Zeolite-T and Zeolite-A had the coarsest distributions. The fineness of the Zeolite-Z powder, which provides a high external surface area for the nucleation and growth of hydration products, is most likely the reason behind its superior performance over the two other coarser zeolites. Additionally, XRD analysis (Table 3.6) of Zeolite-T and Zeolite-A showed them to contain more crystalline impurities than Zeolite-Z, which primarily consisted of clinoptilolite. The purity of Zeolite-Z is likely to be another reason why the strength of the Zeolite-Z mortar was significantly higher than that of the Zeolite-T and Zeolite-A mortar.

In summary, Metakaolin-D and Zeolite-Z were seen to have early reactivity, with their mortars surpassing the strength of the control by 28 days. The presence of fine particles that can increase surface area and act as nucleation and growth sites for hydration products was considered to be one of the reasons for this early reactivity. However, caution must be exercised in using pozzolan surface area as the only predictor of early age mortar compressive strength. For porous pozzolans like zeolites, portions of the surface area can be from internal porosity, and as such, are not available as nucleation and growth sites for hydration products. Factors like particle texture and crystalline impurities of the pozzolans can also play a role in mortar compressive strength and can potentially negate the effect of surface area, as was seen with Vitric Ash-S. Chemical composition of the pozzolans was also seen to affect mortar strength. The early reactivity of Metakaolin-D was partially attributed to its high alumina content. However, beyond 90 days, mortars containing the most siliceous pozzolans like Pumice-D and Perlite-I were observed to have the highest compressive strength. This indicates that although high alumina content can improve early age strength, having high silica content is more crucial for long term strength.

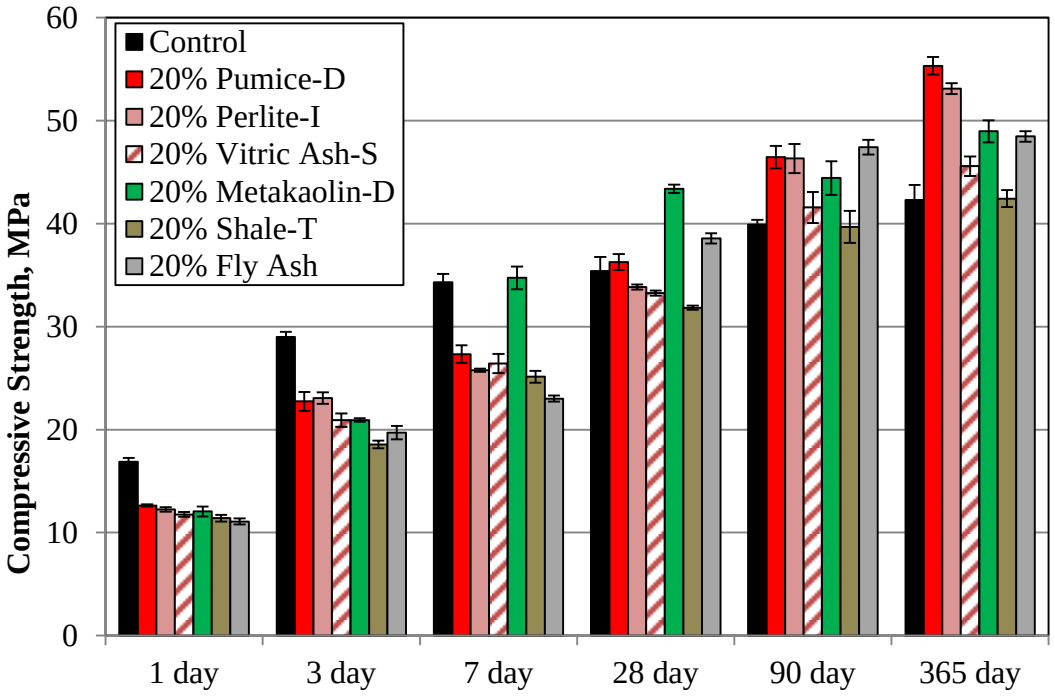

Figure 4.1: Compressive strength of mortar cubes made with w/cm = 0.50

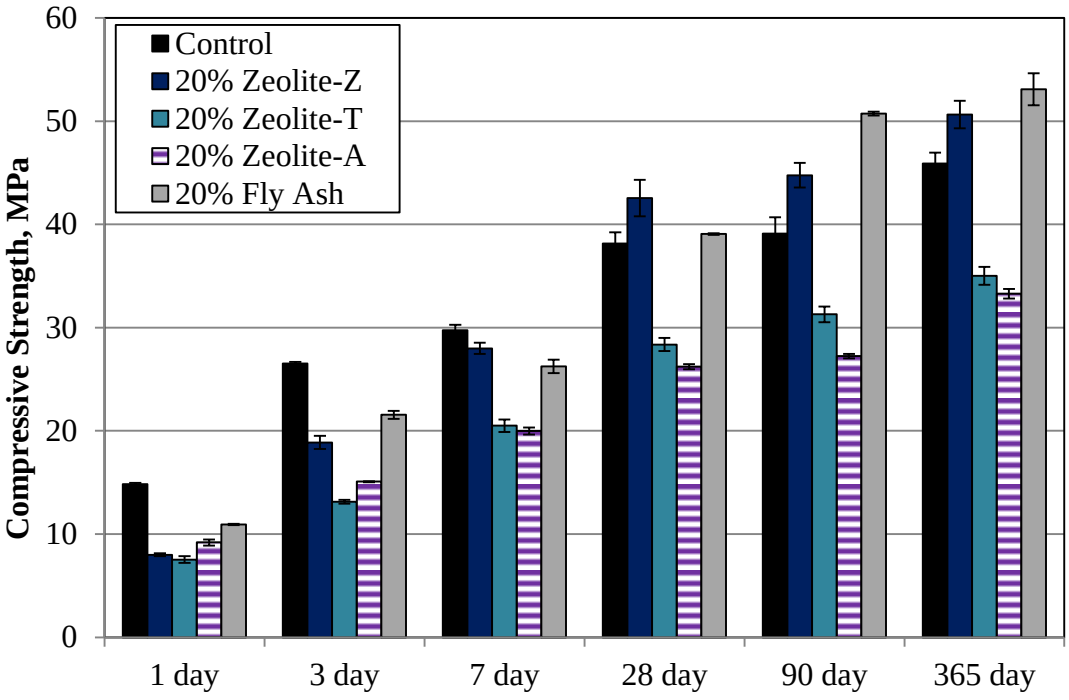

Figure 4.2: Compressive strength of mortar cubes made with w/cm = 0.55

4.1.2 Heat of Hydration

Isothermal calorimetry was performed to understand whether the low strength of pozzolan mortars in the early stages of hydration (1-3 days) was a result of retardation in the cement hydration kinetics caused by the addition of pozzolans. The data from the isothermal calorimetry tests were used to plot curves showing the rate of heat produced during hydration and are presented in Figures 4.3 - 4.5. Please note that the rate of heat evolved has been normalized to the amount of cement in the paste. The shape and position of the heat rate curves for the pozzolan pastes relative to the curve of the control paste provide valuable information regarding the effect of pozzolans on cement hydration. A rightward shift of the pozzolan curve relative to the control curve indicates a delay in the onset of the acceleratory phase of cement hydration, which in turn suggests a retardation of cement hydration kinetics. From Figures 4.3 – 4.5, it can be observed that none of the natural pozzolan paste curves showed a rightward shift that would indicate delay in the onset of the acceleratory phase. This suggests that the addition of the natural pozzolans does not retard cement hydration. Instead, the lower strengths observed in the natural pozzolan mortars were most likely the effect of diluting the cement content (Camiletti et al., 2013; Weerdt et al., 2012) with a slower reacting pozzolanic material. Interestingly, the fly ash curve was shifted slightly to the right, suggesting that the addition of fly ash was retarding cement hydration. This shift of fly ash mixtures has also been seen in previous literature (Nocun-Wczelik, 2001; Fajun et al., 1985).

Other than the Shale-T paste, all of the natural pozzolans exhibited enhanced nucleation of hydration products or the "size filler effect" to some degree, since from Figures 4.3- 4.5 it can be observed that the onset of the acceleratory period came earlier in the pozzolan pastes than in the control paste. Zeolite-Z, having the finest particle size distribution among the eight natural pozzolans being tested as Class F fly ash

replacements, exhibited this phenomenon very strongly, with its acceleratory period starting approximately an hour earlier before that of the control paste (Figure 4.5). This ties into the hypothesis presented in Section 4.1.1 that the fineness of the Zeolite-Z powder could partially account for its enhanced early reactivity compared to the other pozzolans. Additionally, the natural pozzolan pastes were observed to have a slightly longer deceleration phase than the control paste (for example, compare the calorimetry curves for the Shale-T paste and the control paste in Figure 4.4). This is most likely due to the "space filler effect," which refers to the growth of additional hydration products due to increased space per grain of cement, since the pozzolanic materials are not expected to produce hydrates in the very early stages of hydration (Oey et al., 2013; Lothenbach et al., 2011).

The first peak of the rate of heat calorimetry curve, after the initial peak from dissolution, is attributed to the hydration of the silicate phases and is generally higher than the following peak (i.e. the second peak after the initial peak from dissolution), which is attributed to the hydration of the aluminate phases. Interestingly, from Figure 4.4 it can be observed that the second peak of the Metakaolin-D paste is higher than the first. This trend for metakaolin pozzolans has been seen in previous literature (Antoni et al., 2012), and is thought to be an effect of enhanced nucleation, which has been seen to affect the aluminate phases more than the silicate phases (Antoni et al., 2012; Lothenbach et al., 2011). Undersulfation has also been suggested as a reason for the unusual second peak, but it was not conclusively proven in previous literature whether the undersulfation was caused by the participation of aluminates originating from the metakaolin pozzolan itself (Antoni et al., 2012). The second peak in the rate of heat calorimetry curve for the Zeolite-Z paste is also unusual in shape. Given the fine particle size distribution of Zeolite-Z, this unusual second peak could be a result of the enhanced nucleation and

growth of hydration products occurring in the Zeolite-Z paste. Additionally, the Zeolite-Z paste could also have problems of undersulfation like the Metakaolin-D mixture. Finally, it must be noted that undersulfation usually gives rise to a much sharper second peak that what is observed for the Metakaolin-D and Zeolite-Z paste in Figure 4.4 and 4.5. More research needs to be done to conclusively prove whether the unusual second peak is due to enhanced nucleation or undersulfation.

In summary, the calorimetry data showed that the natural pozzolans did not retard the cement hydration. The initial lower strengths of the pozzolan mortars were most likely due to the effect of diluting the cement content with a slower reacting pozzolanic material. However, this dilution benefits the growth of hydration products by providing extra space per grain of cement for the hydration products. Additionally, fine pozzolans can enhance growth of hydration products by providing extra nucleation and growth sites with their high surface area. This was very pronounced for the pastes of the finely ground Metakaolin-D and Zeolite-Z, both of which had high early mortar strengths.

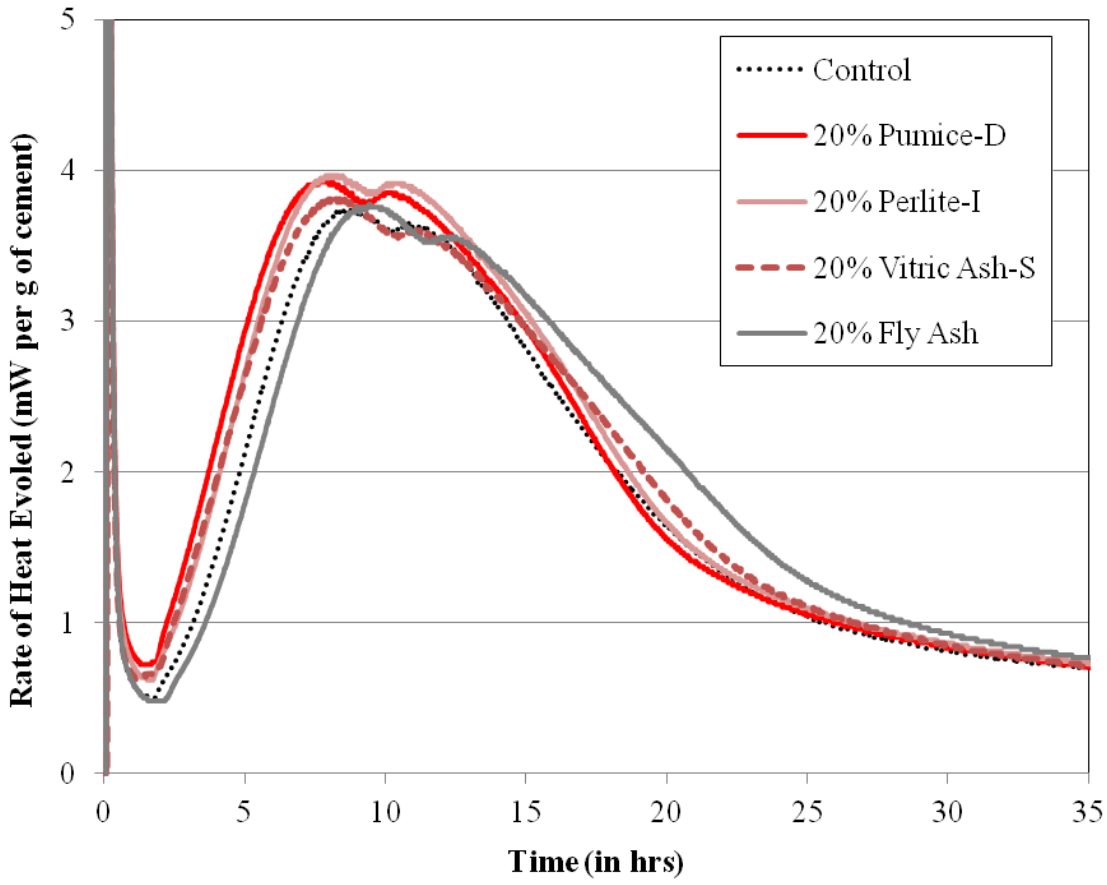

Figure 4.3: Rate of heat evolved per g cement in pastes with unaltered volcanic pozzolans

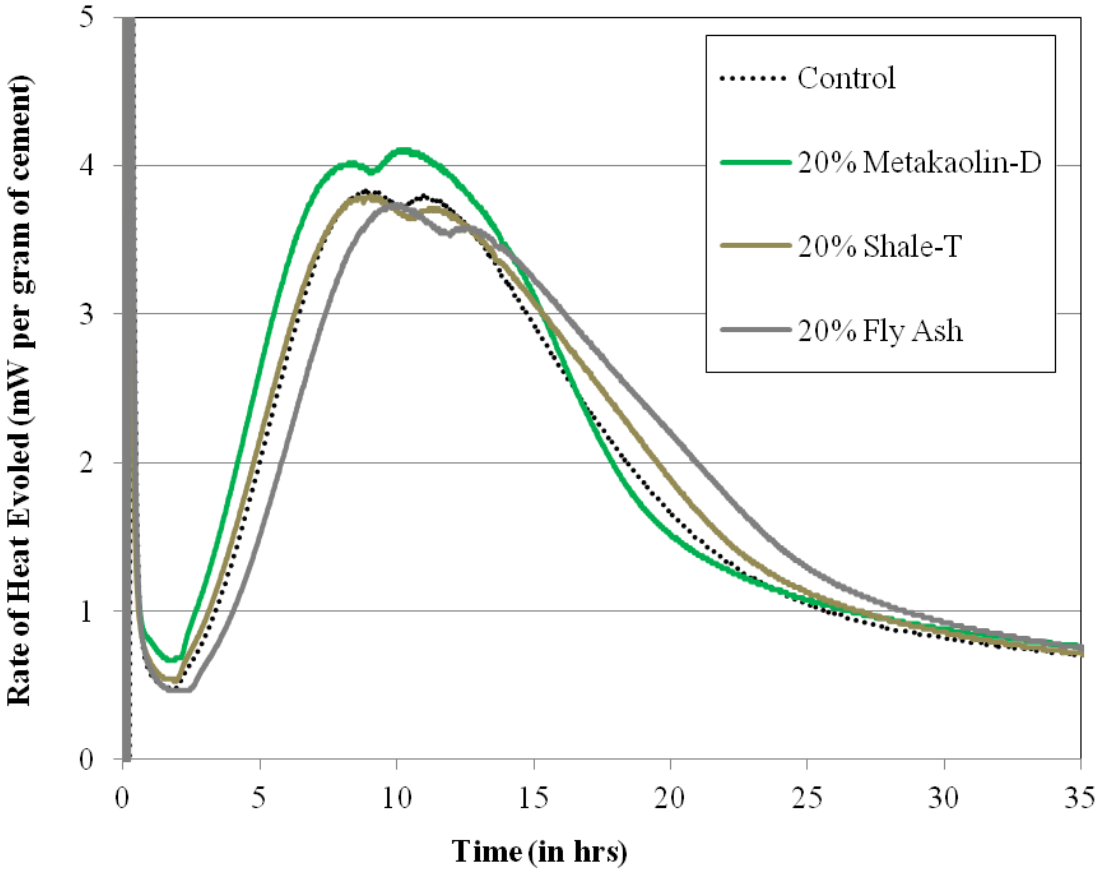

Figure 4.4: Rate of heat evolved per g cement in pastes with sedimentary pozzolans

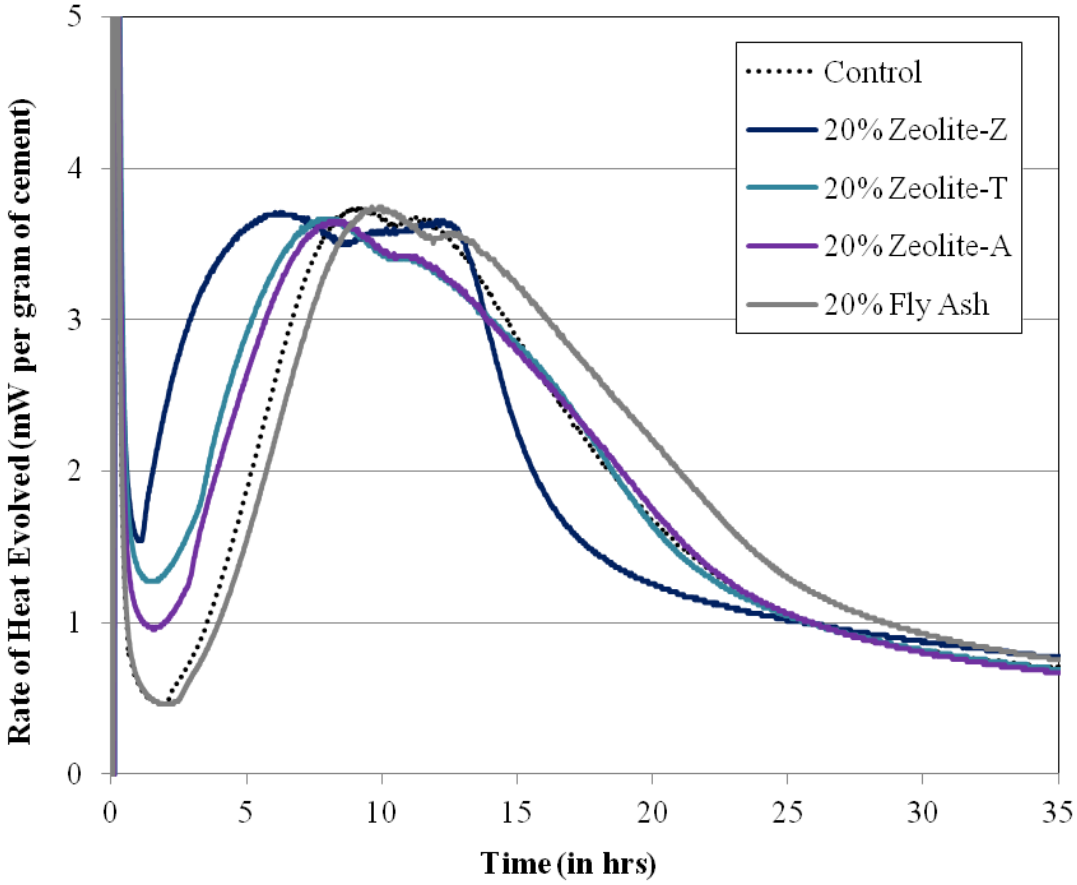

Figure 4.5: Rate of heat evolved per g cement in pastes with zeolites

4.1.3 Calcium Hydroxide Content

The calcium hydroxide contents of the pastes were measured using TGA/DSC to see if increases in mortar strength could be correlated with pozzolanic activity. Pozzolanic activity is defined to be the reaction of calcium hydroxide with the pozzolan to form calcium silicate hydrate (C-S-H). Therefore, increases in pozzolanic activity should manifest itself through the decrease of calcium hydroxide content in cementitious pastes. Figure 4.6 presents the calcium hydroxide contents of the pastes at 7, 28 and 90 days of hydration. The error bars represent the range of the data from duplicate tests. Please note that the data have been normalized to the amount of cement in the paste. Table 4.1 shows the percent reduction in calcium hydroxide content in pozzolan pastes between 7-90 days.

Pozzolanic activity for the Metakaolin-D and Zeolite-Z mixtures was expected to have commenced from an early age, since by 7 days the compressive strengths of the Metakaolin-D and Zeolite-Z mortars, presented in Figure 4.1 and 4.2, had already overcome the dilution effect (Camiletti et al., 2013; Weerdt et al., 2012) and were similar in value to that of the control mortar. Since pozzolanic activity results in the consumption of calcium hydroxide to form C-S-H, the calcium hydroxide content of the Metakaolin-D and Zeolite-Z pastes were expected to be lower than or equal to (taking into account that size and space filler effect increases calcium hydroxide production) that of the control at 7 days. On the other hand, since the compressive strength of the other pozzolan mortars was observed to be much lower than the control mortar at 7 days, their pozzolanic activity was considered to be minimal during the first week of hydration. As such the calcium hydroxide contents per gram of cement for all the other pozzolan pastes, were expected to be the same as that of the control paste, or slightly higher to account for size and space filler effects.

From Figure 4.6, it can be seen that at 7 days the Metakaolin-D and Zeolite-Z pastes had much lower calcium hydroxide contents than the control paste, as anticipated from the compressive strength data. The pastes of Pumice-D and Perlite-I also behaved as expected and had similar calcium hydroxide contents as that of the control paste. Surprisingly, the Vitric Ash-S, Shale-T, Zeolite-T and Zeolite-A pastes, which did not show any indication of pozzolanic activity from their mortar compressive strength results, had lower calcium hydroxide contents than that of the control paste at 7 days. Since the strength results of these pozzolan mortars do not support the hypothesis of significant calcium depletion through pozzolanic activity in the first week of hydration, more research needs to be done to understand the reasons behind this divergence in data.

Since the initial production of calcium hydroxide could be different depending on the size and space filler effects experienced in a pozzolan-cementitious system, perhaps a better way to gauge the level of pozzolanic activity is to look at the difference in calcium hydroxide contents over time, instead of looking at the absolute value at a particular point in time. For example, if one only considered the data in Figure 4.6, which shows the pastes of Vitric Ash-S, Shale-T, Zeolite-T and Zeolite-A to have similar calcium hydroxide contents to those of the Pumice-D and Perlite-I pastes at 90 days, it would indicate that their pozzolanic potentials are similar. However, when looking at the calcium hydroxide content difference between 7 – 90 days from Table 4.1, it can be observed that Pumice-D and Perlite-I reduced the calcium hydroxide content per gram of cement at least twice as much as that of Vitric Ash-S, Shale-T, Zeolite-T and Zeolite-A. This corroborates the results from mortar cube compression testing that have shown the Pumice-D and Perlite-I mortars to have much higher strengths than the Vitric Ash-S, Shale-T, Zeolite-T and Zeolite-A mortars. In fact, as shown in Figure 4.7, the correlation between the 90 day strength of the pozzolan mortars and the reduction in the calcium

hydroxide content of their paste mixtures between 7-90 days were very high, with coefficient of determination (R^2) values of 0.89 for mortar cubes with w/cm of 0.50, and 0.99 for cubes with w/cm of 0.55. This confirms the hypothesis that the increases in mortar strength are related to pozzolanic activity, where calcium hydroxide is consumed to form C-S-H. The fly ash mixture did not follow this trend seen in the natural pozzolan mixtures. Despite having a higher strength than the control mortar at 90 days, the reduction in calcium hydroxide content of the fly ash paste was much lower than the natural pozzolans which had similar improvements to compressive strength. This trend has been observed in previous literature and the high calcium content of the fly ash was forwarded as one of the reasons for the less pronounced reduction of calcium hydroxide (Lothenbach et al., 2011). From the XRF results, presented in Tables 3.2 and 3.3, it can be observed that the fly ash used in this research also had higher calcium content than the other pozzolans.

In summary, the reduction in calcium hydroxide content is a good indicator of pozzolanic activity, which can further be correlated to the increase in mixture compressive strength. In the current research, with a calcium hydroxide content reduction of 0.06 grams per gram of cement, Perlite-I was seen to have the highest pozzolanic reactivity, followed by Zeolite-Z, Pumice-D and Metakaolin-D pastes, in that order. The actual calcium hydroxide reduction from the start of hydration is expected to be larger than what was seen for the Metakaolin-D and Zeolite-Z pastes between 7-90 days, since the onset of pozzolanic activity for these two materials with an early reactivity most likely started earlier than 7 days, unlike the rest of the natural pozzolans.

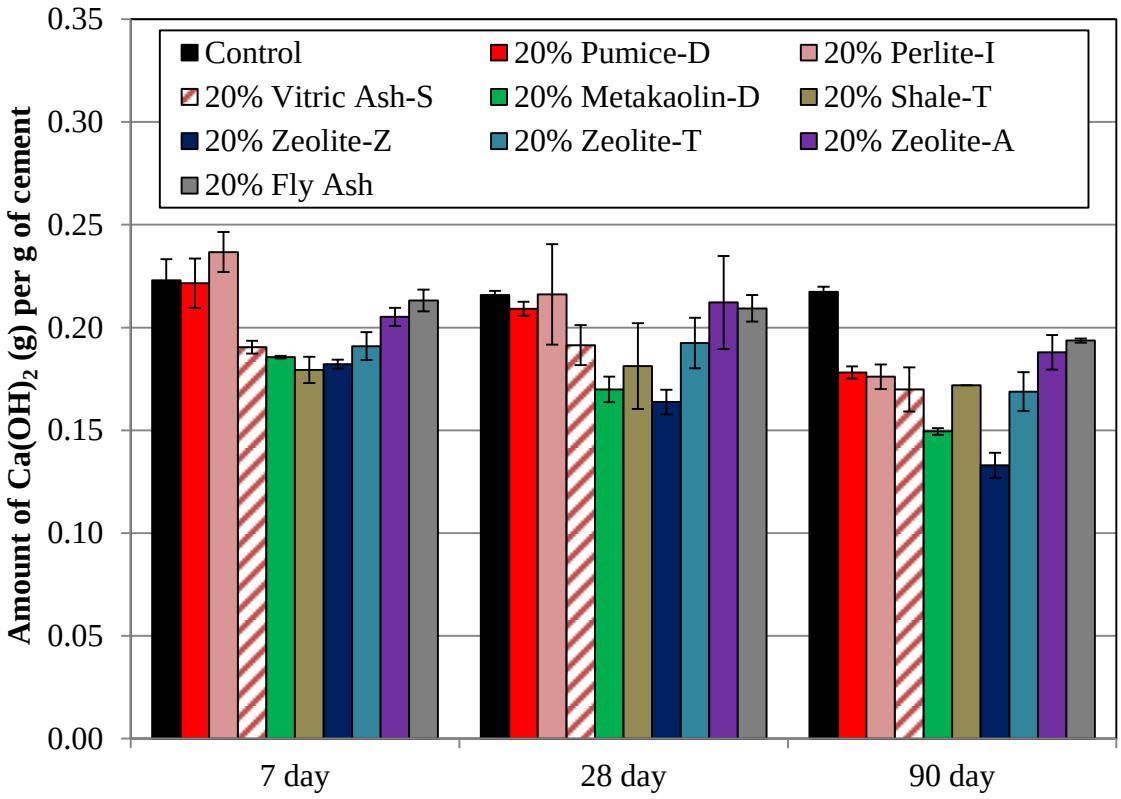

Figure 4.6: Calcium hydroxide contents of the control and pozzolan pastes

Table 4.1: Reduction of Calcium Hydroxide between 7-90 Days in Pozzolan Pastes

Mixture Description	Reduction in $Ca(OH)_2$ in grams per gram of cement
20% Pumice-D	0.04
20% Perlite-I	0.06
20% Vitric Ash-S	0.02
20% Metakaolin-D	0.04
20% Shale-T	0.01
20% Zeolite-Z	0.05
20% Zeolite-T	0.02
20% Zeolite-A	0.02
20% Fly Ash	0.02

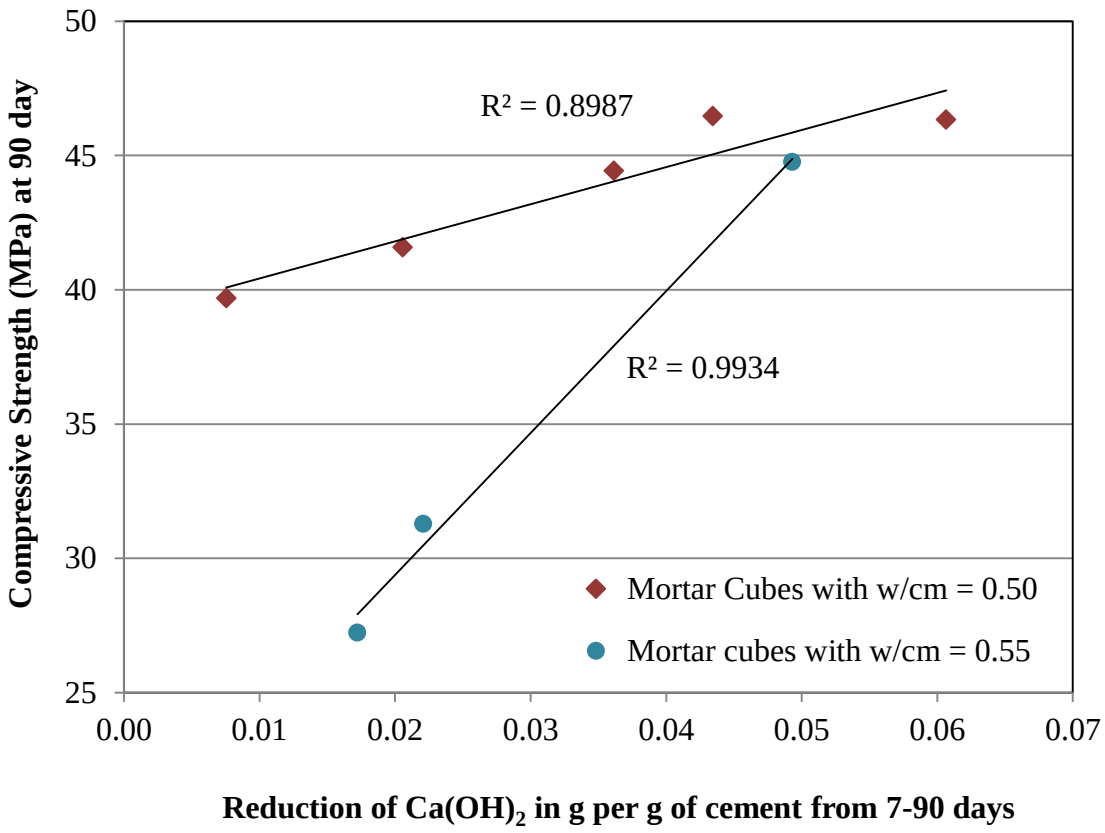

Figure 4.7: Correlation between strength of mortars and $Ca(OH)_2$ reduction in pastes

4.2 Mixture Workability

In this research, the effect of pozzolans on mixture workability was evaluated by measuring the rheological properties of pastes containing pozzolans. Since the focus of the research presented in this dissertation is on the pozzolanic materials, rather than the level of workability needed by a particular application, the success criteria for the pozzolan pastes in terms of rheology was to have a similar workability to that of the control mixture without any pozzolans. Fly ash generally improves the workability of concrete mixtures, owing to the spherical shape of the fly ash particles that act as ball

bearings and reduce interparticle friction (Mindess et al., 2002). As such, pozzolan pastes that have rheological properties similar to the fly ash mixture were also considered to have a good performance in terms of mixture workability.

Figure 4.8 presents representative rheological flow curves of the control and pozzolan pastes, which show how the shear stress in the pastes changed as the shear rate was decreased from 50 s^{-1} to 10 s^{-1}. The Bingham model (Mechtcherine et al., 2014), was used to analyze the flow curves showing a linear trend, whereas the apparent viscosity at each shear rate was used to evaluate the flow curves with a non-linear trend. For additional details on the rheology data analysis, please refer to Section 2.3.2. Table 4.2 presents the Bingham yield stresses and viscosities of the paste mixtures with a linear flow curve, while Table 4.3 shows the apparent viscosities of the paste mixtures with a non-linear flow curve. Table 4.2 and 4.3 also show the ranges of the data from duplicate testing.

From Figure 4.8, it can be seen that at any given shear rate, the Zeolite-Z and Zeolite-T pastes exhibit higher shear stresses than any of the pozzolan or control paste mixtures. This indicates that the use of Zeolite-Z and Zeolite-T as SCMs significantly reduces the workability of cementitious mixtures. These rheology results corroborate the results from the ASTM C 618 water requirement test (Table 3.1), which showed the Zeolite-Z and Zeolite-T mixtures to have a significantly higher water demand than that of the control mixture. However, unlike the water requirement test, the rheology results gave a more thorough understanding of how the zeolites influenced mixture workability. For example, from Figure 4.8, it can be observed that the flow curve of the Zeolite-T paste is different from all the other paste mixtures since it is the only flow curve that exhibits a non-linear response to increasing shear rate. As such, instead of using the linear Bingham model, the workability of the Zeolite-T paste was evaluated by calculating the

apparent viscosity at each particular shear rate. From the results, presented in Table 4.3, it can be observed that the Zeolite-T paste exhibits shear thinning behavior (Mindess et al., 2002), with the apparent viscosity being significantly reduced by 2.8 Pa.s between the shear rates of 10 s^{-1} and 50 s^{-1}. On the other hand, the flow curve of the Zeolite-Z paste showed a linear trend and was evaluated with the Bingham model. Although the viscosity of the Zeolite-Z mixture is very high, it is lower than that of the Zeolite-T paste at lower shear rates, and comparable to that of the Zeolite-T paste at higher shear rates. This illustrates how the rheology results gave further insight into the effect of zeolites on mixture workability than the water requirement test which simply indicated that Zeolite-T had a higher water demand than Zeolite-Z.

The rheology results of Zeolite-Z and Zeolite-T were not surprising since the poor workability of zeolites mixtures has been well documented in previous literature (Bilim, 2011; Ahmadi and Shekarchi, 2010; Perraki et al., 2010). The shear thinning behavior, shown by the Zeolite-T paste in this study, has also been observed in previous literature on zeolite grouts (Sahmaran et al., 2008). The poor workability and the shear thinning behavior of zeolite mixtures can both be explained by the porosity of the zeolites, which range from micropores in the crystalline structure of the zeolite itself to mesopores that are created from voids left between crystal aggregates (Elaiopoulos et al., 2010). The porosity of the zeolites results in a high surface area, as observed in the BET results of Table 3.5. Since particles need to be fully coated with water to flow easily, materials with a high surface area often require higher water contents than materials with a low surface area to achieve the same workability (Mindess et al., 2002). Additionally, the micropores in the zeolites contain cations that can absorb water through charge-dipole interactions (Snellings et al., 2012) and increase the water demand of the material. However, since the water is only weakly bonded to the cations (Snellings et al., 2012), at higher shear rates

the water could be released from the micropores (Sahmaran et al., 2008). This in turn can cause shear thinning, since the released water will be available to facilitate the flow of the particles and decrease the overall viscosity of the mixture (Sahmaran et al., 2008). Finally, the presence of clay impurities, as seen in the XRD results of Zeolite-T (Table 3.6), can also contribute to the high water demand of the material, since clay can absorb water due to the interchangeable cations that are present in its layered structure (Fernandez et al., 2011a; Foster, 1954).

Other than the Zeolite-T mixture, the rest of the paste mixtures exhibited a linear response to increasing shear rate. As such, the viscosities and yield stresses of these mixtures, presented in Table 4.2, were evaluated using the Bingham model. From Table 4.2, it can be observed that the viscosity and yield stress of the Shale-T paste was lower than that of the control. In fact, out of the eight natural pozzolans tested as Class F fly ash replacements, the viscosity of the Shale-T paste was the closest to that of the fly ash mixture, indicating its suitability to be a fly ash replacement in applications where fly ash is typically used to improve concrete mixture workability. The low BET surface area (Table 3.5) of the Shale-T pozzolan and the smooth texture of its particles seen during SEM imaging (Figures 3.11 – 3.13) most likely contributed to the low viscosity and yield stress of the Shale-T paste. Similar conclusions about the particle texture of calcined shale and its effect on mixture workability were made by previous researchers working on self-consolidating concrete (Ramsburg and Neal, 2002).

Similar to Shale-T, Perlite-I was also observed to have a low surface area (Table 3.5) and a high proportion of smooth textured particles (Figure 3.5). However, unlike the Shale-T mixture, the viscosity and yield stress of the Perlite-I mixture were slightly higher than those of the control paste. In fact, the viscosity and yield stress of the Perlite-I mixture was similar to the mixtures of Pumice-D and Metakaolin-D, two pozzolans with

a much higher surface area (Table 3.5) than Perlite-I. Although Perlite-I has a lower surface area, its particle size distribution (Figure 3.1) is similar to that of Pumice-D. This led to the hypothesis that below a certain surface area, particle size distribution might have a greater effect on mixture workability than surface area. The rheology results of the Vitric Ash-S paste are also in agreement with this hypothesis, since contrary to expectations that were made based on the pozzolan's surface area, the viscosity of the Vitric Ash-S paste was found to be lower than that of the control mixture. The rheology results of the Vitric Ash-S paste corresponded better with the particle size distribution results, which showed Vitric Ash-S to be coarser than Pumice-D, Perlite-I and Metakaolin-D, despite Vitric Ash-S having a higher BET surface area.

Figure 4.9 shows a correlation of mixture viscosity and median particle size for pozzolans other than zeolites. With an R^2 of 0.87, the rheology data from this study indicates that below a certain pozzolan surface area, particle size distribution of the pozzolan becomes an important consideration for flow behavior. However, more research needs to be conducted, where particle variables like texture and shape are controlled, to form a conclusive relationship for the effects of particle size vs. surface area on mixture viscosity. For example, being a spherical particle, fly ash does not fit into any of the trends observed for the more angular natural pozzolans in this research.

Finally, it must be noted here that, although the rheology results provided a more complete and thorough information on the effect of pozzolans on mixture workability, the results were generally in agreement with the water requirement results, which accurately predicted whether a pozzolan would cause workability problems in cementitious mixtures. However, this was not the case for Zeolite-A. Although the Zeolite-A mortar failed the water requirement test, the viscosity and yield strength of the Zeolite-A paste was seen to be similar to that of the control in the rheology results. More research needs

to be conducted to understand why the rheology results of the Zeolite-A paste was similar to that of the control paste, despite showing a high water demand in the water requirement testing of ASTM C 618 (Table 3.1).

In summary, the rheology results suggest that, other than Zeolite-Z and Zeolite-T, the natural pozzolans will not cause any significant workability issues in cementitious mixtures when used at a dosage of 20%. Due to the disparity between the mortar and paste results of Zeolite-A, its effect on mixture workability was considered to be inconclusive. The Shale-T and Vitric Ash-S pozzolans were shown to be the best replacements for Class F fly ash in applications where fly ash is typically used to improve the mixture workability of concrete. Finally, owing to the variability in the particle characteristics of natural pozzolans, caution should be exercised in using only one variable like surface area or particle size to be an indicator of the pozzolan's effect on mixture workability. While the high surface area of zeolites seemed to influence its effect on mixture workability, particle size distribution was also shown to be an important consideration for the flow behavior of unaltered volcanic and sedimentary pozzolans. Porosity of the materials as well as particle characteristics like shape and texture were also thought to be important influences on mixture workability.

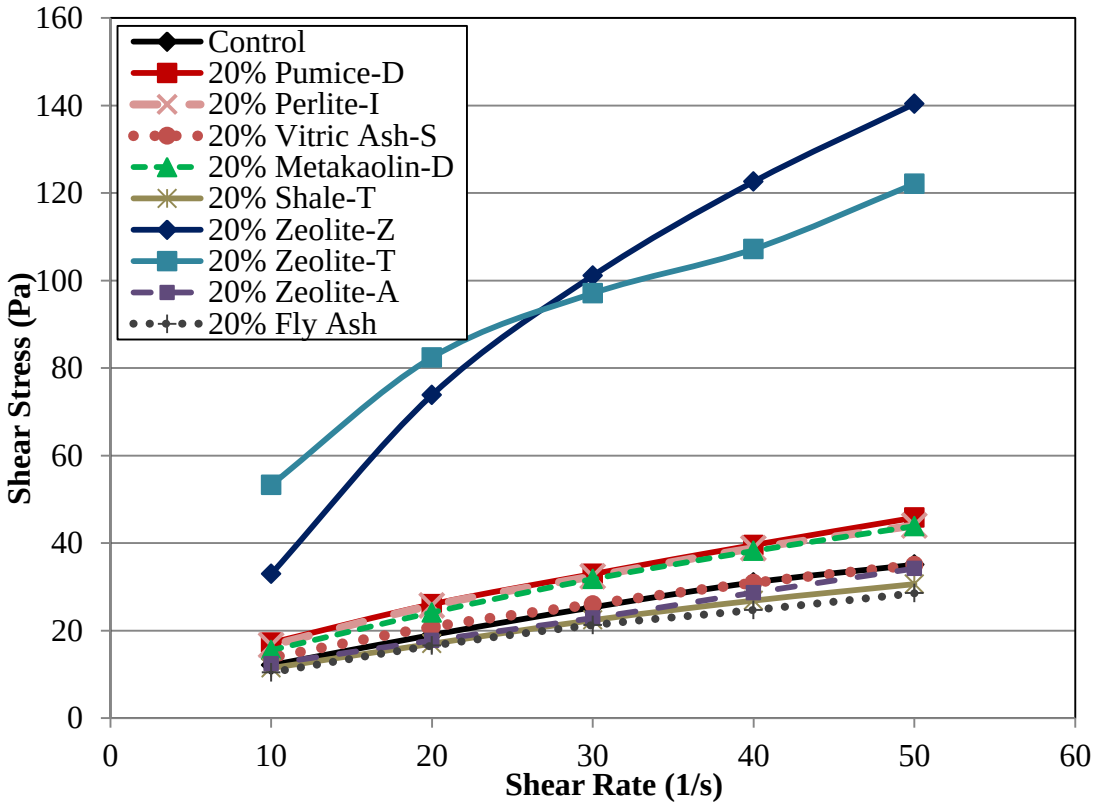

Figure 4.8: Representative rheological flow curves of the control and pozzolan pastes

Table 4.2: Bingham Viscosities and Yield Stresses of Pastes with Linear Flow Curve

Material	Replacement Dosage (%)	Yield Stress (Pa)	Viscosity (Pa.s)
Control	0	7.78 ± 0.64	0.56 ± 0.01
Pumice-D	20	10.72 ± 0.39	0.73 ± 0.03
Perlite-I	20	11.77 ± 0.59	0.67 ± 0.01
Vitric Ash-S	20	9.91 ± 0.32	0.51 ± 0.01
Metakaolin-D	20	10.08 ± 0.60	0.70 ± 0.01
Shale-T	20	7.21 ± 0.01	0.48 ± 0.00
Zeolite-Z	20	15.41 ± 0.34	2.61 ± 0.03
Zeolite-T	20	N/A	N/A
Zeolite-A	20	8.53 ± 1.69	0.55 ± 0.00
Fly Ash	20	7.66 ± 0.64	0.44 ± 0.01

Table 4.3: Apparent Viscosity of Paste with Non-Linear Flow Curve

Shear Rate (1/s)	Apparent Viscosity (Pa.s) of 20% Zeolite-T paste
10	5.29 ± 0.04
20	4.45 ± 0.32
30	3.23 ± 0.01
40	2.70 ± 0.02
50	2.49 ± 0.04

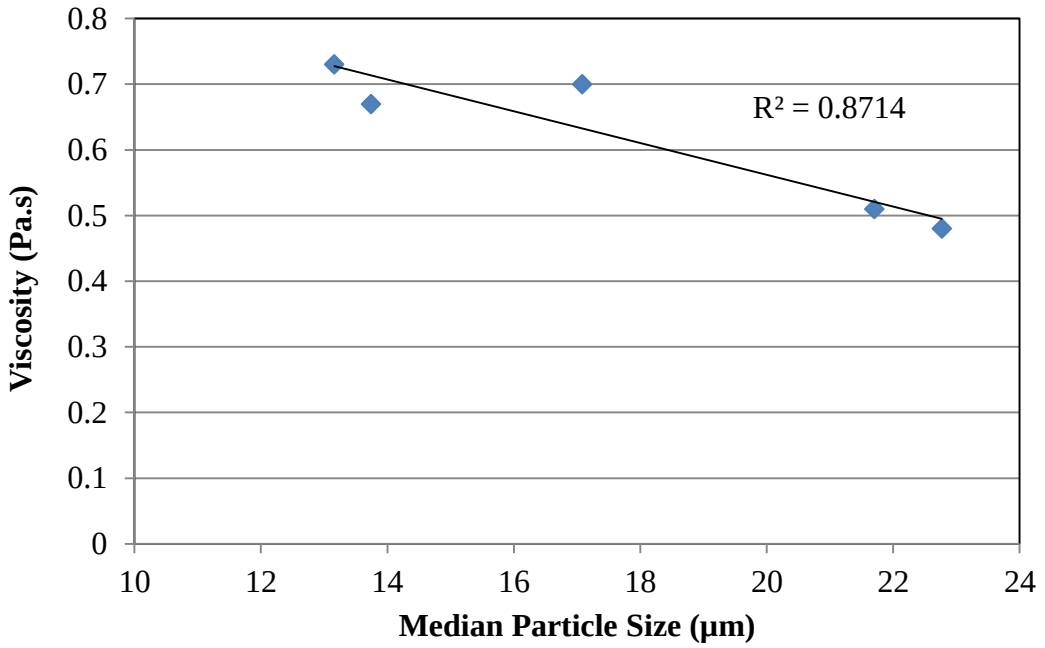

Figure 4.9: Correlation of viscosity and particle size of pozzolans other than zeolites.

4.3 DURABILITY

4.3.1 Alkali Silica Reaction (ASR)

Figure 4.10 shows the results of the ASTM C 1567 (2013) ASR testing on mortar bars where 20% of the cement was replaced with pozzolans. Table 4.4 lists the expansion of the 20% pozzolan-containing mortar bars after 14 days of submersion in NaOH solution, along with the range of the data. The results show that, out of the natural pozzolans, only the Pumice-D, Perlite-I, Metakaolin-D and Zeolite-Z mortar bars had expansions below the ASTM C 1567 limit of 0.1% expansion after 14 days of submersion in NaOH solution. The 20% fly ash mortar also had expansions below the ASTM C 1567 limit. The rest of the mortar mixtures failed the ASTM C 1567 ASR test when a pozzolan replacement dosage of 20% was used. The Vitric Ash-S and Shale-T mortar mixtures just barely missed the limit, exceeding the 0.1% expansion after 12 days of submersion in NaOH solution. However, Zeolite-T and Zeolite-A performed very poorly, crossing the expansion limit at 7 days and 3 days, respectively.

Although previous literature showed no correlation between reduction in ASR expansion in SCM-containing concrete mixtures and calcium hydroxide depletion (Duchesne and Berube, 1994a) it is interesting to note that in this research, other than fly ash, all the pozzolan-mortar bars that passed the ASTM C 1567 test at SCM replacement dosages of 20% had much higher calcium hydroxide depletions (Table 4.1) between 7-90 days than the pozzolan mortar bars that exceeded the 0.1% expansion. This does not mean that the effectiveness of an SCM in mitigating ASR is dependent upon the reduction of calcium hydroxide. More likely, it points to some underlying mechanism due to composition and particle characteristics that make the pozzolans perform well both in calcium hydroxide depletion and ASR mitigation.

Previous literature has shown that the addition of pozzolans mitigate the expansions from ASR by reducing the alkalinity of the pore solution (Chappex and Scrivener, 2012a; Hong and Glasser, 1999; Duchesne and Berube, 1994b; Canham et al., 1987) caused by an increased alkali binding capacity of pozzolanic C-S-H compared to the C-S-H formed from only portland cement (Chappex and Scrivener, 2012a; Hong and Glasser, 1999). Pozzolanic C-S-H is typically considered to have a lower calcium to silicon ratio (Ca/Si), and using synthesized C-S-H, researchers have shown that the binding of alkalis into C-S-H improves as its Ca/Si decreases (Hong and Glasser, 1999). Additionally, in his review of the effect of SCMs on ASR, Thomas (2011) observed that the ability of SCMs to mitigate ASR appeared to be strongly related to their Ca/Si composition. Table 4.5 presents the Ca/Si (calculated from the XRF results) of the natural pozzolans and Class F fly ash used in this research. From Table 4.5, it can be seen that the natural pozzolans with low Ca/Si of 0.01, like Pumice-D, Perlite-I and Metakaolin-D, were effective at keeping expansions from ASR below the 0.1% limit. However, Zeolite-Z and fly ash, which had higher Ca/Si, were also able to keep expansions below the 0.1% limit. This suggests that other factors also influence the ability of SCMs to mitigate ASR. For example, the zeolite framework has a net negative charge, caused by the substitution of Al^{3+} for Si^{4+} in its tetrahedral structure, which is balanced by exchangeable cations in its pores (Snellings et al., 2012). Unreacted zeolites in the mixture could affect the pore solution chemistry, since the cations in its pores are only loosely bounded to the structure (Pabalan and Bertetti, 2001). The substitution of aluminum in the tetrahedral structure of zeolites could lead to the formation of calcium aluminate silicate hydrate (C-A-S-H) instead of C-S-H, which has been suggested in previous literature to have a greater alkali binding capacity than C-S-H (Hong and Glasser, 2002). However, more recent research has shown that instead of changing the alkali binding capacity of C-S-H, the presence of

alumina in SCMs helps mitigate ASR by slowing down the dissolution of the reactive aggregate (Chappex and Scrivener, 2012b). The XRF results (Table 3.3) showed fly ash to have high alumina content, which could be one of the reasons for its effectiveness in mitigating ASR, despite its high Ca/Si composition.

In his review, Thomas (2011) suggested that most SCMs can be used to mitigate ASR, provided that the dosage is high enough. As such, a second round of ASR testing was conducted to find the minimum replacement dosage needed for each natural pozzolan to keep expansions below the ASTM C 1567 (2013) limit. The replacement dosage of Pumice-D, Perlite-I, Metakaolin-D and Zeolite-Z was lowered to 15%, since they passed the ASTM C 1567 (2013) test at a dosage of 20%. For the natural pozzolans that failed to keep expansions below the limit at a replacement of 20%, the dosage was increased until they passed the ASTM C 1567 (2013) test. Figure 4.11 shows the minimum SCM replacement dosages that were required for each mortar mixture to pass the ASTM C 1567 (2013) test. Additionally, Table 4.6 lists the expansion of these mortar bars after 14 days of NaOH submersion, along with the range of the expansion data. The results show that, even at a replacement dosage of 15%, the Pumice-D, Perlite-I, Metakaolin-D and Zeolite-Z mortar bars had expansions lower than the 0.1% limit. The Vitric Ash-S, Shale-T and Zeolite-T pozzolans were able to keep the expansions of their mortar bars below the ASTM C 1567 (2013) limit when used at a replacement dosage of 25%. However, Zeolite-A required a much higher dosage of 35% to pass the ASTM C 1567 (2013) test. This is not surprising since the Zeolite-A mortar had the worst expansion out of all the pozzolan mortar mixtures when tested for ASR resistance at a replacement dosage of 20%. The poor performance of the coarse zeolites, especially Zeolite-A, raised the question of how fineness of a pozzolan could affect its ability to mitigate expansions from ASR. In his review, Thomas (2011) observed that when finely

divided pozzolans agglomerate into sand sized particles, these agglomerated particles can cause ASR since pozzolans are essentially reactive silica. Further research needs to be carried out to see whether grinding the coarser zeolites would result in an improvement in their abilities to mitigate ASR.

In summary, all the natural pozzolans investigated in this research were able to mitigate expansions from ASR, provided that an adequate dosage was used. Most of the pozzolans needed replacement dosages between 15 and 25% to keep expansions below the 0.1% limit of ASTM C 1567 (2013), except for Zeolite-A which needed 35%. A clear trend was not found between the characteristics of the pozzolans and their performance in ASR testing. Pozzolans that needed a low replacement dosage to mitigate expansions were generally observed to have a low Ca/Si ratio. However, Zeolite-Z and fly ash did not fit into this trend. The good performance of these pozzolans was attributed to the presence of alumina in their chemical composition, which has been shown in previous literature to slow down the dissolution of reactive aggregates (Chappex and Scrivener, 2012b).

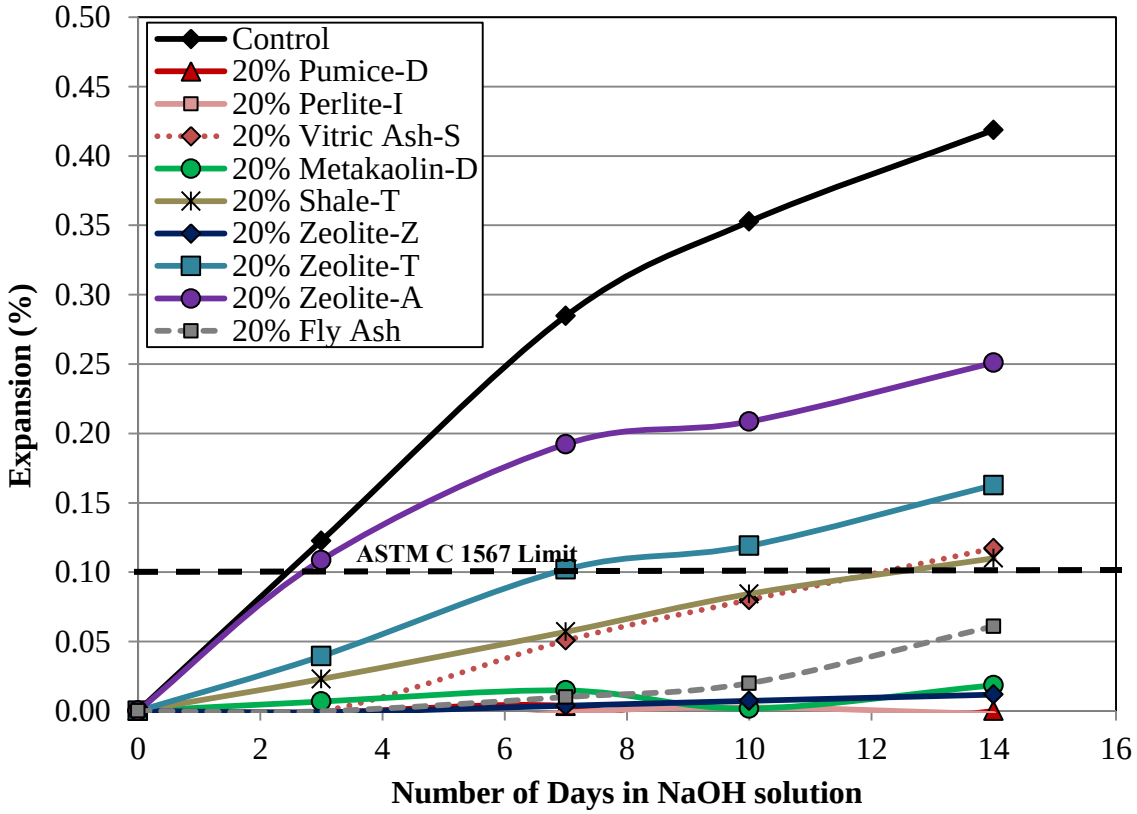

Figure 4.10: Expansions from ASR for mortar bars with 20% pozzolans

Table 4.4: ASR Expansion of 20% Pozzolan-containing Mortar Bars

Mortar Mixture Description	Expansion after 14 days of NaOH submersion
Control	0.419 ± 0.007
20% Pumice-D	0.000 ± 0.004
20% Perlite-I	-0.002 ± 0.003
20% Vitric Ash-S	0.117 ± 0.012
20% Metakaolin-D	0.019 ± 0.009
20% Shale-T	0.110 ± 0.001
20% Zeolite-Z	0.012 ± 0.007
20% Zeolite-T	0.163 ± 0.016
20% Zeolite-A	0.251 ± 0.018
20% Fly Ash	0.061 ± 0.007

Table 4.5: Calcium to Silicon Ratio (Ca/Si) of the Pozzolans

Material Name	Calcium to Silica Ratio (Ca/Si)
Pumice-D	0.01
Perlite-I	0.01
Vitric Ash-S	0.05
Metakaolin-D	0.01
Shale-T	0.04
Zeolite-Z	0.04
Zeolite-T	0.04
Zeolite-A	0.09
Fly Ash	0.22

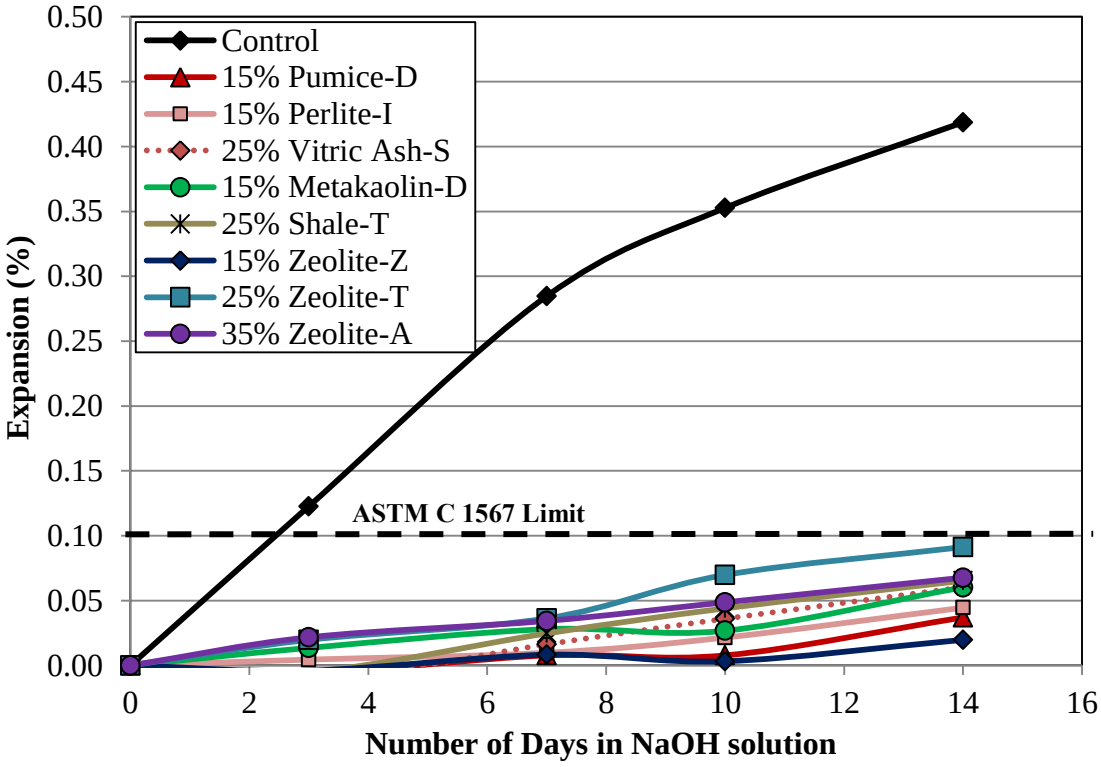

Figure 4.11: Minimum SCM replacement dosage needed to pass ASTM C 1567

Table 4.6: Expansion of Mortar Bars with Minimum SCM Dosage for ASR Mitigation

Mortar Mixture Description	Expansion after 14 days of NaOH submersion
Control	0.419 ± 0.007
15% Pumice-D	0.037 ± 0.004
15% Perlite-I	0.045 ± 0.005
25% Vitric Ash-S	0.060 ± 0.003
15% Metakaolin-D	0.060 ± 0.006
25% Shale-T	0.065 ± 0.006
15% Zeolite-Z	0.020 ± 0.003
25% Zeolite-T	0.091 ± 0.008
35% Zeolite-A	0.068 ± 0.002

4.3.2 Sulfate Attack

Figures 4.12 and 4.13 show expansions of the ASTM C 1012 (2013) mortar bars that were used to test ability of the pozzolans to resist sulfate attack. For clarity, the mortar mixtures with the lower SCM replacement dosage of 15% are presented in Figure 4.12, while the mortar mixtures with the higher SCM dosages of 25% and 35% are presented in Figure 4.13. The yellow dots in the graph represent the "ACI 201.2R: Guide to Durability" (2008) limits of Class 1, Class 2 and Class 3 sulfate exposure. An SCM qualifies for a Class 1 mild sulfate exposure if it can keep expansions below 0.1% for 6 months when tested for sulfate attack using ASTM C 1012. Similarly, an SCM qualifies for a Class 2 moderate sulfate exposure if it can keep expansions from ASTM C 1012 testing below 0.1% for 12 months. Finally, a Class 3 severe sulfate exposure requires the SCM to keep expansions from ASTM C 1012 testing below 0.1% for 18 months (ACI 201.2R, 2008).

From Figure 4.12, it can be seen that at 15% replacement dosage, the mortars of Pumice-D, Perlite-I and Zeolite-Z performed better than the fly ash mortar. All three pozzolans qualify for use in a Class 3 severe sulfate exposure environment, while the fly ash qualifies only for a Class 2 moderate sulfate exposure. Surprisingly, the 15% Metakaolin-D mortar had an inadequate performance under sulfate attack, crossing the 0.1% limit after 18 weeks, and completely cracking after 6 months. However, from Figure 4.13, it can be observed that the sulfate resistance of Metakaolin-D improved when a higher replacement dosage of the pozzolan was used. However, even at a 25% replacement, Metakaolin-D only qualified for a Class 2 sulfate exposure, unlike the Pumice-D, Perlite-I and Zeolite-Z mortars, which qualified for a Class 3 exposure at both 15% and 25% replacement levels. The fly ash mortar also qualified for a Class 3 exposure when a 25% replacement dosage was used. The Shale-T mortar, at 25% replacement, qualified for a Class 1 mild sulfate exposure. The 25% Vitric Ash-S mortar barely missed the Class 1 exposure limit, with its expansion crossing the 0.1% limit just before 6 months. The Zeolite-T and Zeolite A mortars, at replacement dosages of 25% and 35% respectively, had inadequate performances under sulfate attack, with expansions as high as 0.4% by 8 weeks. By 13 weeks, all of the Zeolite-A bars had cracked completely, while the Zeolite-T bars cracked at 15 weeks.

Although there is considerable ambiguity in previous literature about the mechanisms of sulfate attack (Schmidt et al., 2009), it is generally associated with the expansive reaction of penetrating sulfate ions with aluminate hydration phases like monosulfoaluminate (AFm) to form ettringite (Mullauer et al., 2013). As such, common methods of prevention are using low alumina cement, reducing the w/cm and/or incorporating SCMs into the mixture. Using a low alumina cement decreases the formation of aluminate hydration phases in concrete, whereas the use of SCMs and a

lower w/cm reduces the permeability of concrete and slows down the ingress of external sulfate ions into concrete (ACI 201.2R, 2008; Mindess et al., 2002). Previous research has linked the reduction in sulfate expansions when SCMs are used to the increased calcium hydroxide depletion caused from pozzolanic reactions of the SCMs (Janotka et al., 2011; Shehata et al., 2008; Khatib and Wild, 1998; Khatri and Sirivivatnanon, 1997). While the decrease in calcium hydroxide implicitly indicates a reduction of permeability due to the formation of C-S-H from the depleted calcium hydroxide, researchers suggest that an additional benefit of low calcium hydroxide content is that it limits the amount of gypsum formed from the reaction of calcium hydroxide and incoming sulfate ions (Mindess et al., 2002). Although the formation of gypsum does not significantly contribute to expansion, gypsum can react with AFm to produce ettringite, which is the phase that causes expansions when formed in the nanometer-sized pores of concrete (Mullauer et al., 2013; Schmidt et al., 2009). In the study presented here, it was seen that, with the exception of Metakaolin-D, all the natural pozzolans, which had calcium hydroxide reductions of 0.4 g or more per g of cement between 7-90 days (Table 4.1), were able to qualify for a Class 3 severe sulfate exposure at a replacement dosage of only 15%. The high alumina content of Metakaolin-D could be one of the reasons for its poor performance under sulfate attack. Previous research has shown the sulfate resistance of Class C fly ashes with high alumina contents to be inadequate (Tishmack et al., 1999). The researchers suggest that the availability of alumina in the fly ash reduces the ratio of sulfate ions to aluminate ions and favors the formation of AFm instead of ettringite during the initial cement hydration (Tishmack et al., 1999). The higher proportion of AFm becomes detrimental at later ages since it reacts with the incoming sulfate ions to form ettringite, which causes expansion when formed in the nanometer-sized pores of hardened concrete (Mullauer et al., 2013). A phenomenon similar to that of the fly ash

could be occurring with Metakaolin-D, since it also has a high alumina content. The unusual aluminate phase peak seen in the calorimetry curve for the Metakaolin-D paste (Figure 4.4) gives a slight indication of undersulfation, although typically undersulfation manifests as a much sharper aluminate phase peak than what was seen in Figure 4.4. As such, more research needs to be conducted to conclusively prove that undersulfation is occurring in the Metakaolin-D paste. Also, it must be noted that despite previous literature showing trends of undersulfation in calorimetry results of metakaolin, it has not yet been conclusively proven whether the undersulfation was caused by the participation of aluminates originating from the metakaolin pozzolan itself (Antoni et al., 2012).

Out of all the pozzolans, Zeolite-T and Zeolite-A had the worst performance when tested for resistance to sulfate attack. Although these two pozzolans have consistently shown poor reactivity and performance, the high w/cm that was used to achieve constant flow for the zeolite mortar mixtures could have contributed to their poor performance by making the mortar bars more permeable to ingress of sulfate ions. To eliminate the effect of w/cm on performance, a second set of zeolite mortar mixtures was made with a fixed w/cm. The expansion results of these mortar bars with a fixed w/cm are shown in Figure 4.14. From the results it can be observed that although the performance of the Zeolite-T and Zeolite-A mortars improved a little with the lower w/cm, these mortar mixtures still exceeded the 0.1% expansion limit before 4 months, and could not even qualify for a Class 1 mild sulfate exposure. However, it must be noted that although the low w/cm Zeolite-T and Zeolite-A bars crossed the 0.1% expansion limit before 6 months, they did not completely crack until 18 months, unlike the higher w/cm bars that fell apart before 6 months. The effect of w/cm was very apparent for the fly ash mortar mixtures as well. When made with a lower w/cm (0.45-0.46), both the 15% and 25% fly ash mortars had a Class 2 and Class 3 sulfate exposure, respectively.

However, when made at a higher w/cm (0.51), both fly ash mortars only qualified for a Class 1 exposure.

Unlike Zeolite-T and Zeolite-A, w/cm did not significantly affect the performance of the Zeolite-Z mortar, since it qualified for a Class 3 sulfate exposure regardless of the w/cm used. This suggests that Zeolite-Z might be affecting more than just the permeability of the mortar mixture. The unusual aluminate phase peak seen in the calorimetry curve for the Zeolite-Z paste (Figure 4.5) gives a slight indication of undersulfation. However, unlike Metakaolin-D, the amount of alumina in Zeolite-Z is not very high compared to the other natural pozzolans, so the theory of undersulfation due to an increased presence of alumina does not fit for Zeolite-Z. Instead a better hypothesis could be that the sulfates are being tied up with some other hydration phase, which leads to the superior performance of Zeolite-Z in sulfate attack. Another alternate theory, based on previous research on white cements (Skibsted and Anderson, 2013) is that the presence of alkali in the zeolite pores enhances the incorporation of alumina in C-S-H, which increases the ratio of sulfate ions to aluminate ions and favors the formation of ettringite instead of AFm in the early stages of hydration. More research studying the pore solution chemistry and phase assemblages in Zeolite-Z pastes must be done before these hypotheses can be validated. Table 4.7 provides a summary of sulfate expansion of the mortar bars along with the range of the data. With the exception of the 6 month reading for the 15% fly ash mortar (made with a w/cm of 0.51) all ranges are within the limits stated by ASTM C 1012, at expansions below 0.1%. At higher expansions, where the bars are undergoing heavy cracking, the range of the data became wider, as expected.

In summary, other than the two coarse zeolites, Zeolite-T and Zeolite-A, the natural pozzolans were seen to mitigate expansions from sulfate attack in varying degrees. Pumice-D, Perlite-I and Zeolite-Z were seen to have a superior performance to

fly ash, qualifying for Class 3 severe sulfate exposure at dosages of only 15%. Metakaolin-D was able to qualify for Class 2 moderate sulfate exposure at a dosage of 25%. Finally, at dosages of 25%, Shale-T was able to qualify for Class 1 mild sulfate exposure, while Vitric Ash-S barely missed this classification. Generally, pozzolans showing a high calcium hydroxide reduction performed well in the sulfate testing except for Metakaolin-D. The high alumina content of the calcined clay was considered to be the reason for this deviation.

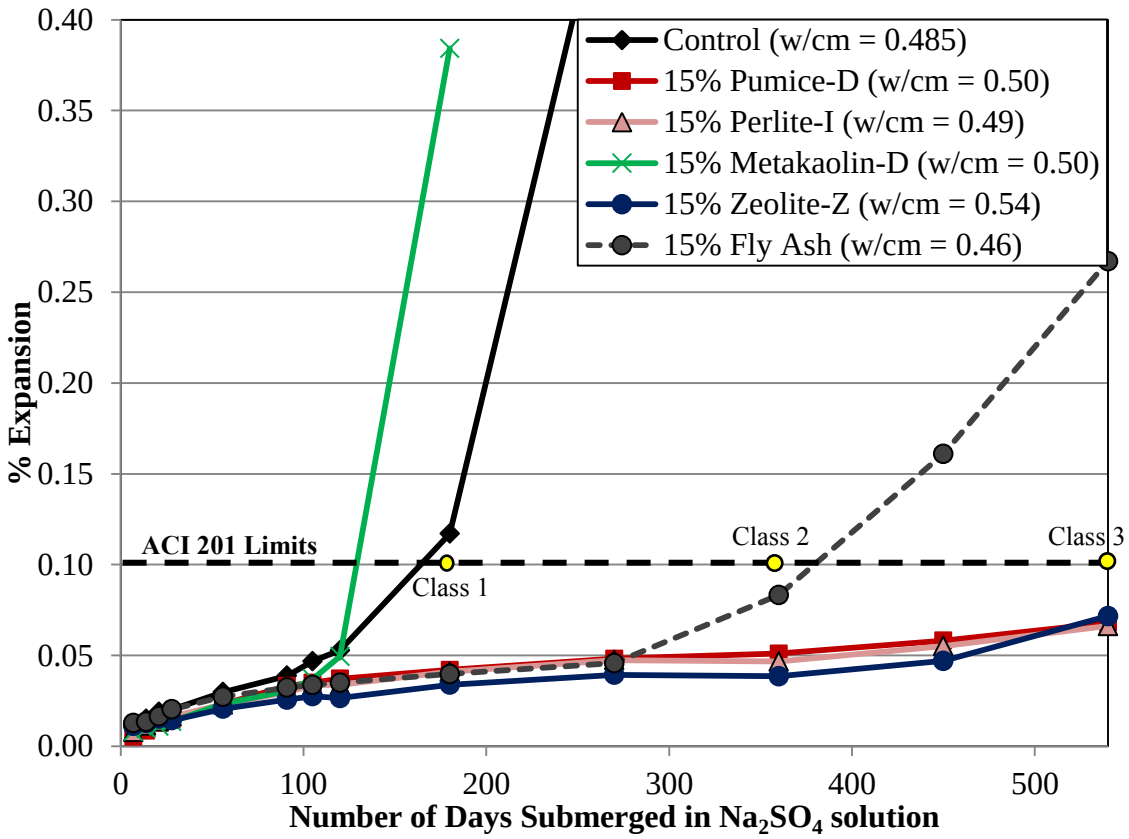

Figure 4.12: Expansions of ASTM C 1012 mortar bars with 15% SCM dosage

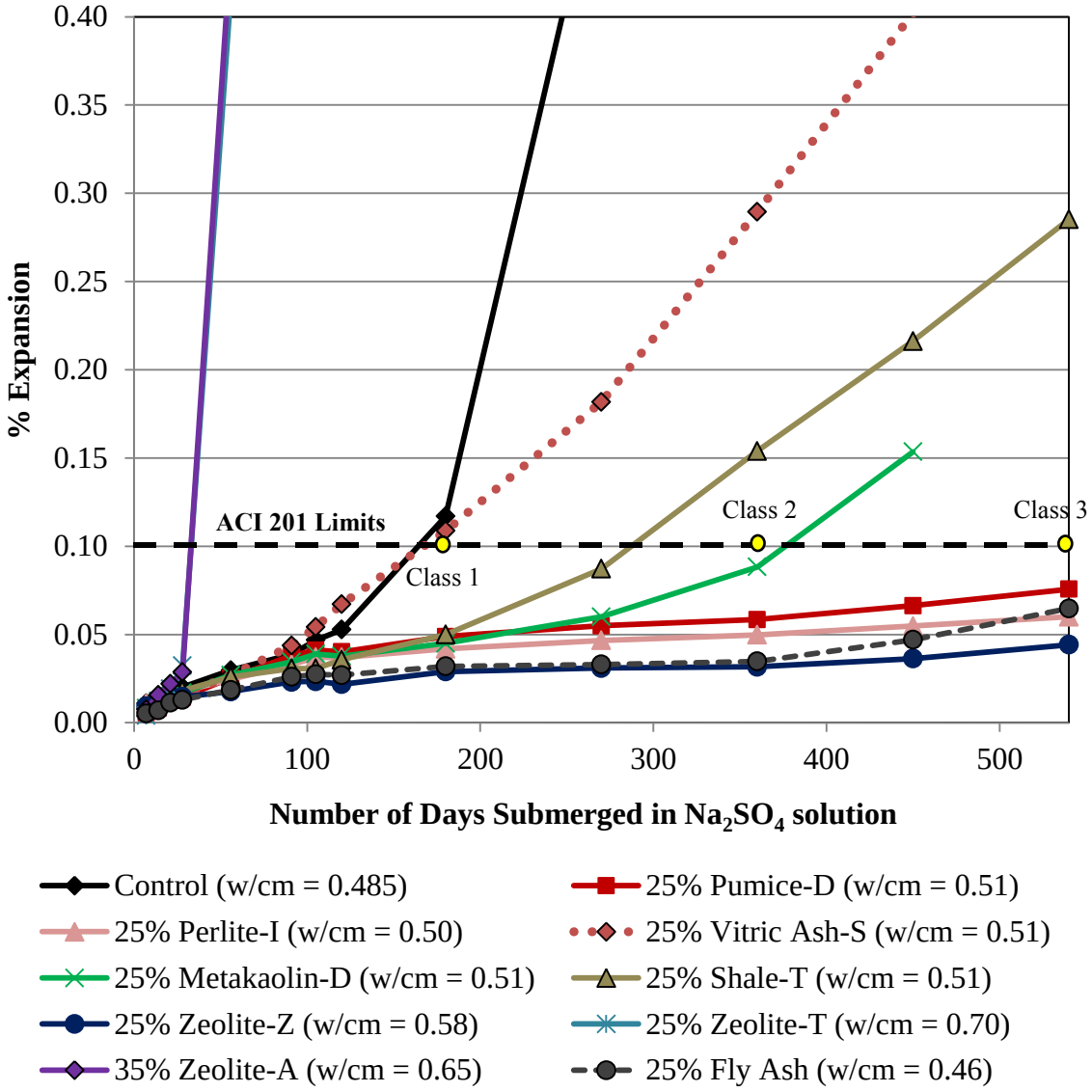

Figure 4.13: Expansions of ASTM C 1012 mortar bars with 25% or 35% SCM dosage

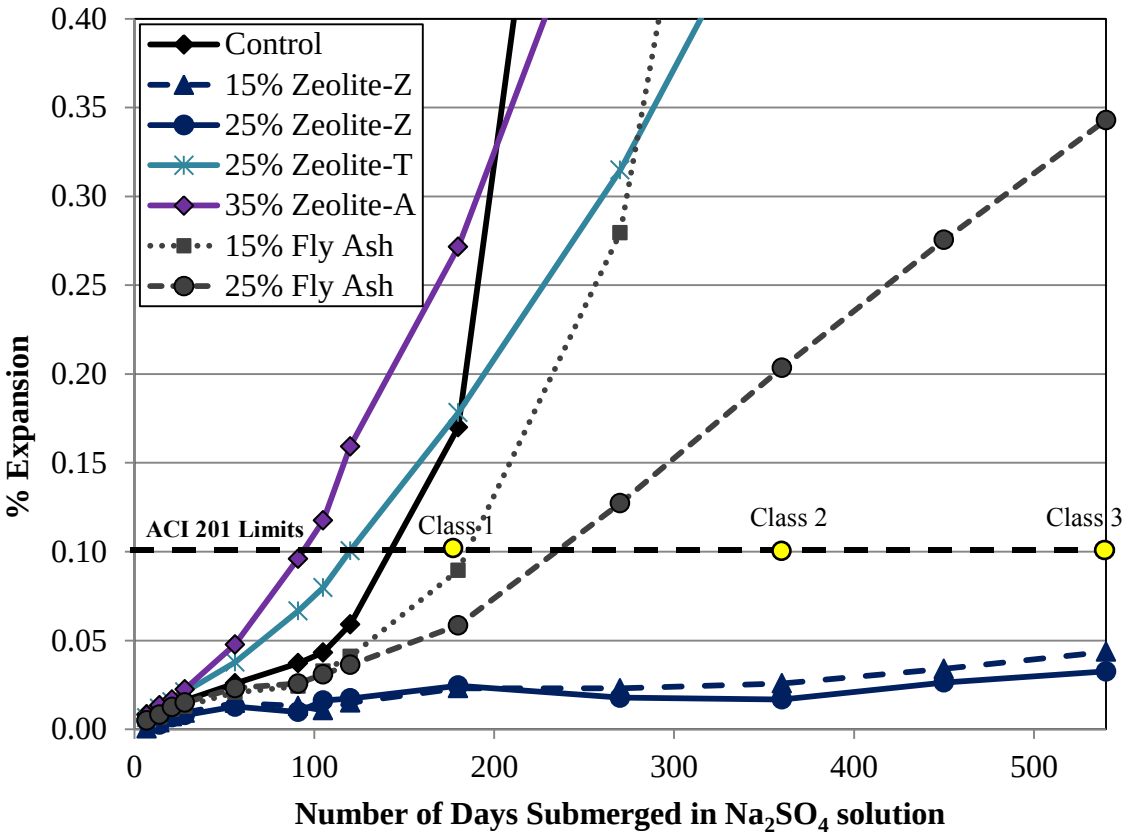

Figure 4.14: Expansions of ASTM C 1012 mortar bars with fixed w/cm ratio

Table 4.7: Summary of Sulfate Exposure Qualification and Mortar Bar Expansion

Mortar Mixture Description	w/cm	Sulfate Exposure	Expansion (%)
Control	0.485	Inadequate for sulfate attack	Exceeds 0.1 at 6 months
	0.51	Inadequate for sulfate attack	Exceeds 0.1 at 6 months
15% Pumice-D	0.50	Qualifies for Class 3	0.068 ± 0.009 at 18 months
25% Pumice-D	0.51	Qualifies for Class 3	0.076 ± 0.016 at 18 months
15% Perlite-I	0.49	Qualifies for Class 3	0.066 ± 0.016 at 18 months
25% Perlite-I	0.50	Qualifies for Class 3	0.060 ± 0.004 at 18 months
25% Vitric Ash-S	0.51	Barely misses Class 1 limit	0.109 ± 0.006 at 6 months
15% Metakaolin-D	0.50	Inadequate for sulfate attack	Cracks at 6 months
25% Metakaolin-D	0.51	Qualifies for Class 2	0.088 ± 0.017 at 12 months
25% Shale-T	0.51	Qualifies for Class 1	0.050 ± 0.005 at 6 months
15% Zeolite-Z	0.54	Qualifies for Class 3	0.072 ± 0.016 at 18 months
	0.51	Qualifies for Class 3	0.044 ± 0.009 at 18 months
25% Zeolite-Z	0.58	Qualifies for Class 3	0.044 ± 0.008 at 18 months
	0.51	Qualifies for Class 3	0.033 ± 0.005 at 18 months
25% Zeolite-T	0.70	Inadequate for sulfate attack	Cracks at 15 weeks
	0.51	Inadequate for sulfate attack	Exceeds 0.1 at 4 months
35% Zeolite-A	0.65	Inadequate for sulfate attack	Cracks at 13 weeks
	0.51	Inadequate for sulfate attack	Exceeds 0.1 at 15 weeks
15% Fly Ash	0.46	Qualifies for Class 2	0.083 ± 0.016 at 12 months
	0.51	Qualifies for Class 1	0.090 ± 0.033 at 6 months
25% Fly Ash	0.45	Qualifies for Class 3	0.065 ± 0.009 at 18 months
	0.51	Qualifies for Class 1	0.059 ± 0.008 at 6 months

4.4 PERFORMANCE PROBLEMS IDENTIFIED

From the results presented in this chapter, it was seen that, other than the two coarse zeolites, Zeolite-T and Zeolite-A, all the natural pozzolans investigated in this research can be used as replacements for Class F fly ash in concrete. Depending on the application, some of the pozzolans showed potential to perform even better than Class F fly ash. In terms of compressive strength, natural pozzolans like Metakaolin-D and Zeolite-Z had higher early age strengths than fly ash, while Pumice-D and Perlite-I

improved the long term strength of mortars more than what was observed for the fly ash. In terms of mixture workability, fly ash, with its spherical particle shape, still had the best performance but pozzolans like Shale-T and Vitric Ash-S did improve the paste viscosities to values similar to that of the fly ash paste. In terms of durability, all the natural pozzolans were able to mitigate ASR, provided an adequate dosage was used. Finally, pozzolans like Pumice-D, Perlite-I and Zeolite-Z had a superior performance compared to that of fly ash in mitigating expansions from sulfate attack.

Although six out of the eight natural pozzolans had good performance and can be used as alternatives to Class F fly ash, there are areas in which the performance of the pozzolans could be improved further. For example, despite improving long term compressive strength, some pozzolans mortars had low strengths during the first week of hydration, which could serve as a barrier to the use of those natural pozzolans in the construction industry. Additionally, the problems with mixture workability that were seen with the use of zeolites could prevent pozzolans like Zeolite-Z from being used in the field, despite having a superior performance to fly ash in terms of strength and durability. The next two chapters of the dissertation focus on ways to modify a subset of pozzolans tested in Chapter 4 so that their performance as SCMs can be further improved.

Chapter 5: Improving Compressive Strength of Pumice Mortars

This chapter focuses on ways to mitigate the low early age compressive strength of pozzolan mortars seen in Chapter 4. Since a variety of natural pozzolans were tested, many different pozzolan characteristics, such as surface area, porosity, chemical composition and crystalline impurities, were seen to influence the compressive strength of the pozzolan mixture. The surface area of the pozzolans, in particular, was observed to have one of the greatest influences on early age strength, since early hydration is dominated by the availability of sites where hydration products can nucleate and grow (Oey et al., 2013; Lothenbach et al., 2011). As such, this chapter investigates whether the early age strength of a pozzolan mixture can be increased by simply decreasing pozzolan particle size to increase surface area. In order to control for other factors that affect compressive strength, like chemical composition or crystalline impurities, only the three pumice pozzolans, with almost identical XRF chemical compositions (Table 3.2) and XRD results (Table 3.6), but different particle size distributions, were used for the research presented in this chapter. A finely ground inert quartz filler was also used to distinguish between the pozzolanic effects and size filler effects of the pumice pozzolans.

Particle size distributions of the three pumice pozzolans and quartz are presented in Figure 3.2, while their surface areas are presented in Table 3.5. From the results shown there, Pumice-N, with a d_{50} value of approximately 3 μm, was observed to have the finest particle size distribution and the largest surface area out of the three pumice pozzolans. Pumice-D is the middle in terms of both particle size and surface area, with a d_{50} value of approximately 13 μm. Pumice-S is observed to have the coarsest distribution and smallest surface area out of the three pumice pozzolans, with a d_{50} value of 20 μm. Since pumice pozzolans are porous (Presley, 2006) some of the surface area included in the BET results

might not be available as nucleation sites. As such, for the rest of the research presented in this chapter, size filler effects will be explained in terms of particle size of the pumice pozzolans rather than surface area. Although Pumice-D has a similar d_{50} value to that of the quartz, the particle size distribution of the quartz is slightly finer than that of Pumice-D. The surface area of quartz is lower than that of Pumice-D, but this is most likely due to the porosity of the pumice pozzolan that makes its BET surface area higher (Presley, 2006).

Compressive strength, isothermal calorimetry and TGA/DSC, the procedures of which are described in Section 2.3.1, were carried out on mixtures with all four materials (three pumice pozzolans and inert quartz) along with a control mixture that had no pozzolans/fillers. The compressive strength results were used to see whether decreasing the particle size of a pozzolan, without any other modification, could lead to increases in the strength of pumice mortars through filler effects. Data from isothermal calorimetry were used to corroborate the compressive strength data and observe whether the onset of the acceleratory phase occurred faster with decreasing particle sizes of the pumices. Additionally, the calorimetry curve of the inert quartz filler was compared with those of the pumice pozzolans to determine if strength losses were a result of diluting the cement content. Finally, the data from TGA were used to observe whether decreasing the particle size could increase the rate of the pozzolanic reaction.

5.1 COMPRESSIVE STRENGTH

Figure 5.1 shows the average compressive strength of the pumice and quartz-containing mortars made at a w/cm of 0.5. The error bars represent the range of the data. All the ranges are within the limits prescribed by ASTM C 109, except for the 3 day

compressive strength of the Pumice-D mortar. The range for this reading was approximately 8% of the average, instead of being less than or equal to 7.6%, as suggested by ASTM C 109 (2011). For more information about the compressive strength data analysis, please refer back to section 2.3.1.1.

From Figure 5.1, the trend of increasing compressive strength with decreasing pozzolan particle size can be clearly observed. The mortar with the finest pumice, Pumice-N, had the highest strength out of the three pumice-containing mortars at all ages. By 7 days, the strength of the Pumice-N mortar was equivalent to that of the control, and by 28 days its strength had surpassed that of the control by 40%. The mortar of Pumice-D, had strength similar to that of the control by 28 days, while the mortar of the coarsest pumice, Pumice-S, reached an equivalent strength to the control mortar at 90 days. Since these pumices are identical in composition, the differences in their mortar's rate of strength gain can be solely attributed to the differences in their particle size distributions.

The compressive strength of the inert quartz mortar gives insight into the role of size and space filler effects on compressive strength. The strength of the inert quartz mortar was always consistently lower than that of the control, and this difference can be completely ascribed to the dilution effect (Camiletti et al., 2013; Weerdt et al., 2012) since quartz, being an inert filler, should not negatively affect cement hydration. Since the replacement dosage was 20%, the strength of the quartz mortar was not expected to exceed 80% of the control mortar, due to dilution. However, the strength of the quartz mortar ranged from 81 - 91% of the control at the different ages that it was tested. Since quartz is not pozzolanic, this increase in strength beyond 80% must be due to size and space filler effects. During the early stages, when hydration is dominated by the availability of sites where hydration products can nucleate and grow (Oey et al., 2013; Lothenbach et al., 2011), the increase in compressive strength of the quartz mortar

beyond 80% is most likely due to size filler effects provided by the fine particles of quartz. At later stages, when hydration is dominated by the impingement of hydration products (Bullard et al., 2011) the increase in strength of the quartz mortar is most likely due to space filler effects, where additional hydration products are formed due to increased space per grain of cement, resulting from the replacement of cement with the filler material. (Oey et al., 2013; Lothenbach et al., 2011).

The influence of size and space filler effects on compressive strength of pumice pozzolans can be observed by comparing the 1 day compressive strength of the pumice mortars to that of quartz mortar. At 1 day, the pozzolanic reactions are considered to be negligible (Lothenbach et al., 2011), and since 20% of the cement was replaced in all the pumice mortars, strength increases beyond 80% of the control at 1 day can be attributed to size and space filler effects. The mortar of Pumice-N, the finest pumice, had 1 day compressive strength that was about 90% of the control, whereas the quartz filler, which was coarser than Pumice-N, had 1 day mortar strength that was approximately 81% of the control. This indicates that the very fine particles of Pumice-N are providing greater amount of nucleation sites than the quartz particles, which results in the higher strength of the Pumice-N mortar, relative to the quartz mortar. Pumice-D and Pumice-S, which were both coarser than quartz, had 1 day mortar strengths that were 75% and 65% of the control, respectively. Since these strengths were lower than 80%, it was assumed that the particles of Pumice-D and Pumice-S do not significantly contribute to size filler effects. Due to dilution of the cement content, all the pumice and quartz pastes were expected to have space filler effects to some degree. Since the replacement was done in terms of cement mass, the quartz paste was expected to have the greatest space filler effect since its density is higher than that of the pumices, which results in a lower volume. Results from the calorimetry provide further confirmation of this hypothesis.

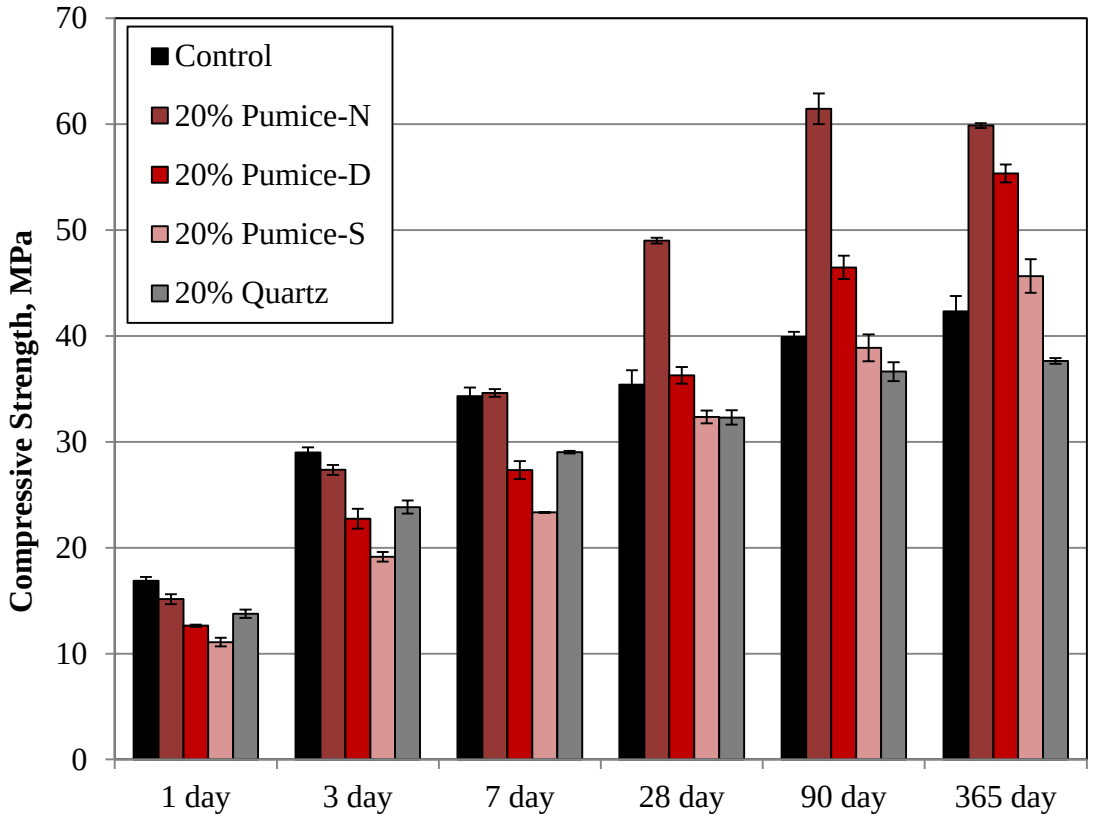

Figure 5.1: Compressive strength of control, pumice and quartz mortars at w/cm of 0.50

5.2 HEAT OF HYDRATION

The data from isothermal calorimetry were used to corroborate the compressive strength data and see how the decreasing particle size of the pumices affected cement hydration. Since quartz is an inert material and cannot retard cement hydration, the calorimetry curves of the pumice pastes were also compared to that of the quartz filler to check if the early age strength decrease seen in the compressive strength data of the pumice mortars was a result of diluting the cement content or due to retardation of cement hydration from the addition of pumice pozzolans. Figure 5.2 shows the rate of

heat produced in the pastes during hydration. Please note that the rate of heat evolved has been normalized to the amount of cement in the paste.

From Figure 5.2, it can be observed that the rate of heat curve for the Pumice-N paste is shifted significantly to the left of the control curve, indicating an earlier onset of the acceleratory period of cement hydration, compared to that of the control paste. On the other hand, the rate of heat curves representing the Pumice-D, Pumice-S and quartz pastes do not show a significant deviation to the left of the control curve. This suggests that the paste containing Pumice N, which has a finer particle size distribution than the cement, exhibited enhanced nucleation and growth of hydration products, whereas the size filler effects are minimal in the pastes containing Pumice-D, Pumice-S and quartz, which all have particle size distributions similar to or larger than cement.

From Figure 5.2, it can be also be observed that the acceleratory phase in the pastes containing the pumices occurred at the same time or faster than that of the paste with quartz, which cannot retard cement hydration due to its inert nature. As such, it can be concluded that like the inert quartz, the addition of the pumice pozzolans does not retard cement hydration. Since the size filler effect of the Pumice-D and quartz mortar was similar, as observed in the rate of heat curves, the higher strength of the quartz mortar at 1 day compared to the Pumice-D mortar (Figure 5.1) must be due to space filler effects, which promote the growth of additional hydration products due to increased space per grain of cement. Space filler effects are shown in the calorimetry rate of heat data by the elongation of the deceleration phase of cement hydration. Although from Figure 5.2 the difference cannot be discerned very easily, the quartz paste is expected to have a higher space filler effect than the pumice pastes due to the higher density of the quartz particles, which leads to higher space being available per grain of cement in the quartz paste compared to the pumice pastes.

Previous literature has shown size filler effects to affect the hydration of the aluminate phases more than that of the silicate phases (Antoni et al., 2012; Lothenbach et al., 2011). This phenomenon was clearly observed in the heat rate curve of the Pumice-N paste, which has a higher aluminate peak (second peak after initial dissolution peak) than the silicate peak (first peak after initial dissolution peak). This effect is not seen in the other two pumice mixtures or the quartz paste, which was not surprising since the Pumice-N paste had the most pronounced size filler effect due to the fineness of the Pumice-N particles.

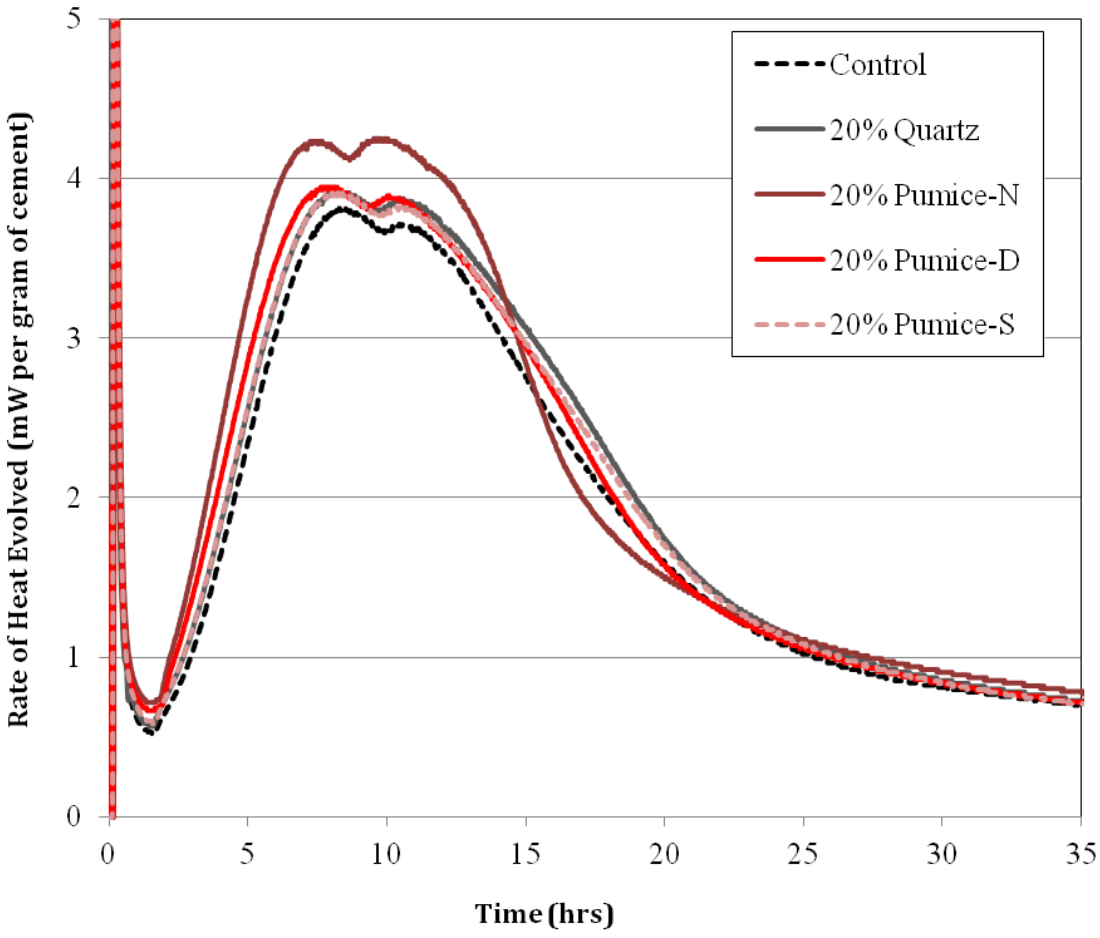

Figure 5.2: Rate of heat produced during hydration for control, pumice and quartz pastes

5.3 CALCIUM HYDROXIDE CONTENT

Calcium hydroxide content of the pastes was measured using TGA/DSC to observe whether decreasing the particle size could, in addition to size filler effects, cause an increase in the rate of the pozzolanic reaction. Figure 5.3 presents the calcium hydroxide content of the pastes, normalized to the amount of cement in the mixture. The calcium hydroxide levels per gram of cement of the pumice and quartz pastes were expected to be the same as the control or higher, to account for the enhanced nucleation of hydration products from size and space filler effects. Over time, the calcium hydroxide content of the pumice pastes was expected to decrease as the pozzolans react with the calcium hydroxide to form calcium silicate hydrate. Since quartz is inert, the calcium hydroxide content of the quartz paste was expected to be the same over time, or increase due to size and space filler effects (Antoni et al., 2012).

From Figure 5.3, it can be seen that as early as 7 days, the Pumice-N paste showed a slight decrease in calcium hydroxide content relative to that of the control. On the other hand, the paste with Pumice-D, which was sourced from the same location as Pumice-N and identical in all aspects except for particle size, did not show a significant decrease in calcium hydroxide content at 7 days. This illustrates that, although pozzolanic reaction is considered to be negligible in the earlier stages of hydration (Lothenbach et al., 2011), it is possible to increase the rate of pozzolanic reaction by grinding pozzolans to a smaller particle size.

Even after 7 days, the rate of calcium hydroxide depletion in the Pumice-N paste continued to be faster than the two other pumice pastes. At 28 days, the calcium hydroxide content in the Pumice-N paste was about 24% lower than that of the control. By 90 days, the calcium hydroxide level was reduced even further to be about 45% lower than that of the control. On the other hand, the Pumice-D paste did not show a significant

reduction in calcium hydroxide content until 90 days, when the calcium hydroxide level was seen to be 18% lower than that of the control. Even at 90 days, the Pumice-S paste did not show any significant reduction of calcium hydroxide content, compared to that of the control. Since the pumices are almost identical in composition, the differences in calcium hydroxide level can be solely attributed to particle size. This is interesting because it shows that effects of particle size play a role even during the late stages of hydration, and that the rate of pozzolanic reactivity can be improved through a decrease in particle size.

The calcium hydroxide content of the quartz paste was observed to be similar to that of the control at 7 days. As expected, over time the calcium hydroxide content of the quartz paste actually increased relative to the control due to size and space filler effects. This trend of increased calcium hydroxide contents of quartz pastes at 28 and 90 days has been seen in previous literature as well (Antoni et al., 2012). Comparing the calcium hydroxide contents of the pumice pastes to that of the inert quartz, instead of the control, perhaps gives a better idea of the total amount of calcium hydroxide that was reduced by the pumice pozzolans, whose pastes also exhibited size and space filler effects. The 90 day calcium hydroxide contents of the Pumice-N, Pumice-D and Pumice-S pastes were lower than that of the inert quartz paste by 50%, 26% and 12%, respectively. However, since the level of size filler effects depend on the particle size of the pozzolans/fillers, comparing the Pumice-N and Pumice-S paste to that of the quartz gives only an approximation, since their particle size distributions are very different. The comparison of the Pumice-D and quartz paste was considered to be more accurate, since the particle size distribution of quartz was the closest to that of Pumice-D.

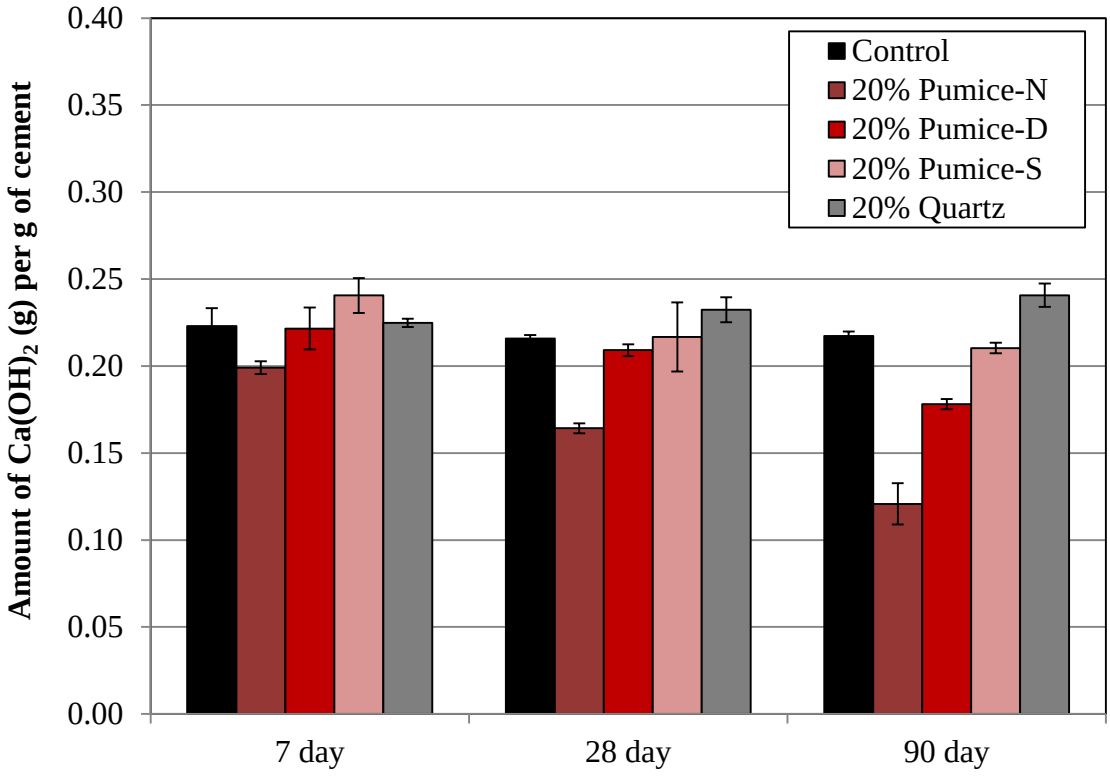

Figure 5.3: Calcium hydroxide content of the control, pumice and quartz pastes

5.4 Conclusions of Strength Improvement Study on Pumice Mixtures

Pumice pozzolans, with almost identical chemical composition but different particle size distributions, were used to study the effect of particle size on compressive strength of mortar. In summary, it was found that decreasing the particle size of a pozzolan resulted in higher early age compressive strength of the mixture due to size filler effects that enhance the nucleation and growth of hydration products. In addition to filler effects, decreasing the particle size of the pozzolan also resulted in an increase of the rate of pozzolanic reaction. These results are significant, since it provides a relatively simple technique to improve the early age strength of unaltered volcanic pozzolans which were seen in Chapter 4 to only benefit compressive strength at later ages.

Chapter 6: Improving the Effect of Zeolites on Mixture Workability

The poor workability of zeolites mixtures has been well documented in previous literature (Bilim, 2011; Ahmadi and Shekarchi, 2010; Perraki et al., 2010). The research presented in this dissertation has also shown zeolites to have a high water demand (Table 3.1) and to increase the viscosity of paste mixtures compared to that of the control mixture with no pozzolans incorporated (Figure 4.8). This chapter focuses on ways to mitigate the high water absorption of zeolites, as problems with mixture workability could serve as a barrier to the use of zeolites as SCMs in the construction industry.

The porosity of the zeolites, which range from micropores in the crystalline structure of the zeolite itself to mesopores that are created from voids left between crystal aggregates (Elaiopoulos et al., 2010), is one of the main reasons behind the poor workability of zeolite mixtures. The porosity of the zeolites results in a high surface area (Table 3.5) that increases the amount of water needed to fully coat the particle surfaces (Mindess et al., 2002). Additionally, the micropores in the zeolites contain cations that can absorb water through charge-dipole interactions (Snellings et al., 2012) and increase the water demand of the material. The presence of clay impurities like montmorillonite, as seen in the XRD results of Zeolite-T (Table 3.6) can exacerbate the water demand of the material as well, since clay can absorb water due to the interchangeable cations that are present in its layered structure (Fernandez et al., 2011a; Foster, 1954).

Previous literature has suggested that calcination causes destabilization of the zeolite crystal latticework and increases the ability of the zeolites to participate in pozzolanic reactions (Fernandez et al., 2011b; Habert et al., 2008; Perraki et al., 2005; Liebig and Althaus, 1998). However, the effect of calcination on zeolite mixture workability has not been investigated in these previous studies. For the research

presented in this chapter, it was hypothesized that calcination of the zeolites would improve its mixture workability as well, since destabilization of the crystal latticework could lead to an alteration of the micropores that absorb water due to the presence of cations. Additionally, research on thermally treated zeolites has shown the surface area of the zeolites to be decreased through calcination (Ates and Hardacre, 2012), although it was not conclusively proven whether the reduction in surface area was due to a decrease in porosity from the destabilization of the zeolite structure, or through an agglomeration of particles, or both. However, it was hypothesized for this research that regardless of the cause, the reduction in surface area of the zeolites would lead to an improvement in mixture workability, since less water will be required to coat the reduced particle surface area (Mindess et al., 2002). Based on previous research (Fernandez et al., 2011a), it was also hypothesized that calcination would dehydroxylate the clay minerals and reduce its water absorption capacity, which in turn would lower the overall water demand of pozzolans like Zeolite-T that contained clay impurities like montmorillonite.

To test the aforementioned hypothesis, the zeolites were calcined at a temperature of 800°C, following the calcination procedures presented in Section 2.4. BET measurements, which use nitrogen gas adsorption to measure surface area, were used to understand the effect of calcination on the zeolite surface area. However, the BET surface area measurements cannot take into account the zeolite micropores, since they are inaccessible to the nitrogen molecules due to the presence of the cations (Elaiopoulos et al., 2010). As such, XRD was conducted to understand the effect of calcination on the zeolite crystalline structure, which can give an indication of the effect of calcination on the zeolite micropores. The procedures of BET and XRD are detailed in Section 2.2.3 and Section 2.2.5, respectively. Additionally, TGA results on the zeolites from Section 3.6 (Table 3.7) are used to explain the changes that are happening to the zeolite structures as

they undergo calcination. Finally, rheology testing, the procedures of which are described in Section 2.3.2, was conducted on pastes with 20% calcined zeolite to see whether calcination decreased the yield stresses and viscosities that were seen in the rheology testing of pastes containing the uncalcined zeolites (Figure 4.8).

6.1 Effect of Calcination on Surface Area and Crystalline Structure of Zeolites

Figures 6.1 – 6.3 show the changes that occurred in the zeolite crystalline structure as it was calcined. For all three zeolites, it can be seen that the clinoptilolite peaks decreased in intensity or completely disappeared after calcination at 800°C, indicating a significant reduction in the crystallinity of the zeolite minerals. The loss of crystallinity of the clinoptilolite minerals suggests that the structure of the zeolites starts to become destabilized at higher temperatures, which could alter the cation containing micropores of the zeolites (Snellings et al., 2012). The TGA/DSC results of the zeolites, originally discussed in Section 3.6 and presented in Figures 6.4 – 6.6, provide further insight into the changes that occur in the structure of the zeolites as they are heated. The DSC plots of all three zeolites had two major endothermic peaks. Previous research by Villa et al. (2013) suggests that the initial endothermic peak at lower temperatures corresponds to the removal of water molecules, while the later peak at higher temperatures corresponds to the collapse of the zeolite structure. Interestingly, from Figure 6.4, it can be observed that the second endothermic peak of Zeolite-Z occurs after 800°C, whereas for both Zeolite-T and Zeolite-A, the second endothermic peak occurs before 800°C (Figure 6.5 and 6.6). This suggests that a higher calcination temperature may be required than the one used in this research to fully destabilize the structure of Zeolite-Z.

Table 6.1 shows the BET surface area of both the uncalcined and the calcined zeolites, along with the range of data from duplicate testing. From the results, it can be observed that calcination significantly reduces the surface area of the zeolites. While the XRD and DSC data suggest that the reduction in surface area is due to the destabilization of the zeolite structure and the collapse of the pores due to dehydroxylation, previous research has suggested that the reduction could also be due to agglomeration and sintering of the zeolite particles themselves (Ates and Hardacre, 2012; Elaipoulos et al., 2010). More research using SEM imaging and porosity analysis needs to be done to conclusively understand the reasons behind the decrease in surface area of zeolites after calcination.

The greatest reduction in surface area was seen for Zeolite-T, the zeolite with the highest initial surface area (Table 3.5). The XRD results (Table 3.6) showed Zeolite-T to be the only zeolite with detectable clay impurities. In addition to the changes occurring to the zeolite particles, the comparatively high surface area reduction of Zeolite-T could also be due to the agglomeration and dehydroxylation of its clay impurities (Fernandez et al., 2011a; He et al., 2000). The surface area reduction of Zeolite-Z and Zeolite-A were similar in value to each other. Despite the reductions in surface area, the relative ranking of the surface areas between the zeolites remained unchanged before and after calcination, with Zeolite-T having the highest surface area, and Zeolite-A having the lowest.

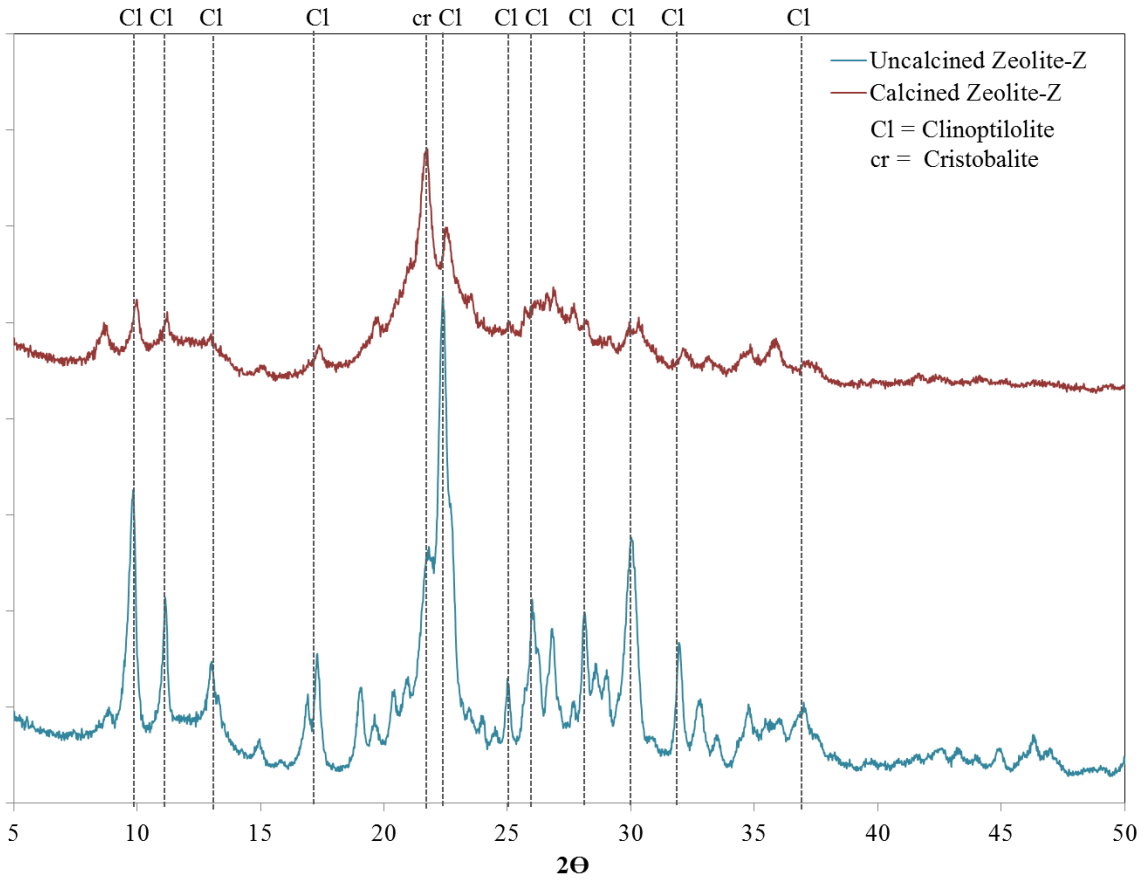

Figure 6.1: Changes to the XRD pattern of Zeolite-Z after calcination

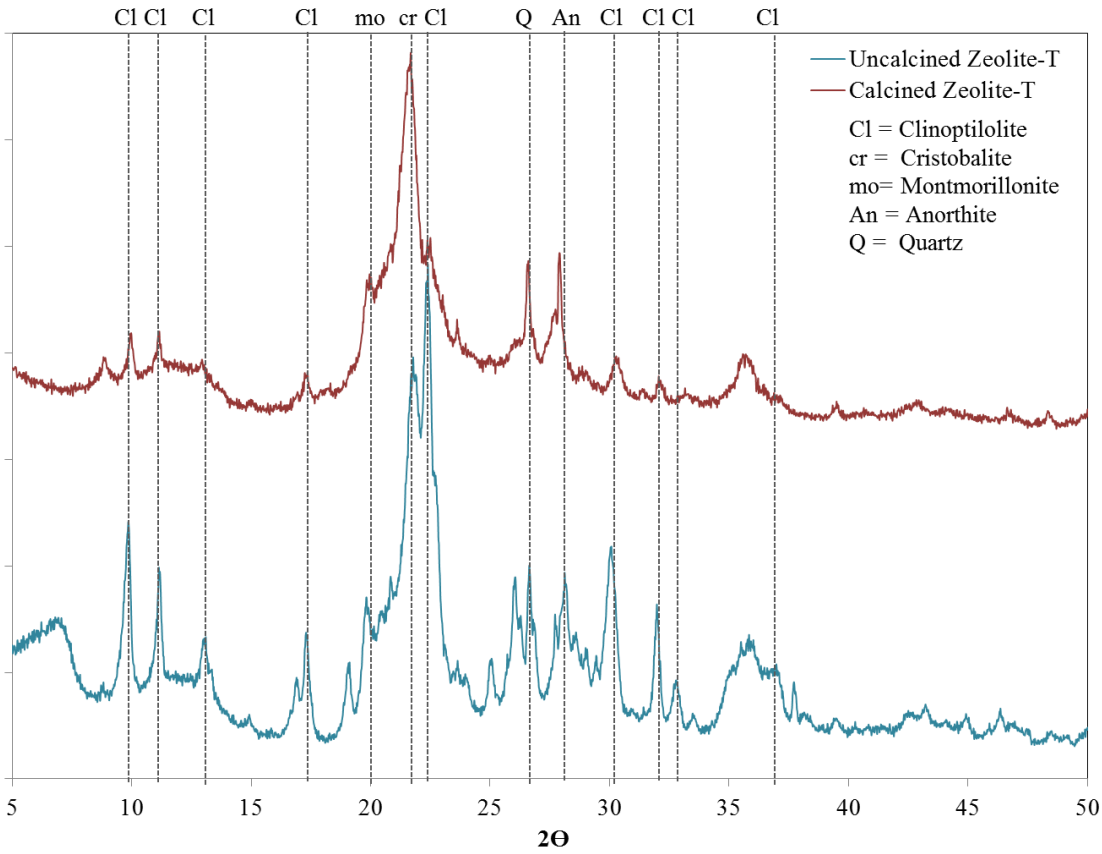

Figure 6.2: Changes to the XRD pattern of Zeolite-T after calcination

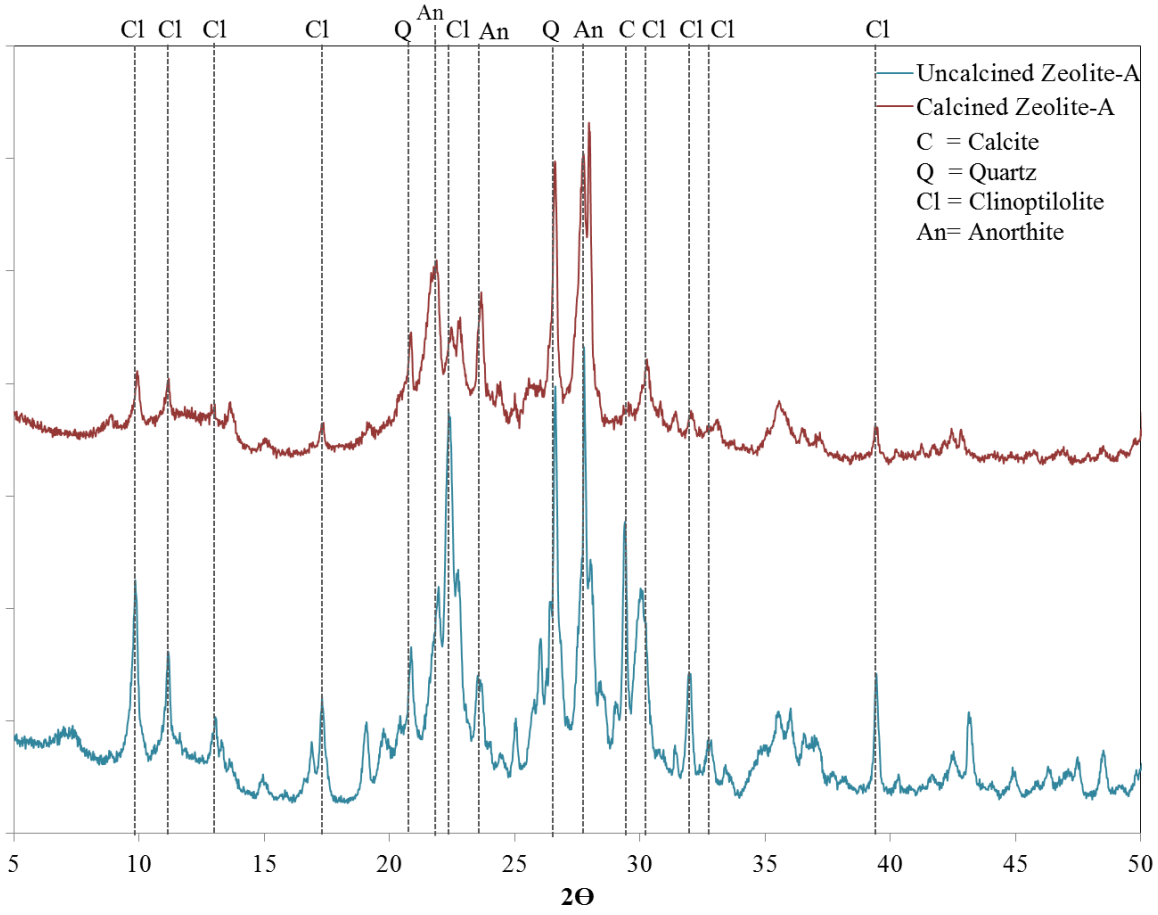

Figure 6.3: Changes to the XRD pattern of Zeolite-A after calcination

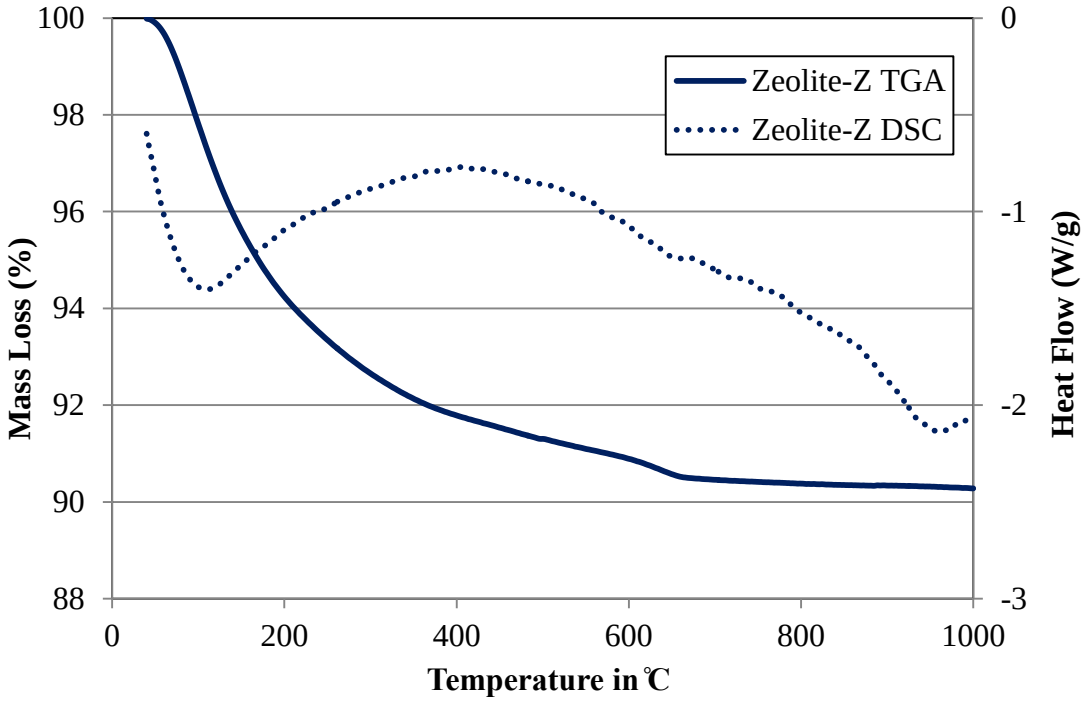

Figure 6.4: TGA/DSC plot of Zeolite-Z

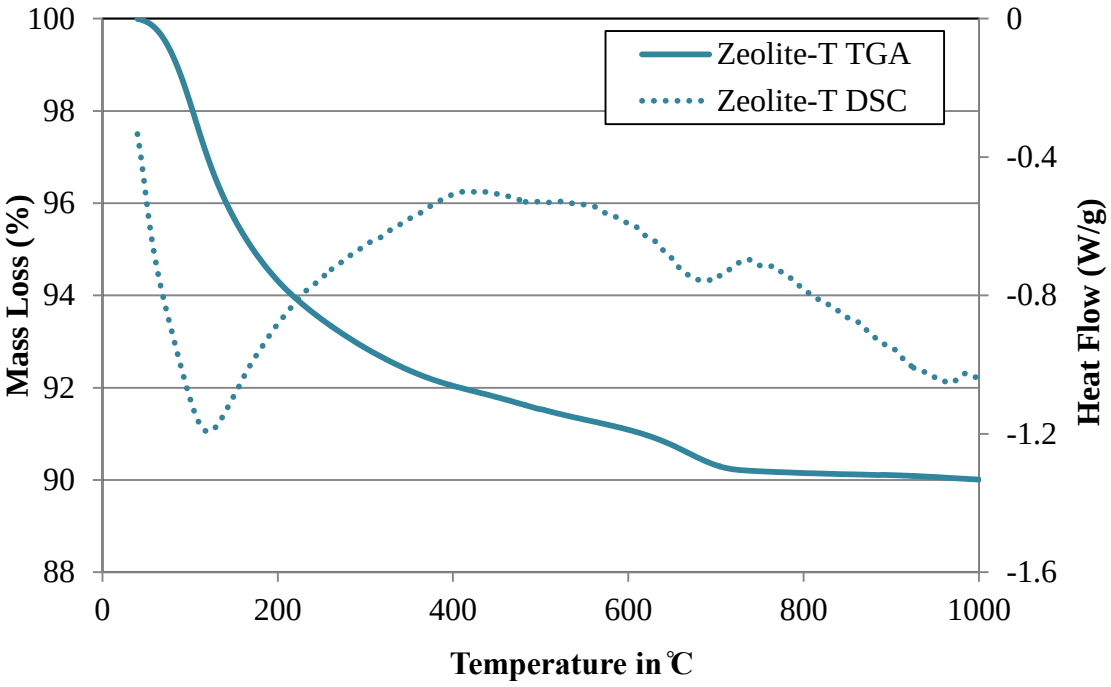

Figure 6.5: TGA/DSC plot of Zeolite-T

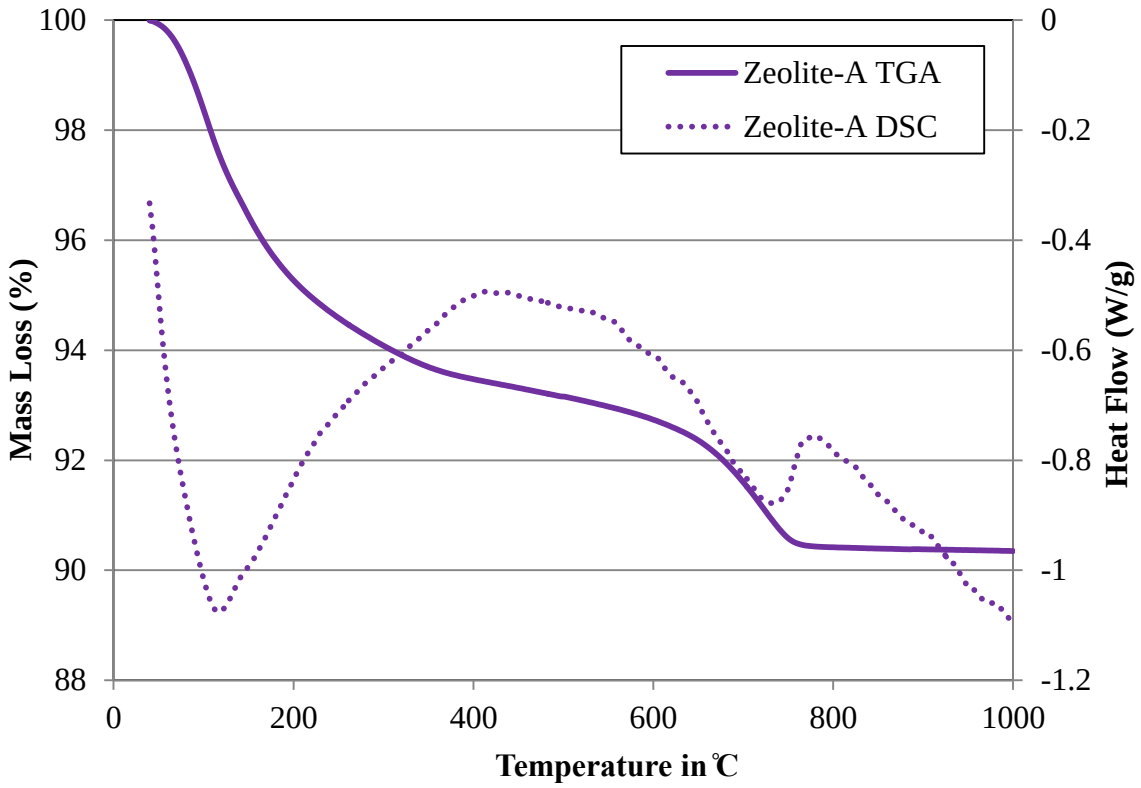

Figure 6.6: TGA/DSC plot of Zeolite-A

Table 6.1: BET Surface Area of Uncalcined and Calcined Zeolites

Material Name	BET Surface Area (m^2/g)		Reduction in Surface Area (m^2/g)
	Uncalcined	Calcined	
Zeolite-Z	42.00 ± 0.57	24.36 ± 0.16	17.64 ± 0.73
Zeolite-T	59.01 ± 0.47	35.05 ± 0.51	23.96 ± 0.98
Zeolite-A	25.98 ± 0.01	7.64 ± 0.15	18.34 ± 0.16

6.2 RHEOLOGY TESTING OF CALCINED ZEOLITE PASTES

Figure 6.7 presents representative rheological curves for the uncalcined and calcined zeolite pastes at a replacement dosage of 20%. For comparison purposes, the same rheological model that was used to interpret the data for the uncalcined zeolite pastes (discussed in Section 4.2) was also utilized to understand the rheological properties of the calcined zeolite pastes. The pastes for the uncalcined Zeolite-Z and Zeolite-A were analyzed using the linear Bingham model. As such, the yield stresses and viscosities of the calcined Zeolite-Z and Zeolite-A pastes, presented in Table 6.2 and 6.3, were also found using the Bingham model. The ranges of the data from duplicate testing are also shown in Table 6.2 and 6.3. The uncalcined Zeolite-T paste, however, was evaluated using apparent viscosity at each shear rate, due to its non-linear response to increasing shear rate. Although the non-linear behavior is not present after calcination, the calcined Zeolite-T paste was also evaluated using apparent viscosity at each shear rate, so that the results between the uncalcined and calcined states could be compared. The apparent viscosities of the Zeolite-T paste are presented in Table 6.4, along with the range of the data from duplicate testing.

Results from the rheology testing confirmed the hypothesis that calcination of the zeolites improved its mixture workability. From Figure 6.7, it can be observed that before calcination, at any given shear rate, the Zeolite-Z and Zeolite-T mixtures exhibited significantly higher shear stresses than the control mixture, indicating the poor mixture workability of the Zeolite-Z and Zeolite-T paste. However, after calcination, both the Zeolite-Z and Zeolite-T mixtures showed lower shear stresses than their uncalcined counterpart across all shear rates, indicating an improvement in the mixture workability. From Figure 6.7, it can be observed that the Zeolite-T paste had the biggest improvement in its mixture workability after calcination, with its shear stresses being lower than the

control paste across all shear rates. From Table 6.4, it can be seen that the reduction in apparent viscosity of the Zeolite-T paste before and after calcination was significant, approximately ranging between 4 to 1 Pa.s across different shear rates. Additionally, it was observed that after calcination, the Zeolite-T paste no longer exhibited significant shear thinning behavior (decrease in apparent viscosity) as the shear rate was increased. Before calcination, the apparent viscosity decreased by 2.80 Pa.s between the shear rates of 10 s^{-1} and 50 s^{-1}, while after calcination this reduction was only 0.43 Pa.s. The improvement after calcination was less pronounced for the calcined Zeolite-Z paste, with its Bingham yield stress and viscosity (presented in Table 6.2 and 6.3) still being much higher than that of the control paste. The reduction in Bingham yield stress and viscosity between the uncalcined and calcined Zeolite-Z paste was less than 4 Pa and 1 Pa.s, respectively. The yield stress and viscosity of the uncalcined Zeolite-A paste was already comparable to that of the control paste before calcination. However, calcination improved the workability of the Zeolite-A mixture even further, with a reduction of about 4 Pa in the Bingham yield stress, and a reduction of less than 0.3 Pa.s in the Bingham viscosity.

The rheology results of the calcined zeolite mixtures were correlated back to the changes observed in the physical properties of the zeolites after calcination, to understand the reasons behind the improved mixture workability. One of the initial hypotheses for this research was that the reduction in surface area through calcination would improve mixture workability due to less water being required to coat the reduced particle surface area (Mindess et al., 2002). From the results, it was observed that Zeolite-T, which had the greatest reduction in surface area after calcination also showed the biggest improvement in its mixture workability. However, even with the largest reduction in surface area, Zeolite-T still had a higher surface area than Zeolite-Z and Zeolite-A. This indicates that, although the reduction in surface area might have partially contributed to

the improvement of mixture workability, the decrease in surface area by itself cannot fully explain the improved mixture workability of the Zeolite-T mixture. Another hypothesis for the research presented in this chapter was that calcination of the zeolites would improve its mixture workability by destabilizing the zeolite crystal structure, which in turn would alter the micropores that absorb water due to the presence of cations and cause shear thinning by releasing the absorbed water at higher shear rates (Sahmaran et al., 2008). The observed loss of shear thinning behavior of the calcined Zeolite-T paste supports this hypothesis, since it suggests that calcination has rendered the zeolite micropores ineffective at absorbing water. The XRD and DSC data of Zeolite-T further corroborate this hypothesis since they respectively show the loss of crystallinity of the zeolite mineral after calcination, as well as the collapse of the zeolite structure before 800°C. The diminished effect of calcination on the workability of the Zeolite-Z paste can also be explained by this hypothesis of calcination improving mixture workability through the destabilization of the zeolite structure. The late occurrence (after 800°C) of the second endothermic peak in the DSC results of Zeolite-Z (Figure 6.4) suggests that the Zeolite-Z structure might not be fully destabilized at 800°C and that a higher calcination temperature might be needed to lower the viscosity and yield stress of the Zeolite-Z paste to values comparable to that of the control paste. In other words, the results presented here suggest that the improvement in zeolite mixture workability is more dependent on changes to the zeolite structure and porosity that dictate its water absorption capacity, instead of a reduction in surface area that lowers the amount of water needed to coat the zeolite particles. Finally, it must be noted that the improvement in mixture workability of the Zeolite-T paste can also be partially attributed to the calcination of its montmorillonite clay impurities (Fernandez et al., 2011a; He et al., 2000).

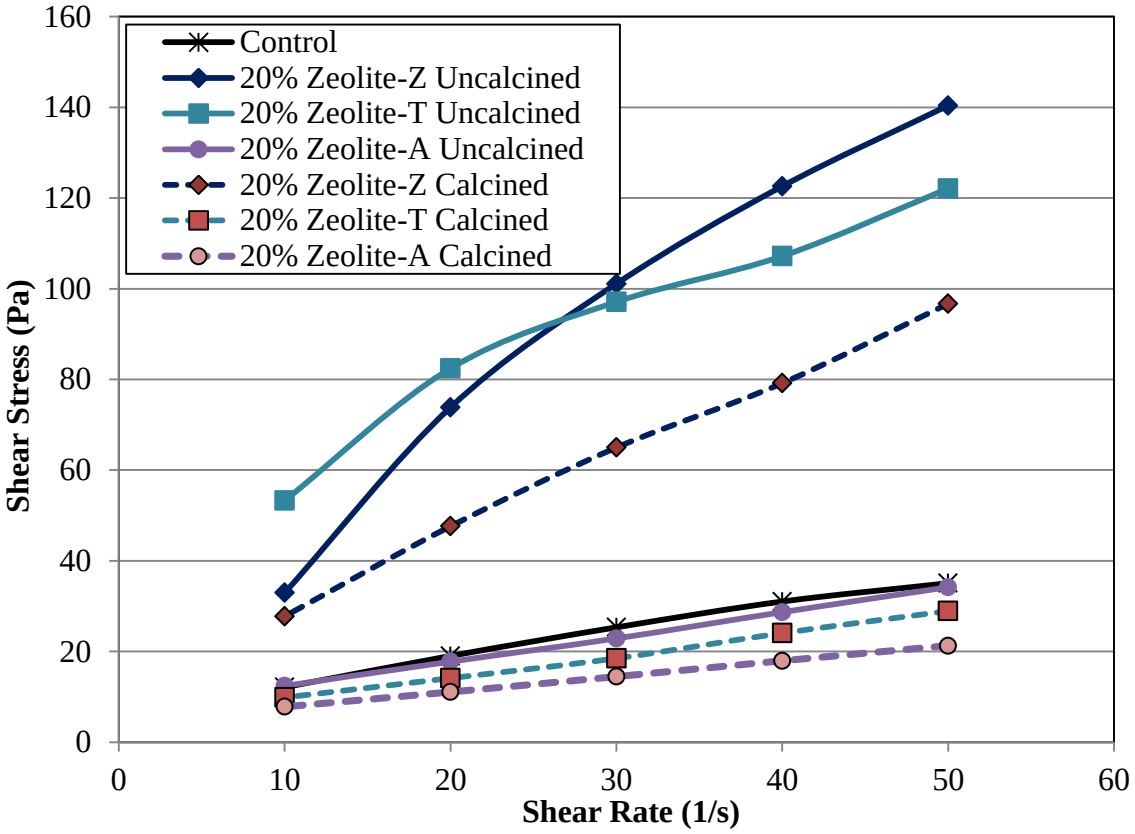

Figure 6.7: Representative flow curves of uncalcined and calcined zeolite pastes

Table 6.2: Bingham Yield Stress for Pastes with Uncalcined and Calcined Zeolites

Mixture Description	Yield Stress (Pa)		Reduction in Yield Stress (Pa)
	Raw	Calcined	
Control	7.78 ± 0.64	N/A	---
20% Zeolite-Z	15.41 ± 0.34	11.55 ± 0.88	3.86 ± 1.22
20% Zeolite-T	N/A	N/A	---
20% Zeolite-A	8.53 ± 1.69	4.10 ± 0.26	4.43 ± 1.95

Table 6.3: Bingham Viscosity for Pastes with Uncalcined and Calcined Zeolites

Mixture Description	Viscosity (Pa.s)		Reduction in Viscosity (Pa.s)
	Uncalcined	Calcined	
Control	0.56 ± 0.01	N/A	---
20% Zeolite-Z	2.61 ± 0.03	1.74 ± 0.04	0.87 ± 0.07
20% Zeolite-T	N/A	N/A	---
20% Zeolite-A	0.55 ± 0.00	0.33 ± 0.01	0.22 ± 0.01

Table 6.4: Apparent Viscosity of the Uncalcined and Calcined Zeolite-T Paste

Shear Rate (1/s)	Apparent Viscosity (Pa.s) of 20% Zeolite-T paste		Reduction in Viscosity (Pa.s)
	Uncalcined	Calcined	
10	5.29 ± 0.04	1.00 ± 0.01	4.29 ± 0.05
20	4.45 ± 0.32	0.70 ± 0.01	3.75 ± 0.33
30	3.23 ± 0.01	0.62 ± 0.00	2.61 ± 0.01
40	2.70 ± 0.02	0.59 ± 0.01	2.11 ± 0.03
50	2.49 ± 0.04	0.57 ± 0.01	1.92 ± 0.05

6.3 Conclusions of Mixture Workability Improvement Study on Zeolites

The results presented in this chapter found that calcination improved the mixture workability of zeolites. While the reduction in the zeolite surface area after calcination, as seen in the BET results, was thought to partially contribute to the improved zeolite paste workability, the improvement was mostly attributed to the destabilization of the zeolite structure through calcination, as seen in the XRD and DSC results, and the alteration of the zeolite micropores, as indicated by the loss of shear thinning behavior of the Zeolite-T paste after calcination. Additionally, the dehydroxylation and agglomeration of clay

impurities through calcination was also thought to improve the workability of the Zeolite-T mixture.

After calcination, the workability of the Zeolite-T and Zeolite-A mixtures were found to be better than that of the control mixture. However, despite some improvement in mixture workability after calcination, the yield stress and viscosity of the calcined Zeolite-Z mixture was still higher than that of the control. Data from the DSC analysis suggests that a higher calcination temperature than what was used in this research maybe required to destabilize the structure of Zeolite-Z further and improve its mixture workability. More research needs to be conducted with the Zeolite-Z pozzolan, calcined at a temperature higher than 800°C, to confirm this hypothesis. Also, additional research utilizing SEM imaging and porosity analysis is needed to understand whether the reduction in surface area solely comes from the destabilization of the zeolite structure, or from agglomeration of the zeolite particles, or a combination of both factors.

Chapter 7: Conclusions

The research presented in this dissertation examined a variety of natural pozzolans to assess their suitability as Class F fly ash replacements in concrete. The physical and chemical properties of the natural pozzolans were extensively characterized, and their performance in cementitious mixtures was evaluated in terms of compressive strength, durability and mixture workability. The performance of the natural pozzolans was then correlated back to the characteristics of the pozzolans to draw meaningful relationships between pozzolan properties and performance. Using this knowledge, some of the under-performing natural pozzolans were also modified to see if changes in their properties could improve their performance in cementitious mixtures. This chapter summarizes the key findings of the research and its contribution to the field. Ideas for future work based on the results and conclusions of this research are also presented.

7.1 Summary of Pozzolan Performance in Cementitious Mixtures

Other than the two coarse zeolites, Zeolite-T and Zeolite-A, all the natural pozzolans investigated in this research can be used as replacements for Class F fly ash in concrete. However, since the ability of these pozzolans to enhance concrete properties is not uniform across all measures of performance, the best natural pozzolan to use will be determined by the needs of a specific application. In terms of compressive strength, natural pozzolans like Metakaolin-D and Zeolite-Z were observed to improve early age strength, with their mortars surpassing the strength of the control by 28 days. On the other hand, Pumice-D and Perlite-I were seen to be more beneficial for long term strength, with their mortars having the highest compressive strength out of all the mixtures tested at 365 days.

In terms of mixture workability, the rheology and water requirement results suggested that, other than the zeolites, the natural pozzolans should not cause any significant workability issues in cementitious mixtures when used at a dosage of 20%. With its spherical shape, fly ash still had the best performance in terms of mixture workability, but rheology results showed pozzolans like Shale-T and Vitric Ash-S to improve the viscosities of their mixtures to values similar to the fly ash paste.

In terms of durability, all the natural pozzolans were able to mitigate ASR, provided an adequate dosage was used. Pumice-D, Perlite-I, Metakaolin-D and Zeolite-Z were the most effective at mitigating expansions from ASR, needing a cement replacement dosage of only 15% (by weight) to keep expansions below the 0.1% limit of ASTM C 1567 (2013). On the other hand, Vitric Ash-S, Shale-T and Zeolite-T needed a higher dosage of 25% to keep their mortar expansions within limits. Zeolite-A was the least effective at controlling expansions from ASR, needing a dosage of 35% to pass the ASTM C 1567 ASR test. In terms of sulfate attack, other than the two coarse zeolites, Zeolite-T and Zeolite-A, the natural pozzolans were able to mitigate expansions from sulfate attack in varying degrees. Pumice-D, Perlite-I and Zeolite-Z were seen to have a superior performance to fly ash, qualifying for Class 3 severe sulfate exposure at dosages of only 15%. Metakaolin-D was able to qualify for Class 2 moderate sulfate exposure at a dosage of 25%. Finally, at dosages of 25%, Shale-T was able to qualify for Class 1 mild sulfate exposure, while Vitric Ash-S barely missed this classification.

In summary, for applications where both early age strength and durability are essential, the best natural pozzolans to use in place of Class F fly ash would be Metakaolin-D and Zeolite-Z. If a severe sulfate exposure is expected, then the use of Zeolite-Z is recommended over Metakaolin-D. Other advantages of Zeolite-Z over Metakaolin-D include its comparatively lower cost of $100/ton compared to $325/ton for

Metakaolin-D. The only disadvantage with Zeolite-Z is its high water demand, which could cause problems with mixture workability if an adequate amount of superplasticizers are not used. Pumice-D and Perlite-I will also perform well to increase the durability of concrete and are recommended in applications where high early strength is not a requirement. Finally, Shale-T and Vitric Ash-S can be used to improve mixture workability and ASR resistance of concrete, and are recommended in applications that do not require high early strength or resistance to sulfate attack. Shale-T has an advantage over Vitric Ash-S due to its lower cost (about $50/ton compared to $100-160/ton for Vitric Ash-S) and its ability to mitigate expansions in a Class 1 mild sulfate exposure.

7.2 CONTRIBUTIONS TO LITERATURE

The research presented here offers comprehensive characterization and performance evaluation of eight different natural pozzolans that could be used as alternatives to Class F fly ash in concrete. A critical difference between previous pozzolan research and the research presented in this dissertation is that here, the performance of the natural pozzolans was correlated back to its physical and chemical characteristics to derive meaningful relationships between pozzolan properties and performance. Finding such relationships was important for understanding the underlying mechanisms of cement and pozzolan interaction, a lot of which are not well established in literature. The wide variety of natural pozzolans used in this research was also helpful in drawing conclusions about why some pozzolans performed better than others in certain areas of performance. Finally, understanding the relationships between pozzolan properties and performance uncovered ways of mitigating the problems of low strength and poor mixture workability that are typically associated with the use of pozzolans as SCMs in previous literature.

Similar to previous literature (Oey et al., 2013; Lothenbach et al., 2011), the presence of fine pozzolan particles that can act as nucleation sites for hydration products was concluded to be one of the main reasons behind the early reactivity of pozzolans like Metakaolin-D and Zeolite-Z mixtures. However, comparisons with the performance results of the other natural pozzolans indicated that caution must be exercised in using pozzolan surface area as a predictor of early age mortar compressive strength for porous pozzolans, where some of surface area could be within pores and cannot act as nucleation sites for the growth of hydration products. Previous literature (Fernandez et al., 2011a) has also shown the presence of alumina to be one of the reasons for the early reactivity of metakaolin. The results of the research presented here corroborate this hypothesis, and extend it by comparing the mortar compressive strength of more siliceous pozzolans like Pumice-D and Perlite-I to that of Metakaolin-D. The results indicate that although presence of alumina can accelerate the rate of strength gain at early ages, having high silica content is more crucial for long term mortar strength beyond 90 days.

Although previous research (Lilkov et al., 2011; Erdem et al., 2007; Hossain, 2003; Campbell et al., 1982) has shown pozzolans to generally decrease early age compressive strength, very little research has been done to understand the reasons behind the low early strength or find ways to mitigate the problem. Isothermal calorimetry was used in this research to prove that the initial decrease in strength is from a dilution effect of replacing the cement, rather than an actual retardation of cement hydration caused by the addition of the pozzolans. Additionally, using pozzolans with identical chemical composition but different particle size distributions, the research here established that early age strength could be increased by simply decreasing pozzolan particle size so that more surface area is available for the nucleation and growth of hydration products. Although the concept of increasing concrete strength through a decrease in pozzolan

particle size exists in previous literature (Erdem et al., 2007) the research presented here extends the theory by using TGA/DSC analysis to show that decreasing particle sizes not only brings about enhanced nucleation and growth of hydration products, but also an actual increase in the rate of pozzolanic reactivity. In other words, despite previous research indicating that the reactivity of pozzolans is negligible in the earlier stages of hydration, and that increases in early age strength is solely from size filler effects, the results of the research presented here show that the onset of pozzolanic activity can be accelerated by grinding the pozzolan particles to a finer size.

In terms of durability, it was seen that pozzolans that needed a low replacement dosage to mitigate expansions from ASR also had a low Ca/Si ratio. This corroborates results from previous literature (Thomas, 2011) that found the ASR mitigation ability of SCMs to be strongly related to their Ca/Si composition. However, Zeolite-Z and fly ash did not fit into this trend, and the good performance of these pozzolans in mitigating ASR was attributed to the presence of alumina in their chemical composition, which has been shown in previous literature (Chappex and Scrivener, 2012b) to slow down the dissolution of reactive aggregates. Although previous literature (Duchesne and Berube, 1994a) showed no correlation between reductions in expansion from ASR and calcium hydroxide depletion in SCM mixtures, it is interesting to note that in this research, other than fly ash, all the pozzolan mortar bars that were able to mitigate expansions from ASR at low dosages had high calcium hydroxide depletions between 7-90 days. This correlation does not mean that the effectiveness of SCMs in mitigating ASR is dependent upon the reduction of calcium hydroxide content, but it does point to some underlying mechanism of pozzolan composition and/or particle characteristics that make the pozzolans perform well in both calcium hydroxide depletion and ASR mitigation.

In terms of sulfate attack, the results of this research showed that pozzolans with a high calcium hydroxide reduction in TGA also performed well in sulfate attack testing except for Metakaolin-D, which needed high replacement dosages to qualify for a Class 2 moderate sulfate exposure. Although previous literature (Al-Akhras, 2006, Khatib and Wild, 1998) has explored the ability of metakaolin pozzolans to mitigate sulfate attack, research has not been done to explain the performance of the metakaolin pozzolan under sulfate attack in terms of the characteristics of the pozzolan. The results from XRF and isothermal calorimetry in this research suggests that the poor performance of the Metakaolin-D mortar under sulfate attack is related to the high alumina content of the calcined clay, which could lead to undersulfation of the system.

Another interesting result of this research is that, unlike the performance of most mortars, the Zeolite-Z mixture did not seem to be affected by w/cm, and qualified for a Class 3 severe sulfate exposure level regardless of the w/cm or SCM replacement dosage used. The unusual aluminate phase peak seen in the calorimetry curve for the Zeolite-Z paste gives a slight indication of undersulfation, which could mean that the sulfates are getting tied up in hydration phases of the Zeolite-Z mixture, resulting in its superior performance under sulfate attack. Another alternative theory, based on previous research on white cements (Skibsted and Anderson, 2013), was that the presence of alkali in zeolite pores could enhance the incorporation of alumina in C-S-H, which favors the formation of ettringite instead of monosulfoaluminate in the early stages of hydration. More research studying the pore solution chemistry and phase assemblages in Zeolite-Z pastes must be done before these hypotheses can be proven.

Another major contribution of this research to literature was evaluating the pozzolan pastes in terms of their rheological properties, like yield stress and viscosity, which provide a more thorough understanding of mixture workability, unlike simplistic

measurements like the slump test. Detailed knowledge of the effects of pozzolans on mixture workability can not only have important implications when trying to optimize fresh state properties in the field, it can also help find ways to modify materials like the zeolites to lower their water demand and absorption capacities. For example, unlike the water requirement tests, the rheology results of the Zeolite-T paste showed shear thinning (decrease in apparent viscosity), which indicated that the weakly bonded water in the zeolite pores could be released at higher shear rates. Understanding that certain zeolite mixtures can have lower viscosities at higher shear rates can help to modify pumping procedures in the field when zeolite-containing concrete mixtures are used.

Comparison of the rheology results with pozzolan characteristics showed that the porosity of zeolites was the main reason behind the poor workability of zeolite mixtures. Although previous research (Fernandez et al., 2011b; Habert et al., 2008; Perraki et al., 2005; Liebig and Althaus, 1998) has investigated the effects of calcination on zeolites, a majority of the research has concentrated on the effects of calcination on zeolite reactivity instead of zeolite mixture workability, as was done in this research. It was seen that calcination significantly improved the workability of zeolite mixtures, lowering viscosity of the zeolite mixtures, in some cases, to values less than that of the control paste with no pozzolans. The improvement of mixture workability was attributed to the destabilization of the zeolite structure through calcination, as seen in the XRD and DSC results, and the alteration of the zeolite micropores, as indicated by the loss of shear thinning behavior of the Zeolite-T paste after calcination. The reduction in the BET surface area of the calcined zeolites and the dehydroxylation of clay impurities after calcination was also thought to partially contribute to the improved zeolite paste workability.

7.3 FUTURE WORK

The research presented in this dissertation extensively evaluated the characteristics of a variety of natural pozzolans and their performance in cementitious mixtures. During analysis of the results, several areas were identified where future work could be done to confirm some of the hypotheses presented in this research. Compressive strength results of the Vitric Ash-S mortar indicated that crystalline impurities may play a big role in the reactivity of a pozzolan. In the research presented in this dissertation, only qualitative XRD was conducted which did not allow the crystalline impurities to be quantified. Future research quantifying these crystalline impurities will enhance the understanding of how these crystalline impurities affect the reactivity of pozzolans and influence the compressive strength of pozzolan mortars. Additionally, some pozzolan pastes showed significantly lower calcium hydroxide content after 7 days of hydration without a corresponding increase in compressive strength. Future work needs to be done to measure the calcium hydroxide content of the pastes after 1 day of hydration to see if the initial formation of hydration products per gram of cement in these pozzolan pastes was lower than that of the control from the very beginning.

The rheology data from this study suggested that below a certain surface area, particle size distribution of the pozzolans can be an important consideration for flow behavior. However, more research needs to be done, where particle variables like texture and shape are controlled, to form a conclusive opinion as to whether particle size can be a better predictor of mixture viscosity than BET surface area. The ASTM C 618 water requirement tests of the pozzolans were generally in good agreement with the rheology results, except for Zeolite-A. More research needs to be conducted to understand why the workability of the Zeolite-A mixture was different depending on the test method being used.

Future research investigating the changes to pore solution chemistry with the addition of pozzolans will greatly enhance the understanding of some the durability research presented in this dissertation. For example, the hypotheses behind the superior performance of Zeolite-Z in mitigating sulfate attack, despite the w/cm or SCM replacement dosage used, can be validated by additional research on the pore solution chemistry and phase assemblages in Zeolite-Z pastes. Quantitative XRD that can measure the relative amount of ettringite vs. AFm that are forming in these pozzolan pastes can also help to understand the underlying mechanism through which pozzolans mitigate expansions from sulfate attack.

Future research investigating Zeolite-T and Zeolite-A, the two coarse zeolites that were not recommended as suitable Class F fly ash replacements, could grind the pozzolans down to a finer particle size distribution to see whether the modification improves their performance in cementitious mixtures, especially in terms of compressive strength and durability. Finally, the results in this dissertation showed that fly ash did not follow most of the trends observed for the natural pozzolans, and improved the strength and durability of cementitious mixture without a significant reduction of calcium hydroxide. This indicates that rather than correlating pozzolanic reactivity to the quantity of C-S-H formed through the depletion of calcium hydroxide, future research needs to measure pozzolanic reactivity based on the quality of C-S-H that is formed from the reaction of pozzolans and calcium hydroxide.

Appendix A – Admixture Dosages

Table A.1: Admixture Dosage for ASTM C 1567 Mortar Mixtures

Material	Admixture Dosage (mL/100 kg cement)			
	15% SCM	20% SCM	25% SCM	35% SCM
Pumice-D	155	127	---	---
Perlite-I	155	127	---	---
Vitric Ash-S	---	127	139	---
Metakaolin-D	155	183	---	---
Shale-T	---	124	155	---
Zeolite-Z	511	651	---	---
Zeolite-T	---	1116	1426	---
Zeolite-A	---	356	806	1348
Fly Ash	---	0	---	---

*Values in red represent dosages that are above the manufacturer recommended dosage

Appendix B – XRD and TGA/DSC Plots

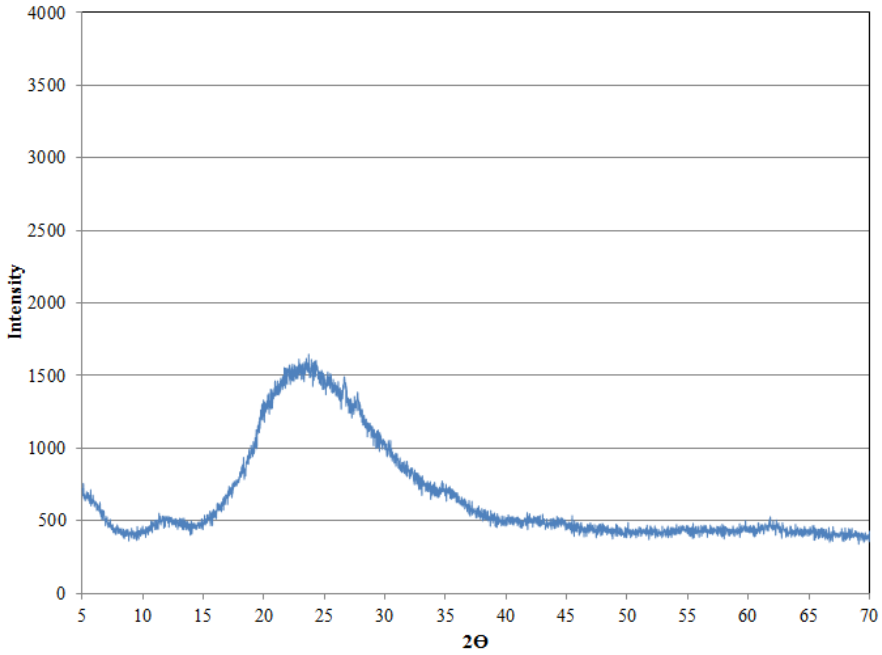

Figure B1: XRD plot of Pumice-D

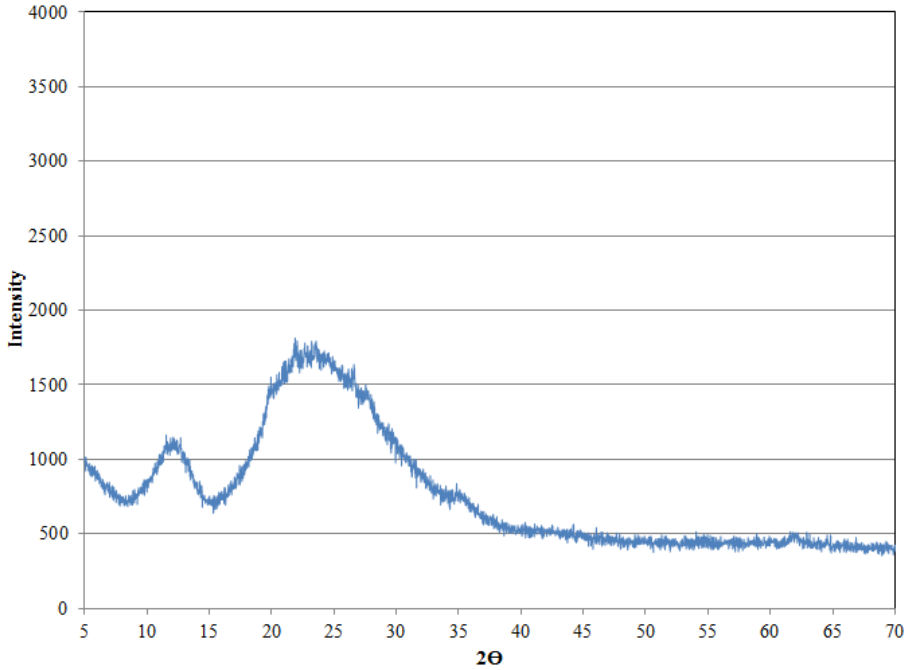

Figure B2: XRD plot of Pumice-N

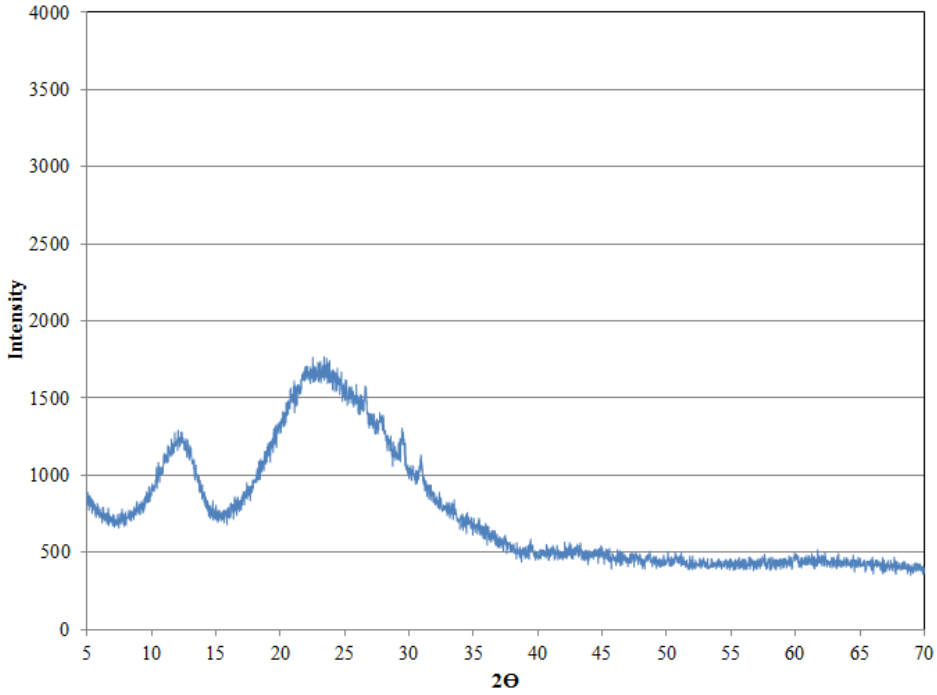

Figure B3: XRD plot of Pumice-S

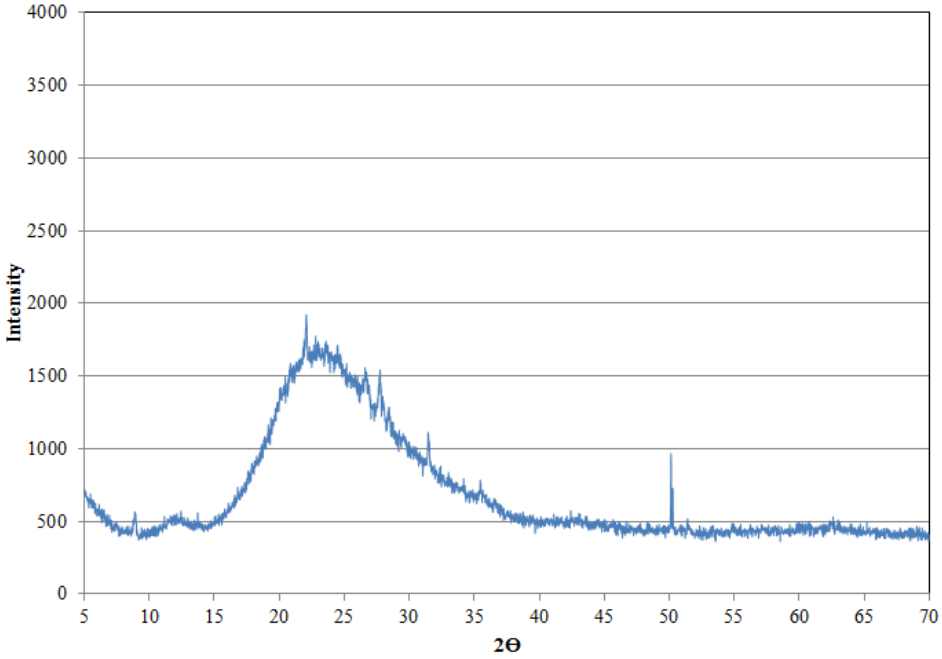

Figure B4: XRD plot of Perlite-I

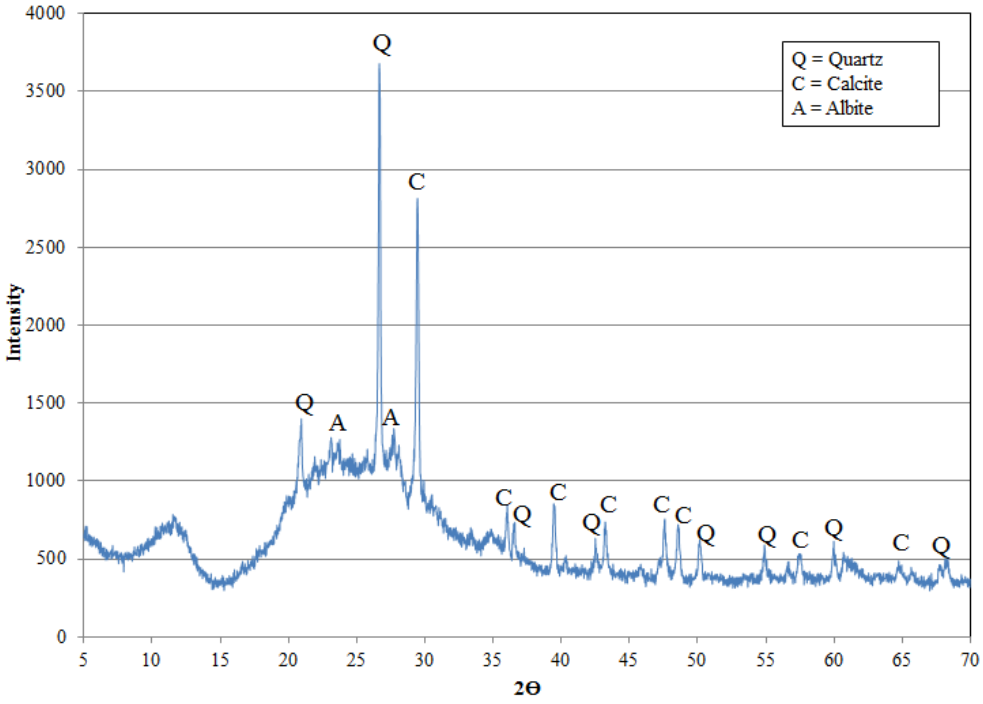

Figure B5: XRD plot of Vitric Ash-S

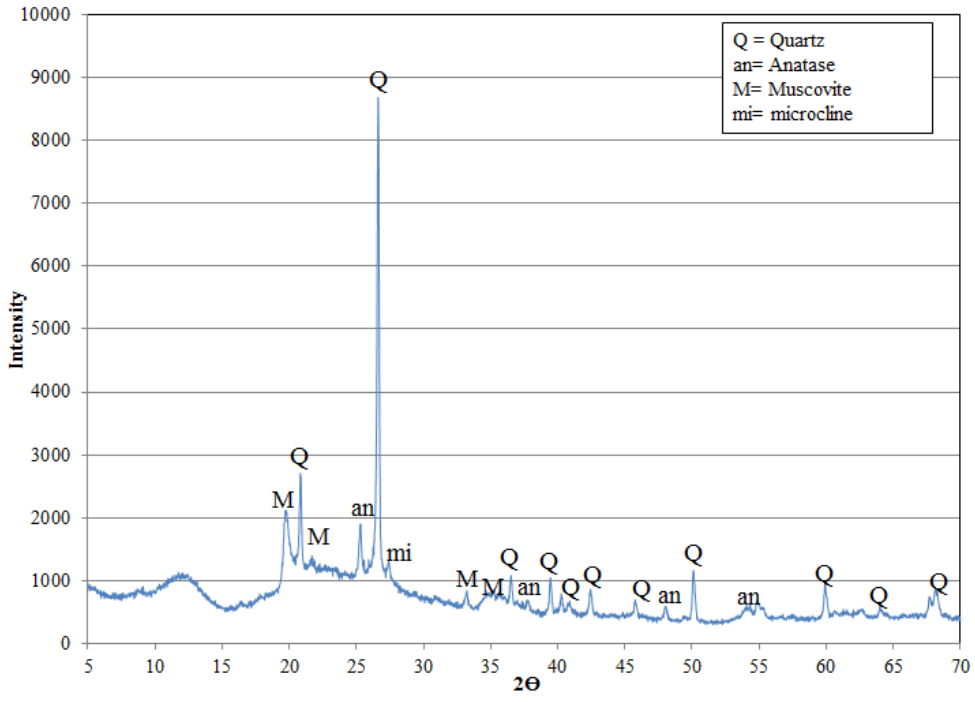

Figure B6: XRD plot of Metakaolin-D

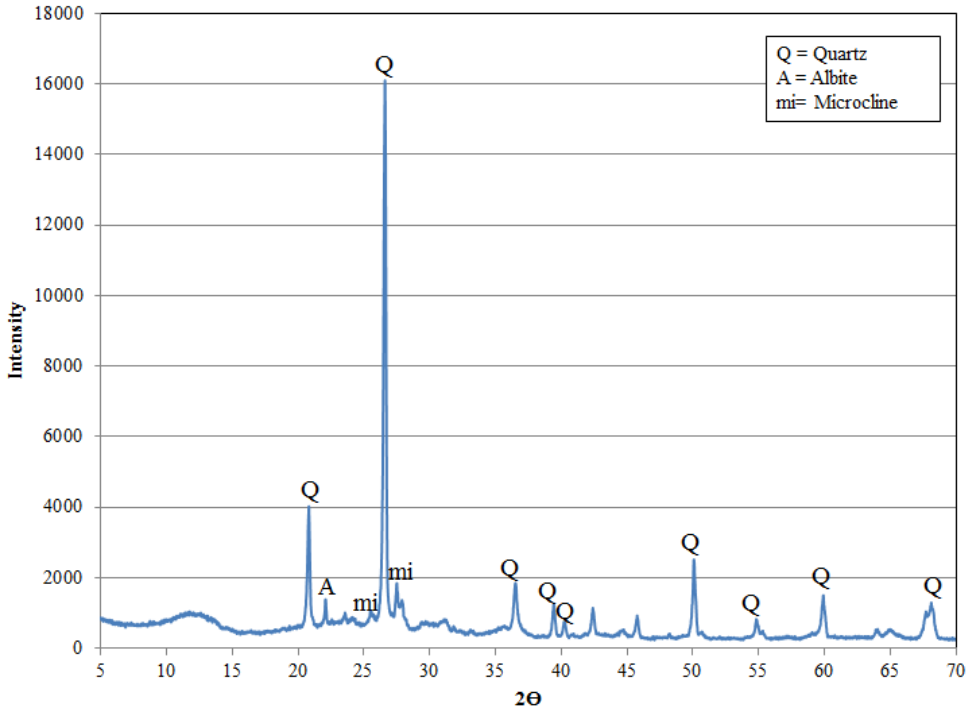

Figure B7: XRD plot of Shale-T

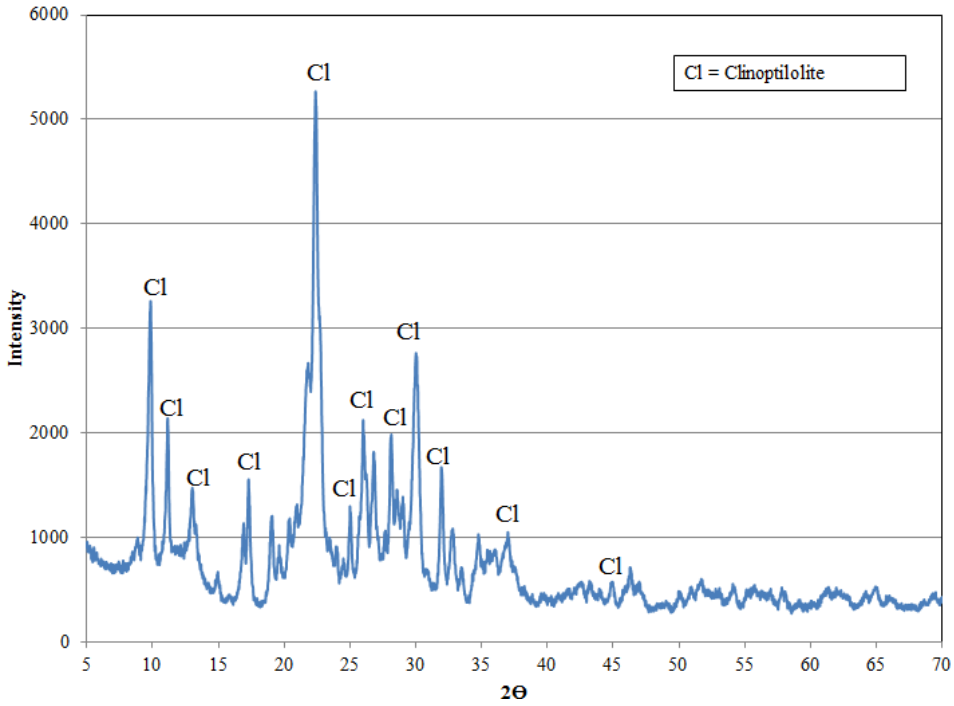

Figure B8: XRD plot of Zeolite-Z

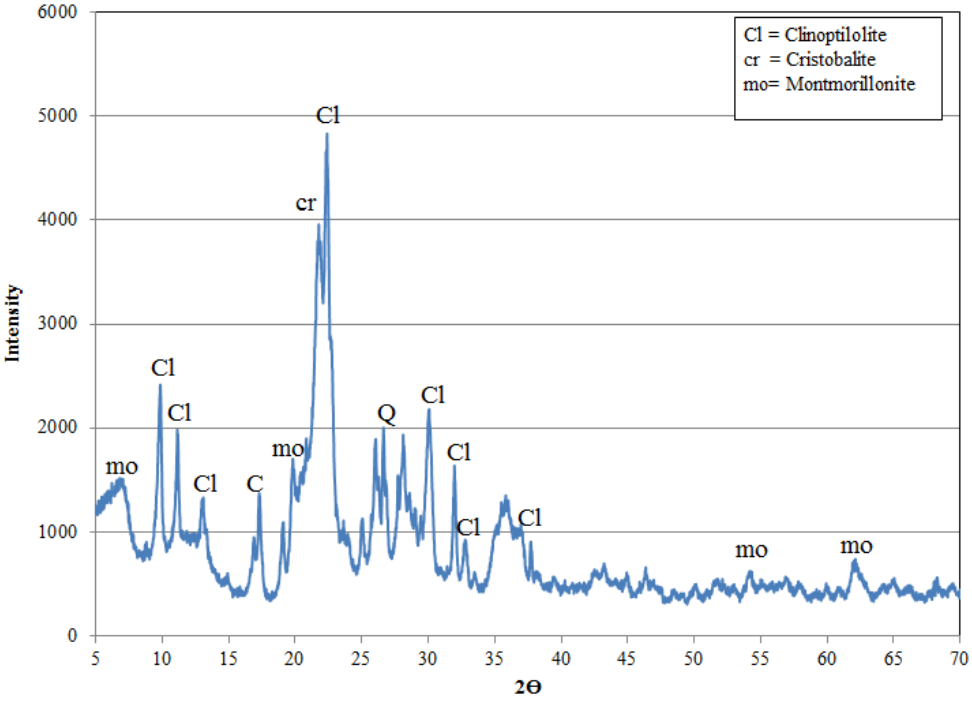

Figure B9: XRD plot of Zeolite-T

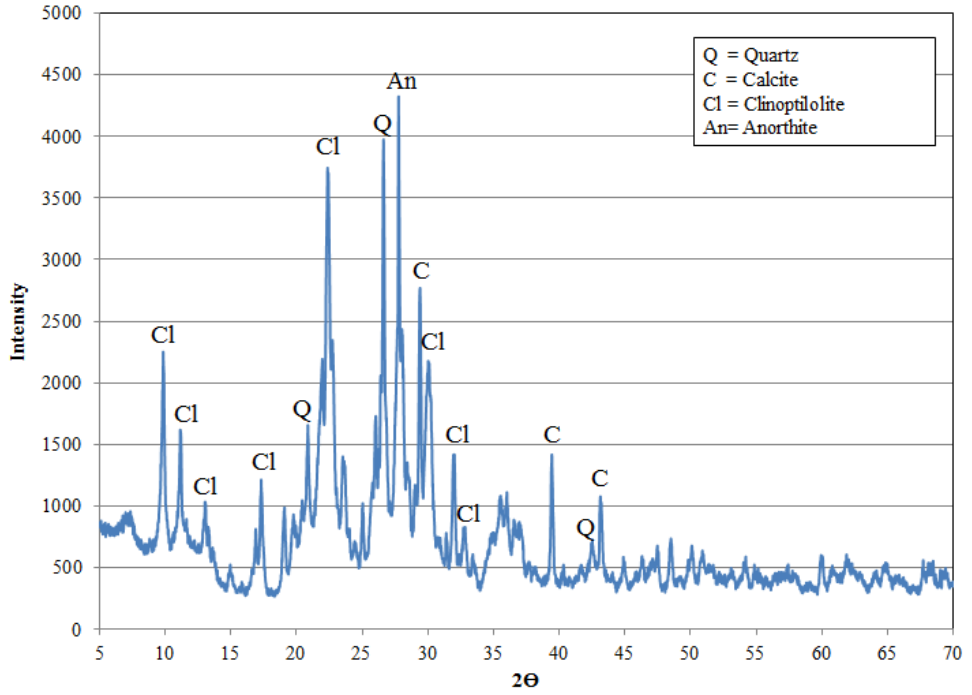

Figure B10: XRD plot of Zeolite-A

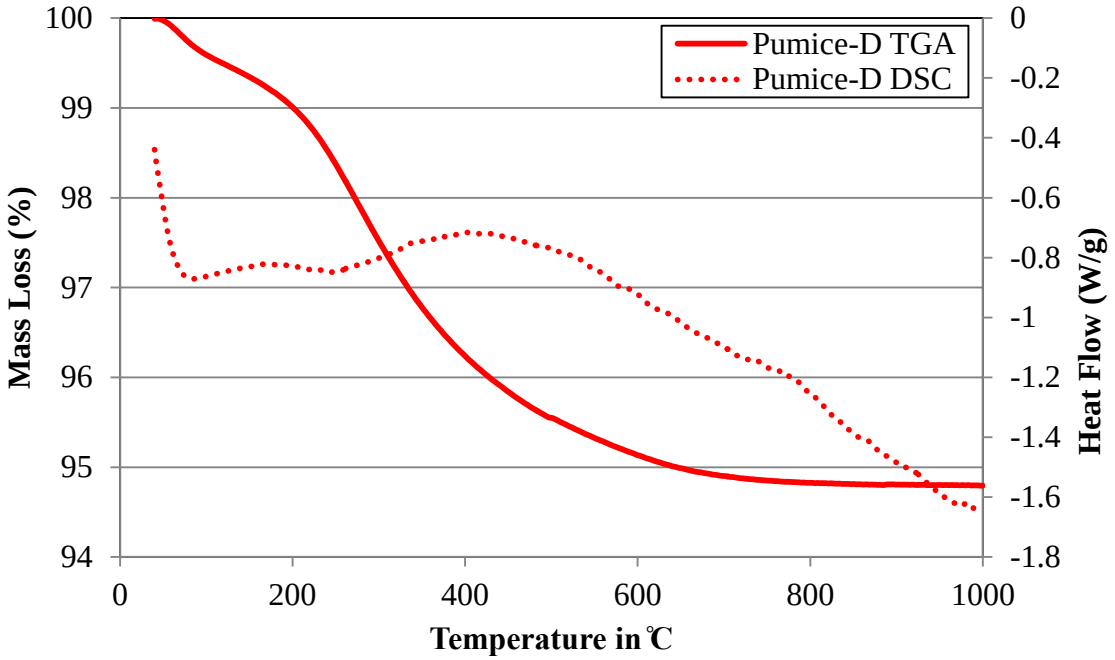

Figure B11: TGA/DSC plot of Pumice-D

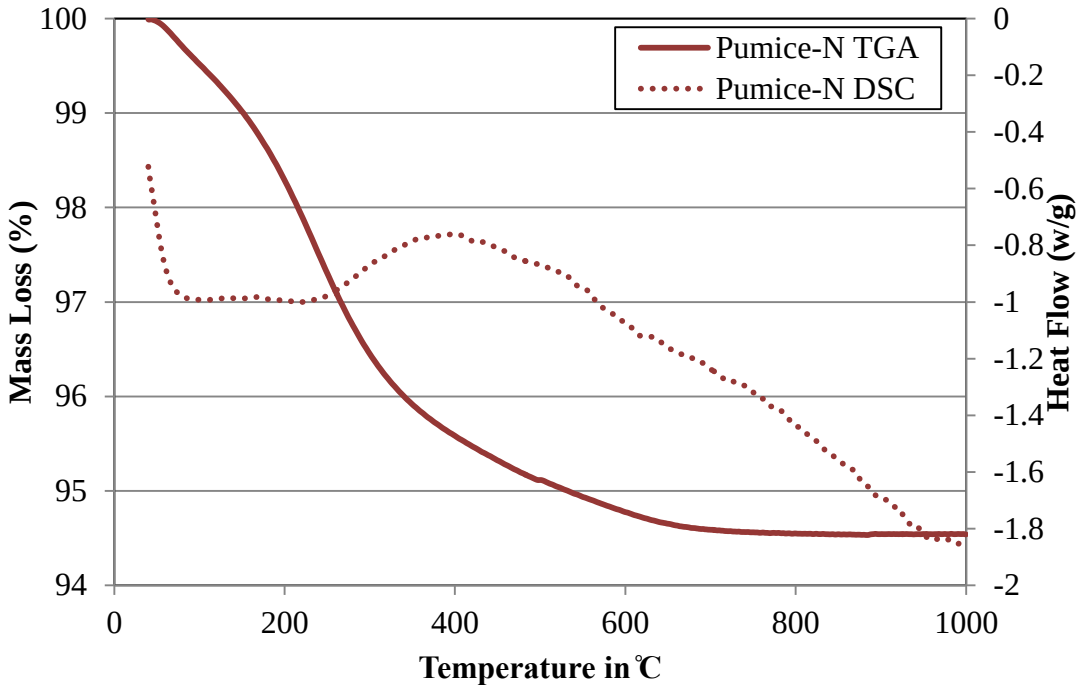

Figure B12: TGA/DSC plot of Pumice-N

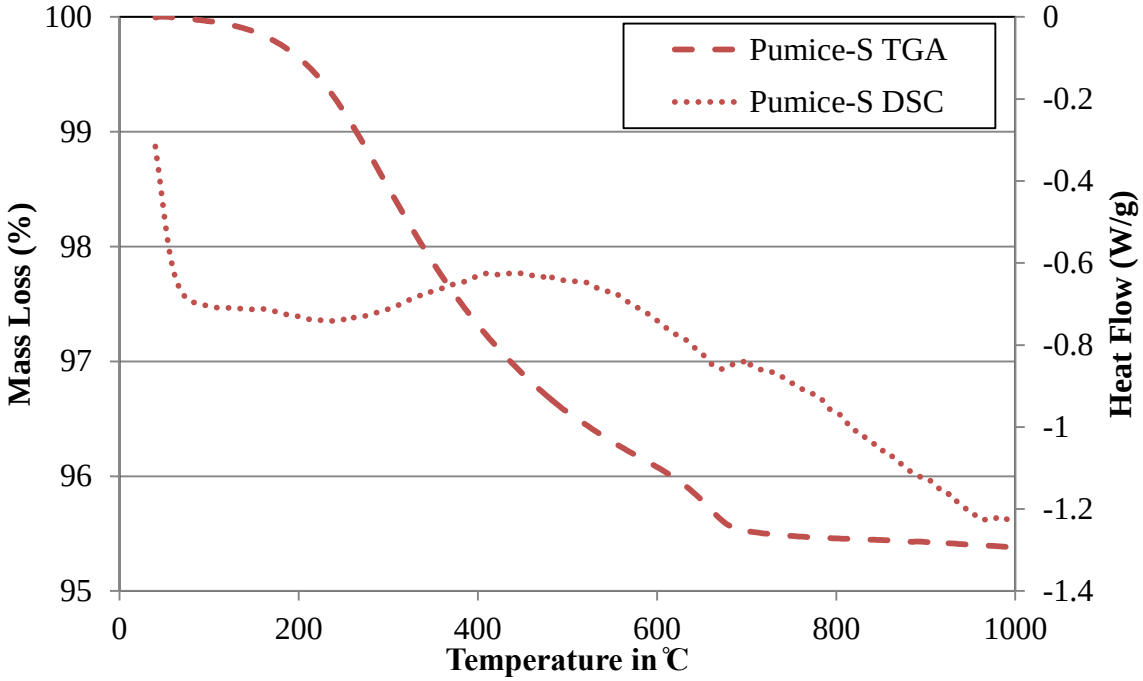

Figure B13: TGA/DSC plot of Pumice-S

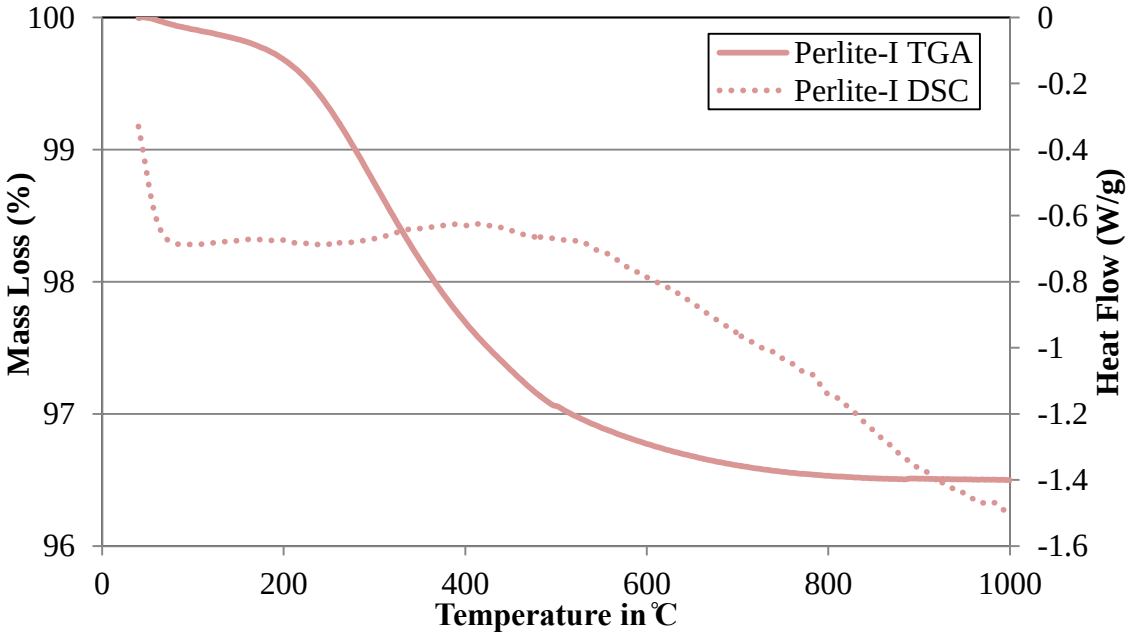

Figure B14: TGA/DSC plot of Perlite-I

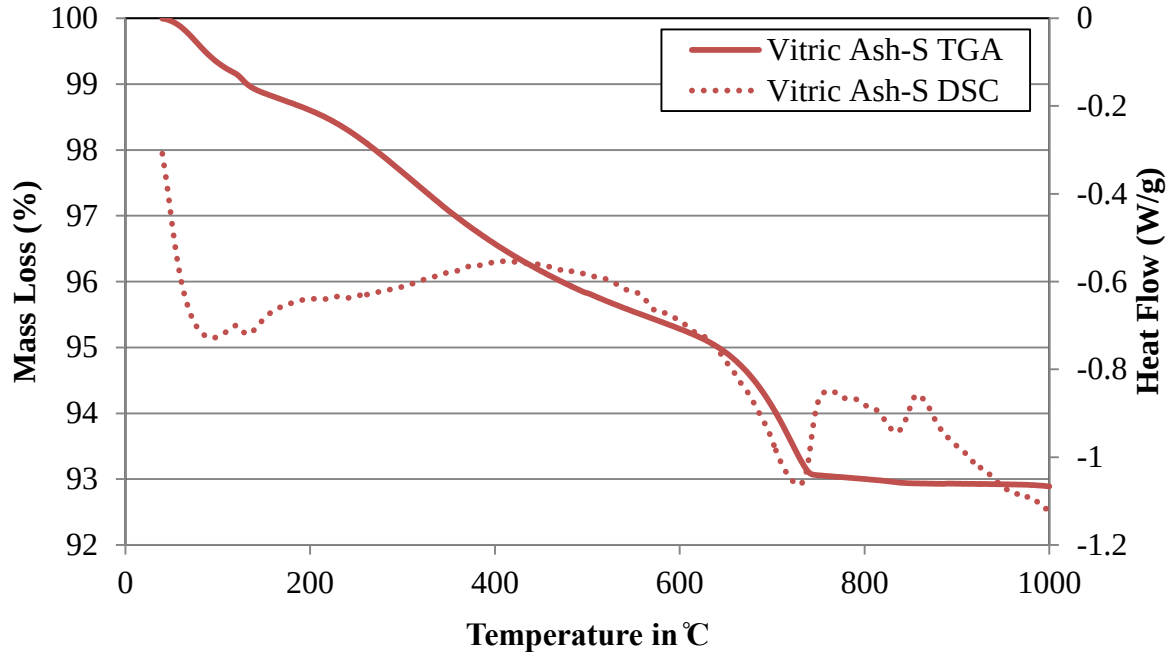

Figure B15: TGA/DSC plot of Vitric Ash-S

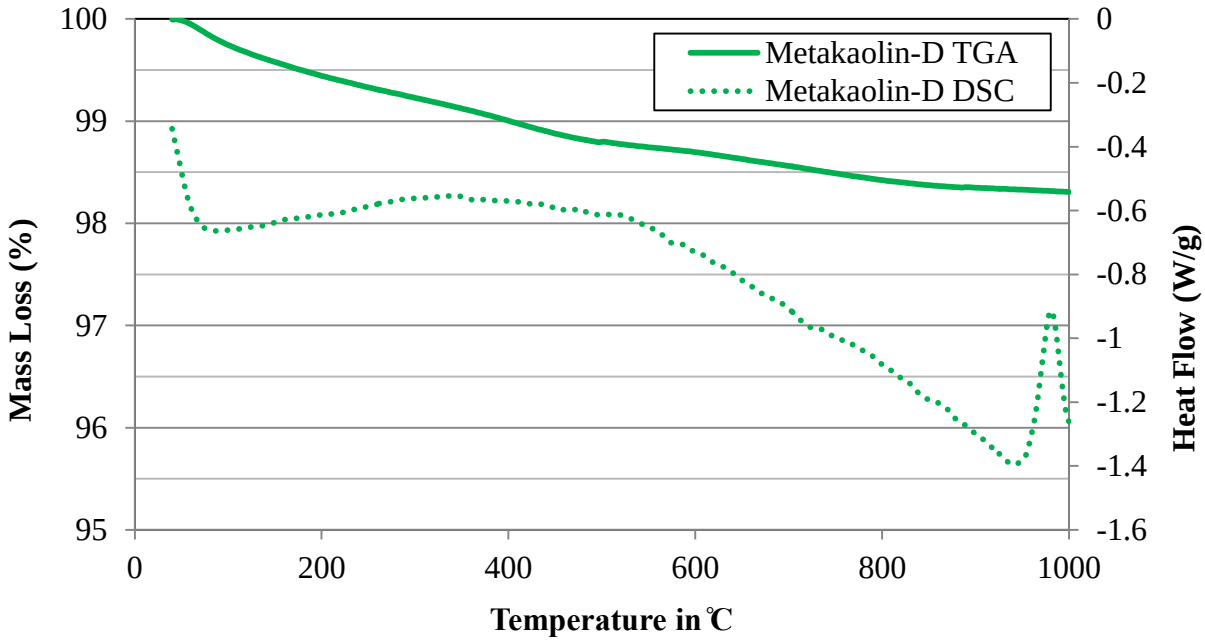

Figure B16: TGA/DSC plot of Metakaolin-D

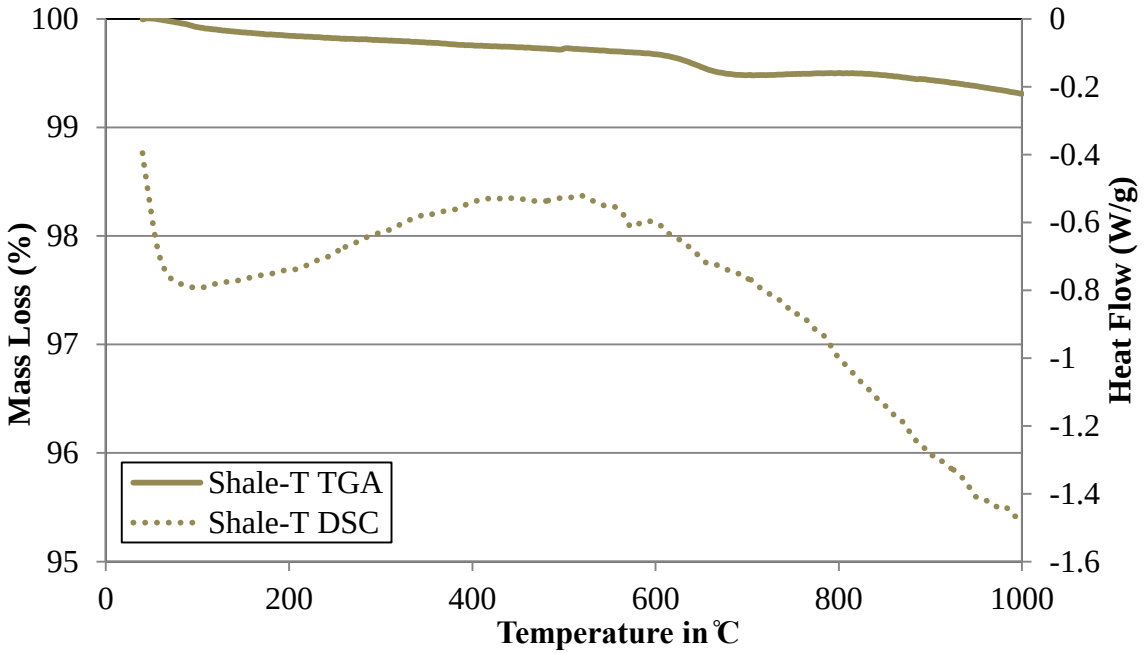

Figure B17: TGA/DSC plot of Shale-T

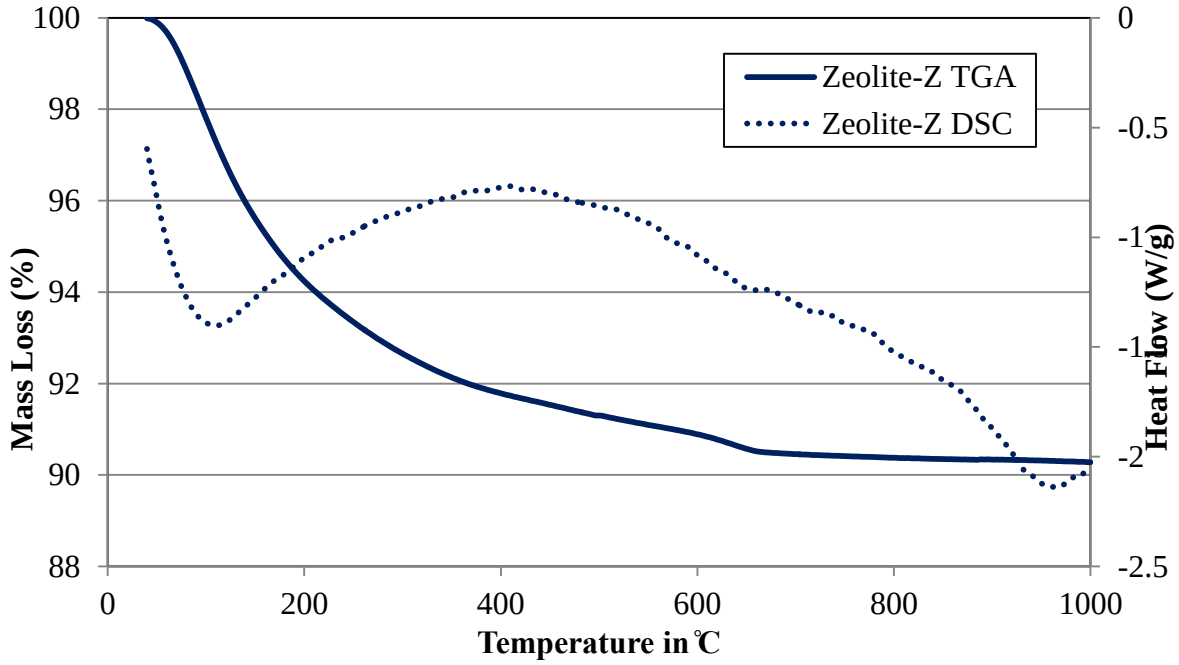

Figure B18: TGA/DSC plot of Zeolite-Z

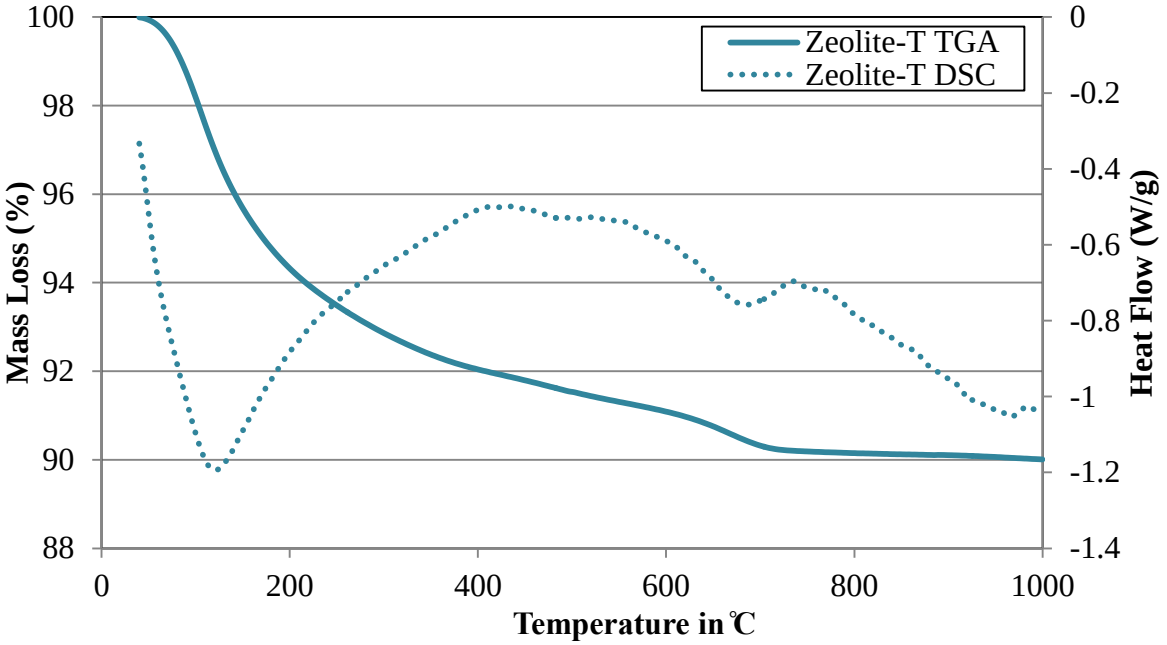

Figure B19: TGA/DSC plot of Zeolite-T

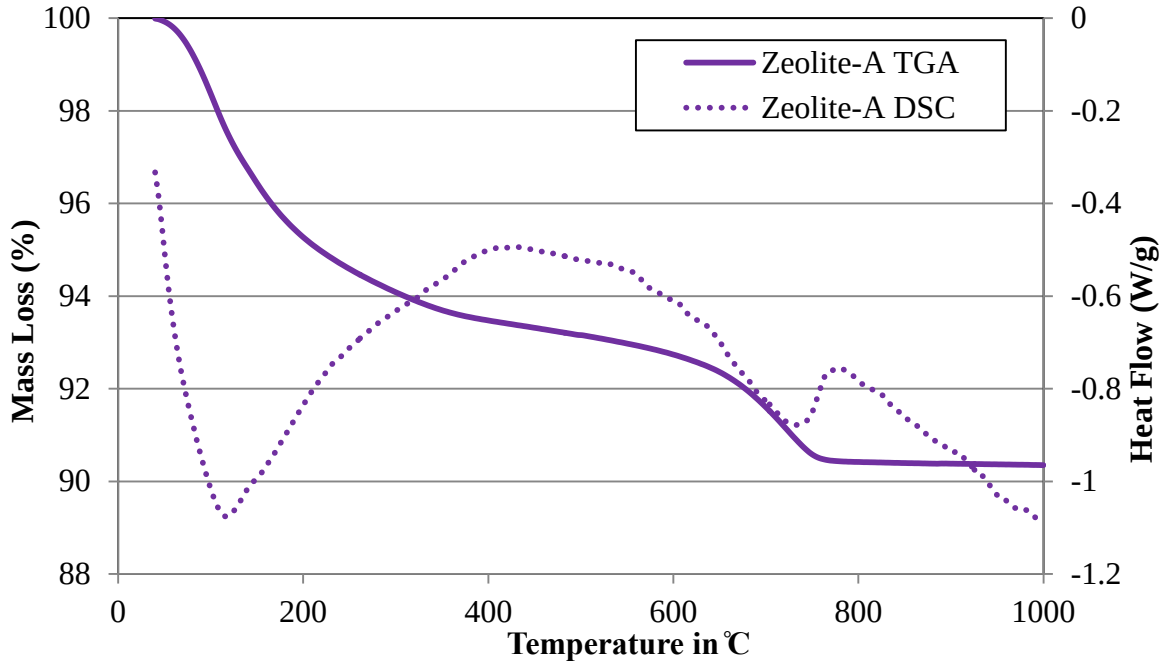

Figure B20: TGA/DSC plot of Zeolite-A

References

ACI 116R (1990b). Cement and concrete terminology. ACI Manual of Concrete Practice, Part 1, American Concrete Institute, Farmington Hills, MI

ACI 232.1R (2012). Report on the Use of Raw or Processed Natural Pozzolans in Concrete. American Concrete Institute, Farmington Hills, MI

ACI 201.2R (2008). Guide to Durable Concrete, American Concrete Institute. Farmington Hills, MI

Ahmadi, B., Shekarchi, M. (2010). Use of natural zeolite as a supplementary cementitious material. *Cement and Concrete Composites* 32, 134-141

Al-Akhras, N.M (2006). Durability of metakaolin concrete to sulfate attack. *Cement and Concrete Research* 36, 1727-1734

Ambroise, J., Murat, M., Pera, J. (1985). Hydration Reaction and Hardening of Calcined Clays and Related Minerals. V. Extension of the Research and General Conclusions. *Cement and Concrete Research* 15, 261-268

Antoni, M., Rossen, J., Martirena, F., Scrivener, K. (2012). Cement substitution by a combination of metakaolin and limestome. *Cement and Concrete Research* 42, 1579-1589

ARTBA Transportation Development Foundation (2011). The Economic Impacts of Prohibiting Coal Fly Ash Use in Transportation Infrastructure Construction. Accessed on September 20th, 2014 from: http://www.circainfo.ca/documents/EconomicImpactsofprohibitingFAinInfrastructure-ARTBASept2011.pdf

ASTM C 109 (2011). Standard Test Method for Compressive Strength of Hydraulic Cement Mortars (Using 2-in. or [50-mm] Cube Specimens). ASTM International, West Conshohocken, PA

ASTM C 125 (2012). Standard Terminology Relating to Concrete and Concrete Aggregates. ASTM International, West Conshohocken, PA

ASTM C 114 (2011). Standard Test Methods for Chemical Analysis of Hydraulic Cement. ASTM International, West Conshohocken, PA

ASTM C 150 (2011). Standard Specification for Portland Cement. ASTM International, West Conshohocken, PA

ASTM C 151 (2009). Standard Test Method for Autoclave Expansion of Hydraulic Cement. ASTM International, West Conshohocken, PA

ASTM C 187 (2011). Standard Test Method for Amount of Water Required for Normal Consistency of Hydraulic Cement Paste. ASTM International, West Conshohocken, PA

ASTM C 311 (2011). Standard Test Methods for Sampling and Testing Fly Ash or Natural Pozzolan for Use in Portland-Cement Concrete. ASTM International, West Conshohocken, PA

ASTM C 430 (2008). Standard Test Method for Fineness of Hydraulic Cement by the 45-μm (No. 325) Sieve. ASTM International, West Conshohocken, PA

ASTM C 494 (2013). Standard Specification for Chemical Admixtures for Concrete. ASTM International, West Conshohocken, PA

ASTM C 604 (2007). Standard Test Method for True Specific Gravity of Refractory Materials by Gas-Comparison Pycnometer. ASTM International, West Conshohocken, PA

ASTM C 618 (2012). Standard Specification for Coal Fly Ash and Raw or Calcined Natural Pozzolan for Use in Concrete. ASTM International, West Conshohocken, PA

ASTM C 778 (2012). Standard Specification for Standard Sand. ASTM International, West Conshohocken, PA

ASTM C 1012 (2013). Standard Test Method for Length Change of Hydraulic-Cement Mortars Exposed to a Sulfate Solution. ASTM International, West Conshohocken, PA

ASTM C 1437 (2007). Standard Test Method for Flow of Hydraulic Cement Mortar. ASTM International, West Conshohocken, PA

ASTM C 1567 (2013). Standard Test Method for Determining the Potential Alkali-Silica Reactivity of Combinations of Cementitious Materials and Aggregate (Accelerated Mortar-Bar Method). ASTM International, West Conshohocken, PA

ASTM D 4326 (2011). Standard Test Method for Major and Minor Elements in Coal and Coke Ash By X-Ray Fluorescence. ASTM International, West Conshohocken, PA

Ates, A., Hardacre, C. (2012). The effect of various treatment conditions on natural zeolites: Ion exchange, acidic, thermal and steam treatments. *Journal of Colloid and Interface Science* 372, 130–140

Badogiannis, E., Papadakis, V.G., Chaniotakis, E., Tsivilis, S. (2004). Exploitation of poor Greek kaolins: Strength development of metakaolin concrete and evaluation by means of k-value. *Cement and Concrete Research* 34, 1035-1041

Barnes, D.I. and Sear, L.K.A (2006). Ash Utilisation from Coal-Based Power Plants. Report COAL-R-274, Hatterrall Associates, UK Quality Ash Association. Accessed on September 20th, 2014 from: http://www.ukqaa.org.uk/wp-content/uploads/2014/02/AshTech-2006-Barnes-Sear.pdf

Bektas, F., Turanli, L., Monteiro, P.J.M. (2005). Use of Perlite Powder to suppress alkali-silica reaction. *Cement & Concrete Research* 35, 2014-2017

Bilim, C. (2011). Properties of cement mortars containing clinoptilolite as a supplementary cementitious material. *Construction and Building Materials* 25, 3175-3180

Bullard, J.W., Jennings, H.M., Livingston, R.A., Nonat, A., Scherer, G.W., Schweitzer, J.S., Scrivener, K.L, Thomas J.J. (2011). Mechanisms of cement hydration. *Cement and Concrete Research* 41, 1208–1223

Camiletti, J., Soliman, A.M., Nehdi, M. L. (2013). Effects of nano- and micro-limestone addition on early-age properties of ultra-high-performance concrete. *Materials and Structures* 46, 881–898

Campbell, D.H., Weise, C.H., Love, H. (1982). Mount St. Helens Volcanic Ash in Concrete. *Concrete International*, July, 24-31

Canham, I., Page, C. L., Nixon, P. J. (1987). Aspects of the Pore Solution Chemistry of Blended Cements related to the Control of Alkali Silica Reaction. *Cement and Concrete Research* 17, 839-844

Chappex, T., Scrivener, K. (2012a). Alkali fixation of C–S–H in blended cement pastes and its relation to alkali silica reaction. *Cement and Concrete Research* 42, 1049–1054

Chappex, T., Scrivener, K. (2012b). The influence of aluminium on the dissolution of amorphous silica and its relation to alkali silica reaction. *Cement and Concrete Research* 42, 1645–1649

Colella, C., Gennaro, M., Aiello, R. (2001). Use of zeolitic tuff in the building industry. *Reviews in Mineralogy and Geochemistry* 45 (1), 551-587

Cook, D.J. (1986) Calcined Clay, Shale and other soils. *Cement Replacement Materials*, 40-72

Denton, J.S., Tuffen, H., Gilbert, J.S., Odling N. (2009). The hydration and alteration of perlite and rhyolite. *Journal of the Geological Society* 166, 895-904

Dhole, R., Thomas, M.D.A, Folliard, K.J, Drimalas, T. (2013). Characterization of Fly Ashes for Sulfate Resistance, *ACI Materials Journal* 110 (2), 159-168

Duchesne, J., Berube, M.A. (1994a). The Effectiveness of Supplementary Cementing Materials in Suppressing Expansion due to ASR: Another Look at the Reaction Mechanisms, Part 1: Concrete Expansion and Portlandite Depletion. *Cement and Concrete Research* 24 (1) 73-82

Duchesne, J., Berube, M.A. (1994b). The Effectiveness of Supplementary Cementing Materials in Suppressing Expansion due to ASR: Another Look at the Reaction Mechanisms, Part 2: Pore Solution Chemisty. *Cement and Concrete Research* 24 (2) 221-230

Elfert, R.J. (1974). Bureau of Reclamation Experiences with Fly Ash and Other Pozzolans in Concrete. Information Circular No. 8640, U.S. Bureau of Mines, Washington DC, 80-93

Elaiopoulos, K., Perraki, T., Grigoropoulou, E. (2010). Monitoring the effect of hydrothermal treatments on the structure of a natural zeolite through a combined XRD, FTIR, XRF, SEM and N2-porosimetry analysis. *Microporous and Mesoporous Materials* 134, 29–43

Engineering News Record (2014). Current Costs. Accessed November 24th, 2014 from: http://enr.construction.com/economics/current_costs/

Erdem, T.K., Meral, C., Tokyay, M., Erdogˇan, T.Y. (2007). Use of perlite as a pozzolanic addition in producing blended cements. *Cement & Concrete Composites* 29, 13–21

Fajun, W., Grutzeck, M.W., Roy, D.M. (1985). The Retarding Effects of Fly Ash upon the Hydration of Cement Pastes: The first 24 hours. *Cement and Concrete Research* 15, 174-184

Fernandez, R., Martirena, F., Scrivener, K.L., (2011a). The origin of the pozzolanic activity of calcined clay minerals: A comparison between kaolinite, illite and montmorillonite. *Cement and Concrete Research* 41, 113 – 122

Fernandez, R., Vigil de la Villa, R., Garcia, R., Rodriguez, O., Frias, M., Villar-Cocina, E. (2011b). Characterization and pozzolanic activity of a calcined natural zeolite. International Conference on the Chemistry of Cement, July 8-10

Foster, M.D. (1954). The Relation Between Composition and Swelling in Clays. *Clays and Clay Minerals* 3, 205-220. Accessed on September 23rd, 2014 from: http://www.clays.org/journal/archive/volume%203/3-1-205.pdf

Guneyisi, E., Gesoglu, M., Mermerdas K. (2008). Improving strength, drying shrinkage, and pore structure of concrete using metakaolin. *Materials and Structures* 41, 937-949

Gokce, H.S., Simsek, O., Korkmaz, S. (2013). Reduction of alkali-silica reaction expansion of mortars by utilization of pozzolans. *Magazine of Concrete Research* 65 (7), 441-447

Habert, G., Choupay, N., Escadeillas, G., Guillaume, D., Montel, J.M. (2009). Clay content of argillites: Influence on cement based mortars. *Applied Clay Science* 43, 322-330

Habert, G., Choupay, N., Montel, J.M., Guillaume, D., Escadeillas, G. (2008). Effects of the secondary minerals of the natural pozzolans on their pozzolanic activity. *Cement and Concrete Research* 38, 963–975

He, C., Makovicky, E., Osbaeck B., (2000). Thermal Stability and pozzolanic activity of raw and calcined mixed-layer mica/smectite. *Applied Clay Science* 17, 141-161

Heidrich, C., Feuerborn, H.J., Weir, A. (2013). Coal Combustion Products: a Global Perspective. 2013 World of Coal Ash (WOCA) Conference, April 22-25, 2013, Lexington, KY. Accessed on September 20th, 2014 from: http://www.flyash.info/2013/171-Heidrich-Plenary-2013.pdf

Hill, R., Sarkar, S., Rathbone, R., J. Hower (1997). An Examination of Fly Ash Carbon and Its Interactions With Air Entraining Agent. *Cement and Concrete Research* 27(2), 193-204

Hong, S.Y., Glasser, F.P. (1999). Alkali binding in cement pastes Part I. The C-S-H phase, *Cement and Concrete Research* 29, 1893–1903

Hong, S.Y., Glasser, F.P. (2002). Alkali sorption by C-S-H and C-A-S-H gels, Part II. Role of alumina. *Cement and Concrete Research* 32, 1101– 1111

Hossain, K.M.A., Lachemi, M. (2006). Performance of volcanic ash and pumice based blended cement concrete in mixed sulfate environment. *Cement and Concrete Research* 36, 1123-1133

Hossain, K.M.A. (2003) .Blended cement using volcanic ash and pumice. *Cement and Concrete Resea*rch 33, 1601-1605

Humphreys, K. and Mahasenan, M. (2002). Towards a sustainable cement industry, Sub-study 8: Climate Change. Accessed on September 20th, 2014 from: http://www.wbcsdcement.org/pdf/battelle/final_report8.pdf

Ideker, J.H., Bentivegna, A.F., Folliard, K.J., Juenger, M.C.G. (2012). Do Current Laboratory Test Methods Accurately Predict Alkali-Silica Reactivity. *ACI Materials Journal* 109 (4), 395-402

Janotka, I., Osacky, M., Krizma, M., Bagel, L. (2011). Performance Study of Slovak Natural Zeolite – Containing Cement Compositions. International Conference on the Chemistry of Cement, July 8-10

Jones, M.R., Sear, L.K.A., McCarthy, M.J., Dhir, R.K. (2006). Changes in Coal Fired Power Station Fly Ash: Recent Experiences and Use in Concrete. Proceedings of Ash Technology Conference, UK Quality Ash Association. Accessed on September 20th, 2014 from: http://www.ukqaa.org.uk/wp-content/uploads/2014/02/AshTech-2006-Jones-et-al.pdf

Karakurt, C., Topcu, I.B. (2011). Effect of blended cements produced with natural zeolite and industrial by-products on alkali-silica reaction and sulfate resistance of concrete. *Construction and Building Materials* 25, 1789–1795

Khanna, R.L., Puri, M.L. (1957).The Use of Calcined Shale as Pozzuolana in Mass Concrete. *Indian Concrete Journal*, August, 257-263

Khatib, J.M., Wild, S. (1998). Sulphate Resistance of Metakaolin Mortar, *Cement and Concrete Research* 28, 83-92

Khatri, R.P., Sirivivatnanon, V. (1997). Role of Permeability in Sulphate Attack. *Cement and Concrete Research* 27 (8) 1179-1189

Lamond, J. F., Pielert, J. H. (2006). Significance of tests and properties of concrete and concrete-making materials. Vol. 169, ASTM International.

Liebig, E., Althaus, E. (1998) Pozzolanic Activity of Volcanic Tuff and Suevite: Effects of Calcination. *Cement and Concrete Research* 28 (4) 567-575

Lilkov, V., Petrov, O., Petkova, V., Petrova, N., Tzvetanova, Y. (2011). Study of the pozzolanic activity and hydration products of cement pastes with addition of natural zeolites. *Clay Minerals* 46, 241-250

Lothenbach, B., Scrivener, K., Hooton, R.D. (2011). Supplementary Cementitious Materials. *Cement and Concrete Research* 41, 1244-1256

Macquaker, J.H.S., Adams, A.E. (2003). Maximizing Information from Fine-Grained Sedimentary Rocks: An Inclusive Nomenclature for Mudstones. *Journal of Sedimentary Research* 73, 735-744

Mechtcherine, V., Gram, A., Krenzer, K., Schwabe, J.H., Shyshko, S., Roussel, N. (2014). Simulation of fresh concrete flow using Discrete Element Method (DEM): theory and applications. *Materials and Structures* 47, 615–630

Meissner, H.S. (1950). Pozzolans used in Mass Concrete. Symposium on Use of Pozzolanic Materials in Mortars and Concretes, STP-99, ASTM, Philadelphia, 16-30

Mielenz, R.C., Witte, L.P., Glantz O.J. (1950). Effect of Calcination on Natural Pozzolana. Symposium on Use of Pozzolanic Materials in Mortars and Concretes, STP-99, ASTM, 43-91

Mindess, S., Young, J.F., Darwin, D. (2002). Concrete 2nd Edition, Pearson Education, New Jersey

Mukherjee, A.B, Zevenhoven, R., Bhattacharya, P., Sajwan, K.S., Kikuchi, R. (2008). Mercury flow via coal and coal utilization by-products: A global perspective. Resources, *Conservation and Recycling* 52, 571–591

Müllauer, W., Beddoe, R.E., Heinz, D. (2013). Sulfate attack expansion mechanisms. *Cement and Concrete Research* 52, 208–215

Nocun-Wczelik, W. (2001). Heat evolution in Hydrated Cementitious Systems admixture with Fly Ash. *Journal of Thermal Analysis and Calorimetry* 65, 613-619

Oey, T., Kumar, A., Bullard, J.W., Neithalath, N., Sant, G. (2013). The Filler Effect: The Influence of Filler Content and Surface Area on Cementitious Reaction Rates. *Journal of the American Ceramic Society*, 1-13

Pabalan, R., Bertetti, P. (2001). Cation-exchange properties of natural zeolites. *Reviews in Mineralogy and Geochemistry* 45 (1), 453-518

Papadakis, V.G. (1999). Effect of fly ash on Portland cement systems Part I. Low-calcium fly ash. *Cement and Concrete Research* 29, 1727–1736

Perraki, T., Kontori, E., Tsivilis, S. Kakali, G. (2010). The effect of zeolite on the properties and hydration of blended cements. *Cement and Concrete Composites* 32, 129-133

Perraki, T., Kakali, G., Kontori, E. (2005) Characterization and pozzolanic activity of thermally treated zeolite. *Journal of Thermal Analysis and Calorimetry*, 82 (1) 109-113

Presley, G. C. (2006). Pumice, pumicite, and volcanic cinder. Industrial Minerals and Rocks: Commodities, Markets, and Uses, Society for Mining, Metallurgy, and Exploration, Inc. 743-753

Ramlochan, T., Thomas, M., Gruber, K.A. (2000). The effect of metakaolin on alkali - silica reaction in concrete. *Cement and Concrete Research* 30, 339-344

Ramsburg, P., Neal, R.E. (2002). The Use of a Natural Pozzolan to Enhance the Properties of Self – Consolidating Concrete. Conference Proceedings of the First North American Conference on the Design and Use of Self-Consolidating Concrete, 401-405

Ravina, D. and Mehta, P.K. (1986). Properties of Fresh Concrete containing large amounts of Fly Ash. *Cement and Concrete Research* 16, 227–238

Rotella, M., Simandl, G. (2002). Marilla Perlite – Volcanic Glass Occurrence, British Columbia, Canada. Geological Fieldwork, Paper 2003-1

Roussel, N., Geiker, M.R., Dufour, F., Thrane, L.N., Szabo, P. (2007). Computational modeling of concrete flow: General overview. *Cement and Concrete Research* 37, 1298–1307

Sahmaran, M., Ozkan, N., Keskin, S.B., Uzal, B., Yaman, I.O., Erdem, T.K. (2008). Evaluation of natural zeolite as a viscosity-modifying agent for cement-based grouts. *Cement and Concrete Research* 38, 930–937

Schmidt, T., Lothenbach, B., Romer, M., Neuenschwander, J., Scrivener, K. (2009). Physical and microstructural aspects of sulfate attack on ordinary and limestone blended Portland cements. *Cement and Concrete Research* 39, 1111 - 1121

Sear, L. K. A. (2009). Coal Fired Power Station Ash Products and EU Regulation, *Coal Combustion and Gasification Products* 1, 63-66. Accessed on September 20th, 2014 from: http://www.ukqaa.org.uk/wp-content/uploads/2014/02/CCGP-Journal-Dec-2009.pdf

Shehata, M.H., Thomas M.D.A, (2000). The effect of fly ash composition on the expansion of concrete due to alkali-silica reaction. *Cement and Concrete Research* 30, 1063–1072

Shehata, M.H., Adhikari, G., Radomski, S (2008). Long-Term Durability of Blended Cement Against Sulfate Attack. *ACI Materials Journal* 105 (6) 594-602

Skibsted, J., Andersen, M.D. (2013). The Effect of Alkali Ions on the Incorporation of Aluminum in the Calcium Silicate Hydrate (C–S–H) Phase Resulting from Portland Cement Hydration Studied by ^{29}Si MAS NMR. *Journal of the American Ceramic Society* 96 (2) 651–656

Snellings, R., Mertens, G., Elsen, J. (2012). Supplementary Cementitious Materials. *Reviews in Mineralogy & Geochemistry* 74, 211-278

Tattersall, G.H., Banfill, P.F.G. (1983). The Rheology of Fresh Concrete. Pittman Advanced Publishing, 1st edition.

Tex-317-D (2012). Test Procedure for Preparation of Cement Samples for Chemical Analysis. Texas Department of Transportation.

Tishmack, J., Olek, J., & Diamond, S. (1999). Characterization of High-Calcium Fly Ashes and Their Potential Influence on Ettringite Formation in Cementitious Systems. *Cement, Concrete, and Aggregates* 21 (1), 82-92

Thomas, M. (2011). The effect of supplementary cementing materials on alkali-silica reaction: A review. *Cement and Concrete Research* 41, 1224-1231

US EIA (2014). Annual Energy Outlook 2014 with projections to 2014. Accessed November 24th, 2014 from: http://www.eia.gov/forecasts/aeo/

US EPA (2014-a). Coal Combustion Residuals - Proposed Rule. Accessed September 20th , 2014 from: http://www.epa.gov/epawaste/nonhaz/industrial/special/fossil/ccr-rule/index.htm

US EPA (2014-b). Clean Air Interstate Rule (CAIR). Accessed September 20th, 2014 from: http://www.epa.gov/cair/index.html

US EPA (2014-c). Cross-State Air Pollution Rule (CSAPR) - Basic Information. Accessed September 20th, 2014 from: http://www.epa.gov/crossstaterule/basic.html

Uzal, B., Turanli L., Mehta P.K. (2007). High Volume Natural Pozzolan Concrete for Structural Applications. *ACI Materials Journal* 104 (5), 535-538

Villa, R.V., Fernandez, R., Rodriguez, O., Garcia, R., Villar-Cocina, E., Frias, M. (2013) Evolution of the pozzolanic activity of a thermally treated zeolite. *Journal of Material Science* 48, 3213–3224

Weerdt, K.D., Haha, M.B., Saout, G.L., Kjellsen, K.O., Justnes, H., Lothenbach, B. (2012). The effect of temperature on the hydration of composite cements containing limestone powder and fly ash. *Materials and Structures* 45, 1101–1114

Zhang, M.H., Malhotra, V.M. (1995) Characteristics of a Thermally Activated Alumino-Silicate Pozzolanic Material and its Use in Concrete. *Cement and Concrete Research* 25, 1713-1725

Vita

Saamiya Seraj was born in Dhaka, Bangladesh in 1987. After finishing her high school in 2005, Saamiya moved to the city of Austin in Texas to start her first year at the Cockrell School of Engineering at UT Austin. She graduated in 2009 with a Bachelor of Science in Civil Engineering. After working for 6 months in an engineering and construction company in Bangladesh, she returned to the US to pursue her graduate degree at UT Austin.

Permanent email: saami.seraj@gmail.com

This thesis was typed by the author.

.